Durability of Superficially Treated Concrete to Ammonium Sulfate and Sulfuric Acid Solutions Combined with Cyclic Environments

By

Amr Magdy Ibrahim

A Thesis submitted to the Faculty of Graduate Studies of

The University of Manitoba

In partial fulfillment of the requirements of the degree of

Master of Science

Department of Civil Engineering

Faculty of Engineering

University of Manitoba

Winnipeg

Abstract

Protecting concrete surface layer is essential for maintaining durability and functionality of concrete infrastructure during their service life. This thesis aimed to investigate the performance of nano-based coatings as superficial treatments for concrete elements exposed to aggravated exposures of ammonium sulfate, commonly found in agricultural, mining, and industrial zones, and sulfuric acid, usually found in wastewater and industrial facilities. Silane (hydrophobic agent) and vinyl ester (membrane-forming polymer) were used as base resins, in which nano-clay and nano-calcium carbonate particulates were dispersed at different dosages (0, 2.5, and 5%). In addition, a colloidal silica solution was used as a surface treatment. These surface treatments were applied to concrete specimens with water-to-binder ratios (*w/b*) of 0.6 (representing deteriorated concrete) and 0.4 (representing good quality concrete). Firstly, the durability of coated concrete specimens was evaluated under two ammonium sulfate exposures: full immersion and combined with cyclic environmental conditions (freezing-thawing and wetting-drying cycles). Degradation of concrete specimens was monitored by visual assessment and quantified in terms of mass and length changes over time. Secondly, the performance of superficially treated concrete specimens was assessed under two sulfuric acid exposures: full immersion and wetting-drying (W/D). Deterioration of concrete specimens was monitored by visual assessment and quantified in terms of mass changes over time. Furthermore, the degradation mechanisms and coatings' performance were studied by thermal, mineralogical, and microstructural analyses.

The results showed that colloidal silica could not adequately protect concrete specimens from these exposures. In addition, neat silane did not provide sufficient protection for concrete under sulfuric acid exposures; however, adding nanoparticles to neat silane significantly

enhanced its performance under such exposures. On the other hand, silane/nanocomposites improved the durability of concrete under ammonium sulfate exposures, and superior performance was generally observed for concrete specimens coated with vinyl ester/ nanocomposites by the end of all exposures.

Keywords: Nanoparticles, Coatings, Concrete, Ammonium sulfate, Sulfuric acid, Durability.

Dedication

I would like to dedicate the enervated efforts and sleepless nights behind this work to my parents and small family, without their valuable support and persistence I would have never got the enthusiasm to fulfill this journey.

Acknowledgments

In the name of Allah, the *Beneficent* and the *Most Merciful*. As a follower of the beautiful religion of Islam, I cannot but acknowledge the countless blessings and mercy that my creator has showered me with and helped me reach the point where I am today. To Him, I declare my gratefulness for bestowing me with the opportunity to pursue research at one of the most prospective research groups in the field of concrete durability. I am honored and blessed to be under the supervision of Dr. Mohamed T. Bassuoni, P.Eng., Professor, Department of Civil Engineering, University of Manitoba who I believe has helped me achieving ingenuity of the subject matter and helped me pursuing my academic achievements. My most sincere gratitude, therefore, goes to him, for his persistent guidance and valuable support in all phases of this research accomplishment. I am sincerely gratitude the cordial support and valuable guidance from my committee member Dr. Ahmed Ghazy, P.Eng., Adjunct Professor, Department of Civil Engineering, University of Manitoba.

I sincerely acknowledge the valuable financial support from Natural Sciences and Engineering Research Council of Canada (NSERC Alliance Program), the City of Winnipeg (COW), and Spray Lock Ltd., that helped me to dedicate myself towards this thesis with full potential.

Table of Contents

Abstract ii
Dedication iv
Acknowledgments v
List of Tables viii
List of Figures ix
Abbreviations/Nomenclatures xv
1. Introduction 1
1.1. Overview 1
1.2. Sulfate-Acid Attack on Concrete 2
1.3. Need for Research 3
1.4. Objectives 6
1.5. Scope of the Work 7
1.6. Thesis structure 8
2. Literature Review 10
2.1. Mechanisms and Features of Ammonium Sulfate Attack 10
2.2. Mechanisms and Features of Sulfuric Acid Attack 12
2.3. Testing Procedures 17
2.3.1. Standard Testing Procedures 17
2.3.2. Non-Standard Testing Procedures 18
2.4. Code provisions 22
2.5. Role of Surface treatments, and Nanoparticles in Resisting Sulfate and Acidic Attacks 25
2.6. Closure 29
3. Experimental Program 31
3.1. Concrete Mixtures 31
3.2. Surface treatments 32
3.3. Testing procedures 34
3.3.1. Characterization of nanocomposites and penetrability of concrete 34
3.3.2. Ammonium sulfate exposures 35
3.3.3. Sulfuric acid exposures 37
3.3.4. Thermal, microstructural, and mineralogical analyses 38

4. Phase I: Results and Discussion for Ammonium Sulfate Attack 41
4.1. Results 41
4.1.1. Dispersion of Nanoparticles in Polymers 41
4.1.2. Wettability of Coated Concrete 42
4.1.3. Penetrability of Concrete 44
4.1.4. Visual Assessment 46
4.1.5. Mass Change 50
4.1.6. Length Change 54
4.2. Discussion 59
4.2.1. Mechanisms of Damage 59
4.2.2. Effect of water-to-binder ratio 64
4.2.3. Effect of Colloidal Silica 65
4.2.4. Effect of Silane/Nanocomposites 67
4.2.5. Effect of Vinyl ester/Nanocomposites 71
5. Phase II: Results and Discussion for Sulfuric Acid Attack 75
5.1. Results 75
5.1.1. Dispersion of Nanoparticles in Polymers 75
5.1.2. Wettability of Coated Concrete 75
5.1.3. Penetrability of Concrete 75
5.1.4. Visual Assessment 75
5.1.5. Mass Change 79
5.2. Discussion 84
5.2.1. Mechanisms of Damage 84
5.2.2. Effect of water-to-binder ratio 89
5.2.3. Effect of Colloidal Silica 91
5.2.4. Effect of Silane/Nanocomposites 93
5.2.5. Effect of Vinyl ester/Nanocomposites 97
6. Summary, Conclusions and Recommendations 100
6.1. Summary 100
6.2. Conclusions for the Ammonium Sulfate Exposures 100
6.3. Conclusions for the Sulfuric Acid Exposures 102
6.4. Recommendations for Future Work 104
7. References 105

List of Tables

Table 2. 1: Stability of cement paste compounds and reaction products under sulfuric acid attack 15

Table 3. 1: Chemical and physical properties of GU cement and Fly ash 32

Table 3. 2: Proportions of concrete mixtures per cubic meter……..32

Table 3. 3: Visual rating for deterioration in concrete specimens……36

Table 4. 1: RCPT results for uncoated and coated concrete specimens……... 46

Table 4. 2: Cumulative mass change (%) of uncoated and coated concrete specimens in the full immersion exposure……...51

Table 4. 3: Cumulative mass change (%) of uncoated and coated concrete specimens in the combined exposure…… 52

Table 4. 4: Cumulative length change (%) of uncoated and coated concrete specimens in the full immersion exposure……...55

Table 4. 5: Cumulative length change (%) of uncoated and coated concrete specimens in the combined exposure…… 58

List of Figures

Figure 2. 1: Summary of sulfate-acid attack: manifestations of damage and failure mechanisms. 16

Figure 3. 1: DSC instrument by which the thermal analysis was conducted. 39

Figure 3. 2: SEM chamber where the fracture specimens were mounted for observation. 39

Figure 3. 3: XRD instrument by which the mineralogical analysis was conducted. 40

Figure 4. 1. Exemplar TEM images of: (a) colloidal silica, (b) silane/nano-calcium carbonate at 5% loading ratio, and (c) silane/nano-clay composites at 5% loading ratio. 41

Figure 4. 2. Exemplar ESEM images of: (a) vinyl ester/nano-calcium carbonate, and (b) vinyl ester/nano-clay composites at 5% loading ratio..... 42

Figure 4. 3. Contact angle of concrete surface treated with various coatings..... 43

Figure 4. 4. Examples of uncoated **concrete** specimens: (a) UC-*w/b* 0.6-full immersion exposure, (b) UC-*w/b* 0.4-full immersion exposure, (c) UC-*w/b* 0.6-combined exposure, and (d) UC-*w/b*=0.4 combined exposure. (Note: numbers between brackets represent the final visual rating). 47

Figure 4. 5. Examples of coated concrete specimens (GU-FA0.6) after 120 days in full immersion exposure. (Note: numbers between brackets represent the final visual rating). 48

Figure 4. 6. Examples of coated concrete specimens (GU-FA0.6) after 120 days in the combined exposure. (Note: numbers between brackets represent the final visual rating). 49

Figure 4. 7. Enthalpy of gypsum (dehydration range of 120-135°C) in uncoated and..... 60

Figure 4. 8. Micro-cracks in uncoated concrete specimens (*w/b* of 0.6) after 120 days in the combined exposure: (a) sub parallel crack close to concrete surface, and (b) micro-crack crossing a void filled with gypsum crystals. 62

Figure 4. 9. Enthalpy of ettringite (average dehydration temperature 90°C) in uncoated and coated specimens (*w/b* of 0.6) after 120 days in the combined exposure. (Note: accuracy of enthalpy determination is ±3%). 63

Figure 4. 10. Gypsum crystals filling a void near the concrete surface of uncoated concrete (*w/b* of 0.6) after the combined exposure and associated EDX. 63

Figure 4. 11. Uncoated concrete specimens (*w/b* of 0.6) after the combined exposure: (a) ettringite clusters filling an air void with associated EDX, and (b) incidental thaumasite formation with EDX. 64

Figure 4. 12. Precipitation of condensed nano-silica particulates on the surface of unexposed concrete coated with CS (*w/b* of 0.6) with shrinkage micro-cracks on the surface and associated EDX for nano-silica particles. (Note: SE refers to the standard error for the average ratio of the marked location). 66

Figure 4. 13. Enthalpy of portlandite (dehydration range of 400-450°C) in uncoated and coated specimens (*w/b* of 0.6) after 56 days of curing. (Note: accuracy of enthalpy determination is ±3%)..... 66

Figure 4. 14. Unexposed concrete specimens (*w/b* of 0.6) coated with: (a) SNC5% with associated EDX, and (b) SNCC5% with associated EDX. (Note: SE refers to the standard error for the average ratio of the marked location)..... 69

Figure 4. 15. XRD patterns of uncoated and coated specimens (*w/b* of 0.6) after 120 days of the full immersion exposure (Note: E = ettringite, G = gypsum, M = mono-carboaluminate, Q = quartz, C = calcite, D = dolomite). 71

Figure 4. 16. Coated concrete specimens (*w/b* of 0.6) with vinyl ester: (a) unexposed, (b) after the full immersion exposure, and (c) after the combined exposure..... 72

Figure 4. 17. Unexposed concrete specimens (*w/b* of 0.6): (a) coated with VENC5% with EDX, and (b) coated with VENCC5% with EDX. (Note: SE refers to the standard error for the average ratio of the marked location)..... 74

Figure 5. 1. Examples of uncoated concrete specimens: (a) UC-*w/b* 0.4-full immersion exposure, (b) UC-*w/b* 0.6-full immersion exposure, (c) UC-*w/b* 0.4-combined exposure, and (d) UC-*w/b* 0.6-combined exposure. (Note: numbers between brackets represent the final visual rating). 76

Figure 5. 2. Examples of coated concrete specimens (GU-FA0.4) after 10 weeks in the full immersion exposure. (Note: numbers between brackets represent the final visual rating). 77

Figure 5. 3. Examples of coated concrete specimens (GU-FA0.4) after 10 weeks in the W/D exposure. (Note: numbers between brackets represent the final visual rating). 78

Figure 5. 4. Mass change of concrete specimens over time in the full immersion exposure: (a) GU-FA-0.4, and (b) GU-FA-0.6. 80

Figure 5. 5. Cumulative mass change of concrete specimens after 10 weeks in the full immersion exposure. 81

Figure 5. 6. Mass change of concrete specimens over time in the W/D exposure: (a) GU-FA-0.4, and (b) GU-FA-0.6..... 83

Figure 5. 7. Cumulative mass change of concrete specimens after 10 weeks in the W/D exposure. 84

Figure 5. 8. Enthalpy of gypsum (dehydration range of 120-135°C) in uncoated and coated specimens (*w/b* of 0.4) after 10 weeks in the full immersion and W/D exposures. (Note: accuracy of enthalpy determination is ±3%)..... 85

Figure 5. 9. SEM micrograph and associated EDX spectrum for gypsum crystals filling a void near the concrete surface of uncoated concrete (*w/b* of 0.6) after the full immersion exposure. . 86

Figure 5. 10. Enthalpy of ettringite (dehydration peak at 90°C) in uncoated and coated specimens (*w/b* of 0.4) after 10 weeks in full immersion and W/D exposures. (Note: accuracy of enthalpy determination is ±3%) 87

Figure 5. 11. SEM micrograph and associated EDX spectrum for ettringite crystals away from the concrete surface of uncoated concrete (*w/b* of 0.4) after the W/D exposure. 87

Figure 5. 12. Micro-cracks in uncoated concrete specimens (*w/b* of 0.6) after 10 weeks in the full immersion exposure. 88

Figure 5. 13. XRD patterns of uncoated and coated specimens (*w/b* of 0.4) after 10 weeks of the full immersion exposure (Note: E = ettringite, G = gypsum, M = mono-carboaluminate, Q = quartz, C = calcite, D = dolomite). 88

Figure 5. 14. SEM micrograph and associated EDX spectrum for uncoated concrete (*w/b* of 0.4) after the full immersion exposure: (a) gypsum crystals covering the surface of concrete specimens, and (b) a dense core with C-S-H in the concrete specimens. 91

Figure 5. 15. Precipitation of condensed nano-silica particles on the surface of unexposed concrete coated with CS (*w/b* of 0.6) with shrinkage micro-cracks on the surface and associated EDX for nano-silica particles. (Note: SE refers to the standard error for the average ratio of the marked location). 92

Figure 5. 16. Enthalpy of portlandite (dehydration range of 400-450°C) in uncoated and coated specimens (*w/b* of 0.4) after 56 days of curing. (Note: accuracy of enthalpy determination is ±3%)..... 93

Figure 5. 17. Unexposed concrete specimens (*w/b* of 0.6) coated with: (a) SC5% with associated EDX, and (b) SCC5% with associated EDX. (Note: SE refers to the standard error for the average ratio of the marked location). 96

Figure 5. 18. Concrete specimens (*w/b* of 0.4): (a) coated with VE before exposures, (b) coated with VE after the full immersion exposure, and (c) coated with VE after the W/D exposure. 97

Figure 5. 19. Unexposed concrete specimens (*w/b* of 0.6) coated with: (a) VEC5% with associated EDX, and (b) VECC5% with associated EDX. (Note: SE refers to the standard error for the average ratio of the marked location)..... 99

Abbreviations/Nomenclatures

C_3A- Tricalcium aluminate, $3Cao.Al_2O_3$

CH - Calcium hydroxide (portlandite)

CS- Colloidal silica

C-S-H - Calcium silicate hydrate

DSC - Differential Scanning Calorimetry

XRD - X-ray Diffraction

SEM - Scanning Electron Microscopy

EDX - Energy Dispersive X-ray analysis

FA - Fly ash

NC- Nano-clay

NCC- Nano-calcium carbonate

NS - Nano-silica

S- Silane

SCMs - Supplementary cementitious materials

VE- Vinyl ester

1. Introduction

1.1. Overview

Agricultural, industrial, and wastewater treatment and collection facilities are essential infrastructure in every community. Due to durability, cost, availability of expert labour, and other factors, concrete as a construction material remains to be the main component in these infrastructural facilities for decades. Chemical deterioration of concrete elements in these applications can initiate from many deleterious environments; however, some are more common to happen than others. For example, sulfate attack on concrete substructures may occur in agricultural areas due to the acidity (pH<7) of some fertilizers in aqueous solutions. Since concrete is vulnerable to acid attacks (high alkalinity is essential for the stability of cementitious matrix), deterioration of concrete elements takes place to different degrees when bare concrete structures are exposed to ammonium-based salts or acids (House and Weiss 2014; Alexander et al. 2013; Bassuoni and Nehdi 2012; Nehdi et al. 2007; Allahverdi and Skvara 2000; Pavlík 1994).

On the other hand, concrete elements in sewage and wastewater facilities are susceptible to severer attack due to continual exposure to sulfuric acid. The constant increment in reported incidents of attack by acidic solutions in these facilities has drawn more attention to this type of damage. In addition, concrete elements, which are not parts of wastewater/sewerage facilities, are also vulnerable to acidic attacks from acid rains or using specific types of aggregate in concrete mixtures. It is well-known that this situation could be attributed to rising sources of acidic media as a result of increased industrial and urban activities (Alexander et al. 2013).

1.2. Sulfate-Acid Attack on Concrete

Ammonium sulfate is a deleterious substance to concrete structures in agricultural, mining, and industrial zones. Ammonium sulfate, as a common fertilizer, has been classified as one of the most severe solutions to concrete as it initiates an 'acid-sulfate' attack (C. Martins et al. 2021; Vishwakarma et al. 2020; Bassuoni and Nehdi 2012; Girardi and Maggio 2011; Mbessa and Péra 2001; Miletić et al. 1999). This sort of attack significantly deteriorates the cementitious matrix resulting in expansion, softening, cracking, and spalling of the concrete structures (Amin and Bassuoni 2018). For example, concrete elements (e.g. floors and tanks) in industrial facilities producing ammonium-based fertilizers experienced signs of deterioration such as swelling and cracking after three years of the start of mass production in the facility (Baxi and Patel 1998).

On the other hand, acidic attack on concrete structures is known since 1895 (Olmstead and Hamlin 1900) and the recent increment in reported attacks on concrete elements by acidic media could be attributed to the rising origins of acidic media as a result of population development which is accompanied by increased industrialisation and urban activities (Alexander et al. 2013). Acidic attack can originate from industrial operations, natural sources, and anthropogenic activities including agricultural and food production activities. In addition, sulfuric acid media can originate from using pyratic aggregates in backfilling or from using pyratic aggregates in concrete (Amin and Bassuoni 2017). Biogenic sulfuric acid attack (BSA) in wastewater facilities is well-known in Europe, North America, Australia, the Middle East, and South Africa (House and Weiss 2014). By the end of last century, the estimated expenses of repair of public and private sewage systems in Germany was about US$100 billion, with around 40% of the damage originated from BSA (Kaempfer and Berndt 1999). A report in 1991 (U.S. EPA 1991) stated that

the estimated cost for maintenance or replacement of 25 miles of deteriorated concrete sewer pipelines, due to BSA, in Los Angeles County is $130 million. Moreover, the city of London, Ontario, Canada, spent over $1 million for the replacement of a trunk sewer, which experienced severe structural deterioration due to sulfuric acid attack (Hewayde, E. et al. 2007).

In order to have concrete with enhanced durability in aggressive environments, it is essential to synthesize solid data on sources and types of ammonium sulfate and acids, which commonly damage concrete elements, along with the mechanisms of deterioration cementitious matrices under such aggressive media. Hence, the current thesis focuses on the harmful effects of deleterious substances on cementitious composites namely ammonium sulfate and sulfuric acid attacks, as well as introduce innovative surface coatings for effective protection.

1.3. Need for Research

In various codes and guidelines for concrete, no specific stipulations are stated to protect concrete from ammonium sulfate attack without/with cyclic environmental conditions. For example, according to the (American Concrete Institute) ACI 201.2R-16 (2016) and CSA (Canadian Standards Association) CSA A23.1-19/A23.2-19 (CSA 2019), it is required to use proper type of cement and dosage/type of supplementary cementitious materials (SCMs; Type F fly ash, slag, silica fume) with a maximum water-to-binder ratio (*w/b*) of 0.4 for concrete exposed to very severe sodium sulfate attack, but no explicit guidance is given on ammonium sulfate attack. On the other hand, stipulations in European standards (BS EN 206-1 (2013)) for concrete elements under aggressive exposures require to use minimum cement content of 360 kg/m^3 with a maximum *w/b* of 0.45 for the highly severe concentration of ammonium ions.

On the other hand, ACI 201.2R-16 (2016) does not include a clear recommendation to protect concrete from severe acidic attack (pH<3). However, stipulations in CSA A23.1 and BS

EN 206-1 (2013) are similar to those of concrete under ammonium sulfate attack. According to ACI 515.2 (2013), it is recommended to apply surface treatments such as epoxy and vinyl ester to protect concrete from the ammonium sulfate and sulfuric acid attacks, but no explicit guidance on whether these coats are valid with harsh environments.

Several research studies illustrated the potential of using surface treatments to improve the durability of concrete to water, chlorides, sulfates, and a variety of acids. (Pan et al. (2017)) categorized surface treatments of concrete into four sets according to their function: sealers providing a membrane on concrete surface (e.g. epoxy, and vinyl ester), hydrophobic impregnations that underlay concrete pores and expel diffusing solutions (e.g. silane), pore blockers that react with paste and precipitate compounds which fill out concrete pores (e.g. sodium silicate), and multifunctional treatments (e.g. ethyl silicate which acts as a pore blocker and hydrophobic agent). However, few studies demonstrated the efficiency of coatings in protecting concrete from sodium sulfate attack. (Ibrahim et al. 1999) reported that silane with an acrylic topcoat reduced the compressive strength loss of concrete by 80% compared to that of uncoated concrete after being immersed in 3.1% sodium sulfate solution for 330 days. Likewise, (Aguiar et al. 2008) stated that applying epoxy on concrete specimens decreased the mass loss of concrete by around 65% compared to that of uncoated concrete after being exposed to 215 g/l sodium sulfate solution combined with eight cycles of wetting-drying.

Recent research studies assessed the performance of nano-modified surface coatings (blended nanomaterials with polymers) for concrete. For example, (Li et al. 2018) found that adding nano-titania and nano-silica up to a dosage of 4% to epoxy, polyurethane, and chlorinated rubber resins increased the contact angle of the concrete surface with water (wettability) by an average of around 20% and decreased its water absorption by an average of around 16% relative

to that of concrete coated with neat resins. (Woo et al. 2008) illustrated that 5% nano-clay mixed with silane significantly reduced the chloride diffusivity in concrete by 69% compared to that of uncoated concrete. A few research studies showed the positive effect of nano-modified coatings in improving the durability of concrete under sodium sulfate attack. For example, (Scarfato et al. 2012) found that combining 4% nano-clay with polymeric coatings reduced relative mass loss of concrete by around 50% relative to that of concrete specimens treated with neat polymers. However, there is still dearth of information on the performance of concrete superficially treated with plain or nano-modified coatings under other types of sulfate solutions such as ammonium sulfate, hence the motive of the first part of this thesis.

The performance of superficially treated concrete under sulfuric acid exposures was studied by many research studies (Elnaggar et al. 2019; Xu et al. 2018; Esfandi et al. 2004; Vipulanandan and Liu 2002; Fattuhi and Hughes 1983). For example, (Fattuhi and Hughes 1983) stated that applying a water proofer on concrete specimens decreased the weight change by 50% compared to that of uncoated concrete after 172 days of immersion in 1% sulfuric acid solution. (Xu et al. 2018) found that applying silane to mortar specimens reduced the compressive strength loss by an average of 37% relative to that of plain mortar specimens after 30 days of immersion in a sulfuric acid solution (0.05 M). (Vipulanandan and Liu 2002) reported that applying glass-fiber mat-reinforced epoxy on dry concrete specimens reduced the mass change by around 96% relative to that of uncoated specimens after 23 days of exposure to a 3% sulfuric acid solution. In addition, (Almusallam et al. 2003) stated that mortar specimens coated with epoxy and polyurethane were relatively intact (visual rating of 2), while uncoated specimens experienced significant deterioration (visual rating of 5) after 60 days of immersion in 2.5% sulfuric acid solution. (Elnaggar et al. 2019) demonstrated that applying asphaltic/polyurethane coatings on

concrete specimens reduced the compressive strength loss by an average of 38% relative to that of uncoated specimens after 28 days of immersion in 3% sulfuric acid solution.

A few research studies showed the positive effect of nano-modified coatings in improving the durability of concrete under acidic attack. For example, (Huang et al. 2021) indicated that concrete specimens superficially treated with nano-modified acrylic coating (modified with 0.15% graphene oxide nano sheets) experienced no mass loss after 30 days of immersion in organic acids, while uncoated specimens experienced 0.15% mass loss. However, there is still dearth of information on the performance of concrete superficially treated with nano-modified coatings under severe sulfuric acid exposure, hence the motive of the second part of this study.

So far, most studies on nano-modified coatings mainly focused on evaluating the transport and barrier properties of concrete, without considering the effect of severe exposures. Therefore, the objective of this thesis was to assess the efficacy of nano-modified coatings to protect concrete under aggressive ammonium sulfate and sulfuric acid exposures (constant/full immersion, and cyclic environments).

1.4. Objectives

The main objectives of this thesis are to:

- Evaluate the performance, in terms of physical characteristics and microstructural patterns, of two concrete mixtures with *w/b* of 0.4 and 0.6 which were superficially treated with colloidal silica and nano-modified coatings made with silane and vinyl ester combined with Nano-clay (NC) and Nano-calcium carbonate (NCC) under aggressive ammonium sulfate exposures (full immersion and combined exposures).

- Assess the durability, in terms of physical characteristics and microstructural features, of concrete (*w/b* of 0.4 and 0.6) coated with colloidal silica and nano-modified composites made with silane and vinyl ester as base resins and combined with NC and NCC to severe sulfuric acid exposures (full immersion and wetting-drying (W/D) exposures).

1.5. Scope of the Work

To evaluate the durability of concrete to ammonium sulfate and sulfuric acid exposures, this research program was sub-divided into two experimental phases to fulfill the two objectives. In the first phase, acid-sulfate (ammonium sulfate) attack exposure that would precipitate insoluble voluminous reaction products was used. In the second phase, an acidic attack with similar anion (sulfuric acid) that would produce similar reaction outcomes was employed.

Phase I: The testing procedures were designed to have rapid deterioration of concrete specimens by ammonium sulfate simulating a high concentration of sulfate ions in sulfate-rich soil (full immersion exposure) and accompanied by climatic changes in the combined exposure. It is expected that the specimens that have satisfactory performance in the aggravated exposures would be able to survive under milder field circumstances. Concrete specimens (*w/b* of 0.4 and 0.6) coated with colloidal silica and nano-modified composites made with silane and vinyl ester as base resins and combined with NC and NCC (dosages of 0, 2.5, and 5%) were exposed to the severe exposures for 120 days. The performance of these superficially treated specimens was evaluated by physical parameters such as visual assessment, mass and length changes. To examine the deterioration of microstructure in the specimens, thermal, microscopy, and mineralogical analyses were conducted.

Phase II: The chemical test procedure of the sulfuric acid exposure was designed to observe rapid degradation in the specimens by a highly concentrated sulfuric acid solution (full immersion exposure) and combined with cyclic environmental conditions in the W/D exposure. Specimens from two concrete mixtures with a *w/b* of 0.4 and 0.6 and superficially treated with colloidal silica and nano-modified coatings made with silane and vinyl ester combined with NC and NCC at dosages of 0, 2.5, and 5 were subjected to these aggravated exposures for 10 weeks. The deterioration of these specimens was evaluated by visual assessment and mass change. To distinguish the mechanisms of deterioration, the alteration of microstructure in the damaged specimens was studied by thermal, microscopy, and mineralogical analyses.

1.6. Thesis structure

This thesis is divided into six chapters:

Chapter one includes introduction, overview of sulfate-acid attack, need for research, research objectives and scope of the work.

Chapter two contains a literature review of ammonium sulfate and acidic attacks on concrete. This includes classification of attacks, damage mechanisms and manifestations, standard and non-standard testing procedures, durability performance of various surface treatments, and codes/guidelines stipulations related to these exposures.

Chapter three presents the experimental program, materials and mixtures used in this research program. It also demonstrates exposure regimes for sulfate and sulfuric acid experiments, testing procedures for physical characteristics, thermal, microstructural, and mineralogical analyses.

Chapter four illustrates results and discussion for the ammonium sulfate exposures including mechanisms of damage and effects of various nano-modified surface treatments on concrete

durability against severe ammonium sulfate attack. It also gives insights on possible refinements in the existing codes and guidelines stipulations for such exposures.

Chapter five demonstrates test results and discussion of sulfuric acid exposures. In addition, it explains the performance of concrete superficially treated with nano-modified composites under aggravated acidic exposures with the mechanisms of deterioration, which covers the research gaps in the literature.

Chapter six includes a summary of the thesis work, conclusions based on the test outcomes and insights for future research.

2. Literature Review

This chapter presents an overview of the literature on aggressive attacks (ammonium sulfate and sulfuric acid exposures) on concrete. The effect of several surface treatments on the durability of cementitious materials under these exposures is also discussed in this chapter.

2.1. Mechanisms and Features of Ammonium Sulfate Attack

Concrete foundations, abutments, flatwork, and underground tanks in agricultural and mining zones are susceptible to serious attack by ammonium sulfate. In addition, it was reported that concrete elements in facilities (e.g. flatwork and storage silos) producing ammonium-based fertilizers (ammonium sulfate) are vulnerable to aggressive chemical deterioration (Amin and Bassuoni 2018; Alexander et al. 2013; Akman and Guner 1984). Despite the deleterious effects of ammonium sulfate on several structures, only few research studies evaluated the performance of cement-based materials under ammonium sulfate attack (around 10 research studies over the last two decades) (Martins et al. 2021).

Ammonium sulfate attack on cement-based materials is known as the most aggressive sulfate deterioration driven by acid-sulfate reactions resulting in expansion, cracking, strength loss, and transformation of cementitious matrix into a softened mass (Alexander et al. 2013; Bassuoni and Nehdi 2012; Mbessa and Pe´ra 2001). The combined effect of ammonium and sulfate ions on concrete elements is so aggressive that even when there is a group of different deleterious substances ($(NH_4)_2SO_4$, Na_2SO_4, $MgSO_4$, NaCl, KH_2PO_4) acting together, the ammonium sulfate predominates the effect of other substances (Girardi and Maggio 2011; Mbessa and Pe´ra 2001; Miletić et al. 1998). The type of associated cation significantly affects the mechanism of concrete deterioration under sulfate attack (Miletić et al. 1998). For example, in the case of

ammonium sulfate attack, because of the acidic effect of ammonium ions (NH_4^+), the deterioration process is aggravated (Eqs. 2.1-2.3) (Mahmud Amin 2017), by leaching of portlandite and subsequently decomposing the C-S-H. Generally, ammonium sulfate reacts with calcium hydroxide (CH) in the hydrated paste of concrete forming gypsum, resulting in a decrease in pH and increase in concrete's surface porosity (Rendell and Jauberthie 1999). Posterior or prior to the complete consumption of CH, calcium silicate hydrate (C-S-H) declassifies as a result of the reduction of pH in the pore structure of concrete and/or direct attack from ammonium sulfate. The decalcification of C-S-H starts with a decrease in the calcium-to-silicate ratio (*C/S*) with a progressive loss of cohesion, adhesion, and eventually its disintegration (Marchand et al. 2001). The ammonium sulfate also interacts with the cementitious matrix in the interfacial transition zone (ITZ) resulting in aggregate debonding as a result of formation of gypsum and/or ettringite in ITZ.

$$NH_4^+ \leftrightarrow NH_3 + H^+ \quad \text{(Eq. 2. 1)}$$

$$Ca(OH)_2 + (NH_4)_2\,SO_4 \rightarrow CaSO_4\,.2\,H_2O + 2NH_3 \quad \text{(Eq. 2. 2)}$$

$$xCa.SiO_2.aq + x(NH_4)_2SO_4 + xH_2O \rightarrow SiO_2.aq + xCaSO_4.\,2H_2O + 2xNH_3 \quad \text{(Eq. 2. 3)}$$

Along with the precipitation of gypsum and ettringite, there is an intense dissolution of C-S-H with a decline in the calcium-to-silicate ratio (*C/S*) which eventually transforms into hydrous silica (Bassuoni and Nehdi 2012). The deterioration of concrete is not always caused by precipitation of voluminous ettringite. In alite pastes with total absence of C_3A, ammonium sulfate induced remarkable expansion of 1.28% in 60 days, which was attributed to the exaggerated precipitation of gypsum (Tian and Cohen 2000).

Ammonium sulfate attack on cementitious materials is also accompanied by the emission of gaseous ammonia; however, the effect of gaseous ammonia in the deterioration process is debatable. (Torrenti et al. 2008) disregarded the effect of the released gaseous ammonia on the deterioration of concrete, while (Escadeillas and Hornain 2008) indicated that gaseous ammonia decreases the basicity of the cementitious matrix and prohibits the reaction from attaining equilibrium. Another research study by (Jauberthie and Rendell 2003) discovered that when portland cement mortars were washed after being immersed in ammonium sulfate, rapid cracking occurred as a result of surface shrinkage and probably the emission of ammonium gas from the cementitious matrix.

2.2. Mechanisms and Features of Sulfuric Acid Attack

In general, excessive precipitation of gypsum on (or in) cement-based materials in contact with sulfuric acid medium can be considered as a noticeable damage manifestation of sulfuric acid $H_2(SO_4)$ attack. Based on the source of the acidic media, sulfuric acid aggression on the cement-based materials can be categorized as microbial/biogenic or chemical attack (De Belie et al. 2004; Monteny et al. 2000, 2001). The biogenic sulfuric acid attack (BSA) requires the coexistence of moisture, H_2S, and acidophilic microorganisms to create sulfuric acid solution (House and Weiss 2014). It was found that five kinds of acidophilic microorganisms (*Thiobacillus*) could affect the BSA on concrete elements in wastewater facilities: *T. thiooxidans, T. thioparus, T. neapolitanus, T. novellus, and T. intermedius* (Islander et al. 1991). On the other hand, the chemical sulfuric acid attack can initiate from acidic rains in industrial zones, incidental spillage of the sulfuric acid, or chemical interactions between the concrete constituents. The provenance of sulfuric acid can also be known as ‘internal’ or ‘external’, with various signs of deterioration. (Alexander and Fourie 2011) conducted a field study on sewer

pipelines (external sulfuric acid attack) in South Africa, they described the damage manifestations due to the BSA as a wet eroded concrete surface with white gluey reaction products (calcium sulfate salts) with corrosion blisters and debris on the surface. On the other hand, petrographic analysis conducted by (Tagnit-hamou et al. 2005), demonstrated direct relation between damage manifestations (cracking) of foundations of numerous houses in Canada only after two years of construction and internal sulfuric acid attack originated due to using aggregates containing pyrrhotite phases in concrete. The severity of deterioration caused by internal sulfuric acid attack is noteworthy and was also addressed in other research studies (Rodrigues et al. 2012).

The well-known reported issue of external sulfuric acid attack on concrete is in sewage pipelines (e.g. Wang et al. 2022; Wu et al. 2020; Yuan et al. 2015; O'Connell et al. 2010; Islander et al. 1991; Parker 1951), which belongs to the BSA category. External sulfuric acid attack can also initiate from backfill with pyrrhotite or pyritic-bearing aggregates (Tagnit-hamou et al. 2005; Hobbs and Taylor 2000) while internal attack occurs when using such aggregates as concrete constituent (Rodrigues et al. 2012; Tagnit-hamou et al. 2005). In the external sulfuric acid attack on cement-based materials, acidic solution can infiltrate into pores of the cement paste by diffusion and/or capillary suction due to the pH difference in the pore structure between the front surface and inner core of concrete. In the internal sulfuric acid attack on cementitious matrices, oxidation of pyrrhotite or pyratic-bearing aggregates in conjunction with water formulates sulfuric acid (e.g. Eq. 2.4) (Mahmud Amin 2017). The produced sulfuric acid interacts with the calcium-bearing compounds (foremost portlandite and C-S-H, with lack of portlandite) in hydrated cementitious matrix to form gypsum (Eq. 2.5) (Mahmud Amin 2017) and probably ettringite, far from the reaction domain (Eq. 2.6) (Mahmud Amin 2017). If

carbonates are existing, thaumasite precipitation is also possible (Eq. 2.7) (Mahmud Amin 2017). Thus, the damage manifestations of cement-based materials, in the external sulfuric acid attack, are identified by softening, cracking, and expansion (Rodrigues et al. 2012; Tagnit-hamou et al. 2005; Monteny et al. 2000). These reaction products are similar to that of ammonium sulfate attack as previously discussed; however, the damage mechanisms and manifestations of H_2SO_4 and $(NH_4)_2SO_4$ are different.

$$FeS_2+15/4\ O_2+5/2\ H_2O \rightarrow FeOOH+2H_2SO_4 \quad \text{(Eq. 2. 4)}$$

$$H_2SO_4+Ca\ (OH)_2 \rightarrow CaSO_4.2H_2O \quad \text{(Eq. 2. 5)}$$

$$3CaO.Al_2O_3+3CaSO_4.2H_2O+26H_2O \rightarrow 3CaO.Al_2O_3.3CaSO_4.32H_2O \quad \text{(Eq. 2.6)}$$

$$SO_4^{2-} + 3Ca^{2+} + CO_3^{2-} + SiO_3^{2-} +15H_2O \rightarrow 3CaO.SiO_2.CO_2.SO_3.15H_2O \quad \text{(Eq. 2. 7)}$$

Regardless of the origin of attack, calcium ions are released (firstly from portlandite and then from C-S-H) which may precipitate as insoluble (water solubility of 0.241 ($g/100cm^3$) at 0°C) salts (e.g. gypsum) (Gutberlet et al. 2015). This softening procedure could be combined with expansion, based on the precipitation of excessive amounts of gypsum (Israel et al. 1997; Torii and Kawamura 1994; Attiogbe and Rizkalla 1988) or ‘ettringite’ precipitating away from the acidic zone (Tagnit-hamou et al. 2005; Monteny et al. 2000).

The durability of concrete to sulfuric acid attack is a function of the characteristics of the cement and the pH level of the acidic media (H.W. Dorner 2000). Therefore, the deterioration rate and mechanism of damage are influenced by the acidic concentration along with amount and composition of the hydration products exposed to the acidic medium. The hydration products do not interact with the acidic environment simultaneously. The progress of acidic attack on the

cementitious matrix depends on the stability of the hydrated compounds and reaction products, which is based on the pH level of the attacking environment. There is still debate on reaction products synthesis, quantity, and specific effects on the cement matrix (O'Connell et al. 2010). Based on the available literature, the stability of main phases in the hydrated cementitious matrix and predicted reaction products from sulfuric acid aggression at different levels of pH are illustrated in Table 2.1. From this table, it can be inferred that the damage patterns of acidic aggression may vary depending on the severity of attacking media.

Table 2. 1: Stability of cement paste compounds and reaction products under sulfuric acid attack (Mahmud Amin 2017; Alexander et al. 2013; Gaze and Crammond 2000; Dorner 2000; Dorner 2002; Hobbs and Taylor 2000; Pavlík 1994a; b; Mori et al. 1992)

Unreacted compounds in hardened cementitious matrix	pH level	Stable reaction products
C-S-H*, portlandite, ettringite, aluminate or ferrite hydrates	12.6- 14.0	Gypsum, ettringite, thaumasite, calcite, aluminium, and ferric (hydro) oxides
C-S-H*, ettringite, aluminate or ferrite hydrates	10.5-12.45	Gypsum, ettringite (at core), thaumasite, calcite, aluminium, and ferric (hydro) oxides
Aluminate or ferrite hydrates	6.0-10.5	Gypsum, ettringite (at core), thaumasite, calcite, hydrous silica gel**, aluminium, and ferric (hydro) oxides
Aluminate or ferrite hydrates	5.0-6.0	Gypsum, ettringite (at core), calcite, hydrous silica gel, aluminium, and ferric (hydro) oxides
Aluminate or ferrite hydrates	3.0-5.0	Gypsum, ettringite (will be an incidental feature), hydrous silica gel, aluminium, and ferric (hydro) oxides
Ferrite hydrates	1.5-3.0	Gypsum, hydrous silica gel, and ferric (hydro) oxides
N/A	0.0-1.5	Gypsum and hydrous silica gel and incidental ferric oxides.

* *The C-S-H is not the secondary compound generated from pozzolanic reactions*

** *Hydrous silica gel is formed when C-S-H participates in interaction*

Based on the available literature, the authors deduce that the damage manifestations and mechanisms of different aggressive attacks are distinguishing (e.g. ammonium sulfate attack and sulfuric acid attack). A generic discrimination between some aggressive attacks on concrete is illustrated in **Fig 2.1**.

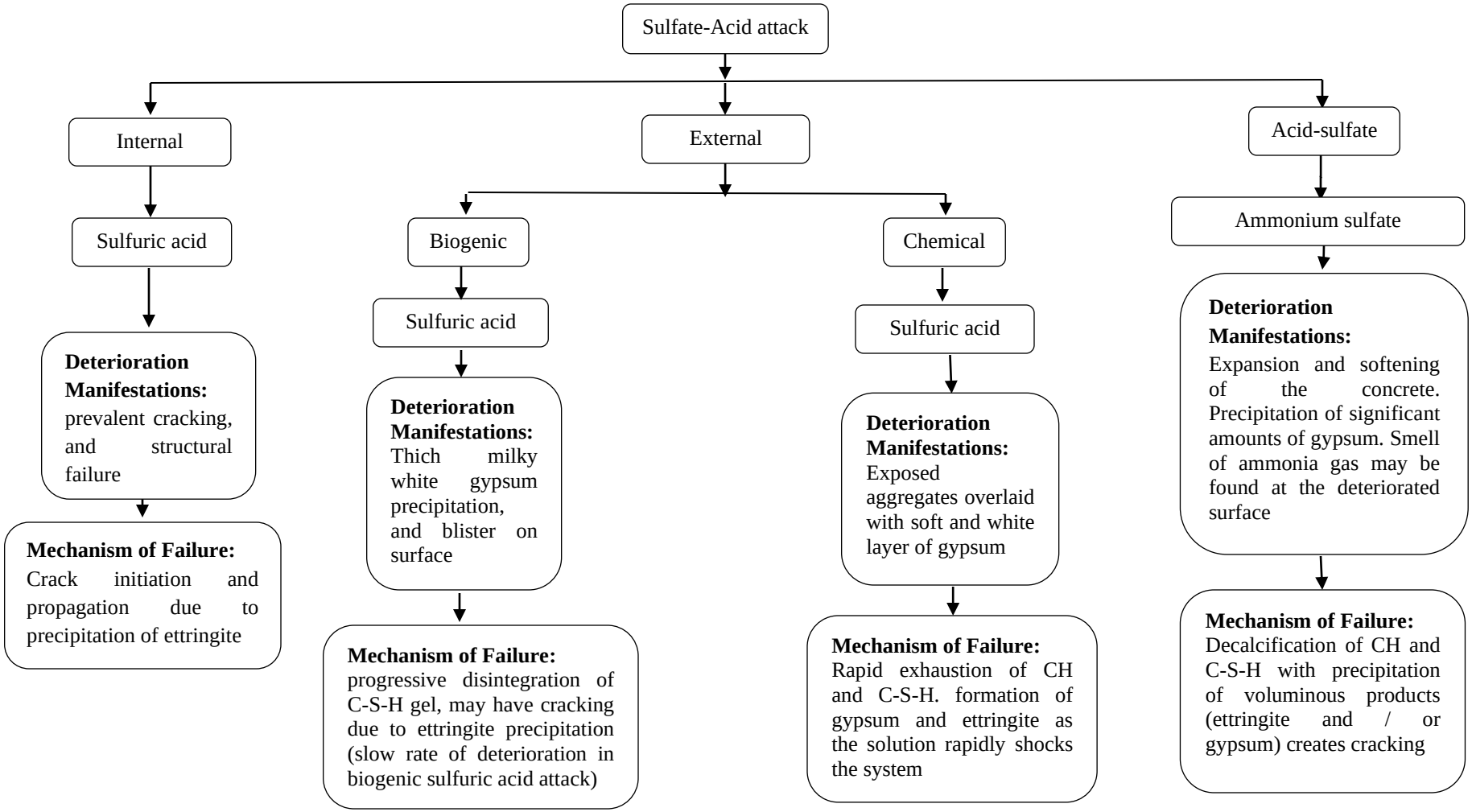

Figure 2. 1: Summary of sulfate-acid attack: manifestations of damage and failure mechanisms.

2.3. Testing Procedures

2.3.1. Standard Testing Procedures

Up to date, there are a few standard tests that evaluate the performance of cement-based materials under aggressive ammonium sulfate and acidic attack, which represent the scope of this study. For example, ASTM C1012 (2018) assesses the deterioration of mortar prisms under sulfate exposure by measuring expansion of the prisms during the exposure. The test is conducted on mortar prisms (25 x 25 x 285 mm), which are immersed in 5% (50 g/l) sodium sulfate solution [without controlling the pH level] at 23°C, and the measurements of expansion are routinely recorded for 12 or 18 months. This test does not represent a standard procedure for evaluating the deterioration of concrete by either ammonium sulfate or sulfuric acid attacks because of the mechanisms involved (as discussed in the aforementioned sections). Acid-insolubility test SANS 6242 (2002) is a standard test in South Africa, which assesses the convenience of concrete mixtures for sewage networks. This test is used to detect the gross acid-insoluble remnants of concrete mixtures by assimilation. However, (Alexander and Fourie 2011) stated that this test does not give information on possible reactions of various binders nor the dissolution kinetics. ASTM C267 (2020) provides general guidelines for evaluating the chemical resistance of mortars and polymer concretes by immersing the specimens in chemical solutions with appropriate concentrations and temperatures to stimulate the service conditions. The changes in mass and compressive strength are recorded accurately during the exposure duration (84 days). On the other hand, ASTM C1898 (2020) evaluates the chemical resistance of concrete specimens to acidic attack. This test is conducted on concrete prisms (50 x 50 x 200 mm), which are soaked in a sulfuric acid solution with pH of 0.5 and 2 [with controlling the pH level by renewing the solution every 7 days] at 23°C. The changes in mass and flexural strength are

recorded routinely during the exposure until the end of exposure after 84 days. EN 13529 (CEN 2003) tests the performance of surface coatings for concrete specimens (750 x 400 x 50 mm) under chemical attacks. The coated concrete specimens are exposed to a localized sulfuric acid solution with pH of -0.19 (the tested area is a circle with a diameter of 100 mm with a solution height of 10 mm). The acidic solution was under pressure during the 28 days of testing. The performance of surface treatments is assessed by visual ratings according to ISO 1990, ISO 2003b, ISO 2003c and ISO 2003d by the end of exposure. Other standard tests such as ISO 7150-1& 2 (water quality-determination of ammonium: Manual spectrometric procedure and automated spectrometric procedure) and German standard DIN 4030-2 (assesses the soil acidity).

Apart from the aforementioned testing procedures, there are limited standard tests to determine the efficacy of nano-modified surface treatments to protect concrete under aggressive ammonium sulfate and sulfuric acid exposures (full immersion, and cyclic environments), which represents the scope of this study.

2.3.2. Non-Standard Testing Procedures

There is lack of standard testing procedures to assess the durability of concrete under ammonium sulfate exposures. The majority of the test studies have adopted simple methods such as soaking the tested specimens in ammonium sulfate solution in the laboratory rather than taking it out to a real field exposure. The current available research studies vary from each other in terms of mixture designs, dimensions of samples, concentration of solution, and duration of exposure. Most of the research studies (Martins et al. 2021; Amin and Bassuoni 2018; Wang and Pan 2017; Bassuoni and Nehdi 2012; Mbessa and Pe´ra 2001; Miletic´ et. al. 1998; Mehta 1985) were conducted on different cement-based materials. It should be demonstrated that research conducted on mortar or paste cannot always stimulate concrete (Cohen and Mather 1991). The

exposure durations in literature varied from 182 days (Mehta 1985) to 378 days (Bassuoni and Nehdi 2012). The periods are longer when lower concentration of ammonium sulfate solutions is used. The sample dimensions also vary and range from standard size (50 x 50 x 285 mm or 75 x 75 x 285 mm) cylinders (Amin and Bassuoni 2018; Bassuoni and Nehdi 2012) to customized sample sizes (Mehta 1985). Concentrations of the ammonium sulfate solutions also varied from 5% (Amin and Bassuoni 2018) to 20% (Mbessa and Pe´ra 2001).

The shortage in standardized test procedures to evaluate the acidic resistance of concrete led research studies into different directions. For instance, a test method was conducted by Pavlík (1994a, b) on paste specimens (d= 45 mm, h = 75 mm) that were prepared into glass tubes with one plane side opened to allow for the axial attack. The specimens were suspended in the aggressive environments, opened side downwards. Another test was carried out by (Mori et al. 1992). In this study, the biogenic sulfuric acid attack was stimulated and conducted laboratory scale testing in a stimulation chamber on mortar specimens (40 × 40 × 160 mm), as well as in a plant consisting of a pipe with a length of 20 m and a diameter of 150 mm. In another study, (Vipulanandan and Liu 2002) tested the performance of concrete cylinders (76 × 152 mm) coated with glass-fiber mat epoxy by immersing half of the specimens in 3% sulfuric acid solution. This study also included testing large scale pipes with an inner coated diameter of 900 mm under hydrostatic pressure. (Padilla et al. 2010) vertically suspended concrete specimens (50 x 50 x 20mm) from commercially produced sewer pipes in reactors with 600 ml of wastewater with active microorganisms at 25^{o}c for 227 days. (Leemann et al. 2010a) exposed concrete cubes (200 × 200 × 200 mm) into the environment of wastewater plants. The pH values were kept constant at 7 by adding alkaline solutions, this value is required to have effective nitrification by enclosing the stability of the microorganisms. The specimens were soaked in an aerated

nitrification basin after reaching an age of 90 days and suspended (1.2m above the floor) at a depth of 5.0m. After two years, the cubes were studied in the laboratory. (Merachtsaki et al. 2021) evaluated the performance of concrete specimens (50 x 50x 20 mm) coated with slurries with magnesium hydroxide micro particles at dosages of 0, 20, 40, and 60% under sulfuric acid exposure. The coated specimens were sprayed by a 0.2 M sulfuric acid solution for 4 days in a controlled chamber. Furthermore, (Merachtsaki et al. 2020) assessed the durability of concrete specimens (50 x 50x 20 mm) coated with slurries containing magnesium hydroxide micro particles at dosages of 0.1, 0.4, and 1% to sulfuric acid attack. The coated concrete samples were immersed in a 0.2 M sulfuric acid solution for one month with circulation of the solution using a peristaltic pump, applying a flow rate, with a horizontal velocity of 0.05 m/s.

Although on-field exposures provide more realistic results, majority of the studies used simple methods to test specimens with acidic solutions inside the laboratory. The available studies differ from each other in terms of surface coatings, mixture designs, dimensions of specimens, solution concentration, type of exposure, and exposure duration. Among the conducted research studies to date, some (Özalp et al. 2023; Merachtsaki et al. 2021; Dashti and Nematzadeh 2020; Mahmoud and Bassuoni 2019; Amin and Bassuoni 2017; Fan and Luan 2013; Leemann et al. 2010a; Bassuoni and Nehdi 2007; Ghrici et al. 2007; Gutierrez-Padilla 2007; De Belie et al. 2004; Vincke et al. 2002; Gu et al. 1998) have tested concrete specimens while others (Chintalapudi and Pannem 2022; Muthu et al. 2021; Khan et al. 2019; Siad et al. 2015; Chatveera and Lertwattanaruk 2014; Soleimani et al. 2013; Donatello et al. 2013; Makhloufi et al. 2012; Urkel et al. 2007; Okochi et al. 2000; Pavlík 2000; Torii and Kawamura 1994; De Ceukelaire 1992; Chandra 1988) conducted tests on either paste or mortars. It should be considered that tests carried out on mortar or paste samples cannot always represent concrete

performance (Cohen and Mather 1991). The exposure durations in literature varied from 14 days (Muthu et al. 2021) to two years (Leemann et al. 2010a,b) if not more. The duration is significantly long, especially with lower concentrations of acidic solutions. The sample dimensions ranged from standard size (50mm x 50mm x 285mm or 75mm x 150mm or 100mm x 200mm) (Amin and Bassuoni 2017; Aydın et al. 2007; Bassuoni and Nehdi 2007; Hewayde et al. 2007) to customized sample sizes and shapes (Muthu et al. 2021; Dashti and Nematzadeh 2020; Chatveera and Lertwattanaruk 2014; Ariffin et al. 2013; Ghrici et al. 2007; Allahverdi 2005; De Belie et al. 2004). Concentrations of the acidic solutions varied in the existing literature from 10% (Mahmoud and Bassuoni 2019) to 1% (Chang et al. 2005; Attiogbe and Rizkalla 1988), while some (De Belie et al. 2004) used concentrations as low as 0.5%. Similarly, the pH level of the solutions varied among the studies. Recently a drive (Jiang et al. 2023; Ibrahim et al. 2021; Alani and Faramarzi 2014; Beddoe and Dorner 2005) to mathematical modeling has been noticed, as a tool for predicting durability and reducing the time factor without disruption of the deterioration mechanisms (Glasser et al. 2008). However, some variations between the rate of damage of cement paste and cement-matrix composites are detected and thus the mathematical models found to stimulate the degree of deterioration of the paste as a function of time are not recommended to be used to detect the extent of deterioration of mortar or concrete (Pavlík and Unčík 1997).

The scale of the testing process can significantly affect the test results, as it may affect parameters such as the rate of renewal of aggressive solutions, use of real-life or stimulated aggressive solutions, specimen surface area/liquid ratio, presence of an interfacial transition zone (ITZ) (concrete vs. paste specimens), choice of a close-to-reality or aggravated test, etc. (Alexander et al. 2013). Clearly, there is a need for a standard testing procedure for evaluating

the ammonium sulfate and sulfuric acid resistance of superficially treated concrete which specifies the attacking solution, the concentration and pH level of the solution, temperature, rate of solution renewal, existence and type of mechanical actions, alternate wetting-drying cycles if any, alternate freezing-thawing cycles if any, pressure, sample dimensions, shape and type, etc. There is also a need for future research about specimen preparation methods before applying surface treatments and the concrete age at the time of testing. The selection of the reference specimen should be done wisely, as test results are usually in comparison with a reference specimen (Alexander et al. 2013). Up to date, the available literature is scattered. It is thus urgent to develop a unified testing procedure addressing these issues soon so that results of different concretes and coatings can be judged based on a single platform.

2.4. Code provisions

Up to date, general requirements are found in the latest version of the American Concrete Institute (ACI) 201.2R-16 (2016): Guide to Durable Concrete on ammonium sulfate and acidic attacks. There are no specific stipulations on protecting concrete from ammonium sulfate attack. The only clear requirement found in the American stipulations is using silica fume to increase the durability of concrete to acids accompanied with suitable protective-barrier systems or coating ACI 515.2R (2013). In ACI 201.2R, it is stated that “no hydraulic-cement concrete, regardless of its composition, will long withstand water of high acid concentration (pH of 3 or lower)”. According to Table 6.2 in the same document, it is recommended to increase the binder content for better durability against acids; however, the exact content of the cementitious binders is not specified. This document overlooks the mechanism of damage of sulfate-acid attack caused by ammonium sulfate exposure and oversimplifies the attack by different types of acids. Overall, this document provides general recommendations for enhancing the durability of

concrete to sodium sulfate attack and does not state clear requirements to protect concrete from harsh sulfuric acid attack (pH<3).

CSA A23.1-19 (CSA 2019) requires to use proper type of cement (e.g., Sulfate Resisting) and dosage/type of supplementary cementitious materials (SCMs; Type F fly ash, slag, silica fume) with a maximum water-to-binder ratio (*w/b*) of 0.40 for concrete exposed to very severe sulfate attack (related to sodium sulfate) with a minimum compressive strength of 35 MPa at 56 days, air content of 4-9% based on coarse aggregate size, and a certain curing type (based on Table 19 and Table 2), but no explicit guidance is given on ammonium sulfate attack.

Canadian standard CSA A23.1-19/A23.2-19 (CSA 2019), indicates that sulfate-resistant cement, like other portland or blended cements, are not durable to most acids or other highly aggressive substances. A good guidance and explanation for internal sulfuric acid attack by oxidation of aggregates containing iron sulfide phases can also be found in CSA A23.1-19/A23.2-19 (CSA 2019). The Canadian code recommends that when pyrrhotite (a metastable form of iron sulphide FeS) is detected in the aggregate, a maximum total sulphur content of 0.1% (as S) in both aggregate and filler is required. It also requires not to use of the aggregates containing pyrrhotite phase. The CSA A23.1-19/A23.2-19 (CSA 2019) detects that dolostones of Lake Ontario area and the St. Lawrence Lowlands (Quebec) contain remarkable amounts of cubic pyrite. The detection of other forms of sulphides, such as marcasite and pyrite, in the aggregate, has also been considered as a problem in the raw materials due to the sulfate release that initiates sulfate attack on the cement paste. The code states that if the total content of sulphide sulphur is less than 0.1%, the aggregate can be used without further tests. Otherwise, the origin of the sulphide mineral phases should be detected. French standard, NF P18-301, put a limit on total sulphur content to 1% as SO_3 (0.4% as S). This limit was increased in the European

standard as NF EN 12 620 stipulated that the total sulfur content (S) of the fillers and aggregates, shall not exceed; (a) 1% S by mass for aggregates other than air-cooled blast-furnace slag; and (b) 2% S by mass for air-cooled blast-furnace slag.

The CSA A23.1-19 (CSA 2019) also categorizes the sewer pipe (the 'crown'; most susceptible part to biogenic sulfuric acid attack) as A-XL and limits the requirements for concrete as maximum *w/b* of 0.4, a minimum compressive strength of 50 MPa after 56 days, air content of 4-9% based on coarse aggregate size, a certain curing type (based on Table 19 and Table 2), and a chloride ion penetrability of < 1000 coulombs within 91 days. Thus, both the ACI 201.2R-16 (2016) and CSA A23.1-19/A23.2-19 (CSA 2019) recommend reduced physical penetrability against sulfuric acid attack. Similarly, British standards relate the durability of concretes to chemical attack to a high degree of impermeability. For more than 60 years, British standards for designing ground concrete elements, requires that these elements should be resistant to aggressive attack from commonly found substances, such as sulfates and acids. BRE Special Digest 1 (2005) provides general information on the deterioration of concrete by ammonium sulfate and sulfuric acid attacks but does not provide specific stipulations. The British code specifies the Aggressive Chemical Environment for Concrete (ACEC) classification of sites based on the pH level, type of ground, and water mobility. In section D5.3.2, the code recommends using super sulfated cement (providing a high-quality concrete) and calcium aluminate cement (formation of a resistant surface layer) as they have good sulfate and acidic resistance provided the concrete surface is properly cured. However, the only specific requirement for acidic exposures in this code is a *w/b* ratio of not more than 0.40 and a minimum cement content of 400 kg/m^3. It also requires preventing drying out of the concrete surface during the first day of curing to maintain a protective surface zone and ensure continued

hydration. In a few cases, the BRE Special Digest 1 (2005) also used oversimplification. For example, the code dissociates expansion from acidic attack. It also states that neither thaumasite nor ettringite is stable in acidic solutions which is incomplete information (Table. 2.1 of this document). Other documents such as BS EN 206-1 (2013), in Table 2, state that a level of NH_4 of 15–30 mg/l is classified as slightly aggressive, 30–60 mg/l is considered as moderately aggressive, and greater than 60 mg/l as is classified highly aggressive. Another document from BRE (Garvin et al. 2000) states that excavation and removal of soil contaminated with ammonium (where concrete will be placed) is not generally essential rather, specifying a high-quality concrete with a low penetrability to resist infiltration of ammonium ions will be satisfactory. An exception is given in a case where there is a possibility of having high ammonium concentrations. In such cases, coatings were required for additional protection. Various options for protective coating against ammonium sulfate and sulfuric acid attacks are discussed in ACI 515.2R (2013) and BS EN 1504-2 (BS EN 1504-2 2004). it is recommended to apply surface treatments such as epoxy and polyurethane to protect concrete from such environments.

2.5. Role of Surface treatments, and Nanoparticles in Resisting Sulfate and Acidic Attacks

Treatment by coatings is an effective strategy for protecting the surface of new or existing concrete structures, as well as repairing concrete exposed to aggressive environments to restore its performance and prolong its service life. (Pan et al. 2017) classified surface treatments of concrete into four classes: hydrophobic agents resisting diffusing solutions (e.g. silane), sealers providing a membrane on concrete surface (e.g. epoxy, and vinyl ester), pore blockers that react with the cement paste precipitating compounds which fill the pores (e.g. sodium silicate), and multifunctional coatings (e.g. ethyl silicate which acts as a hydrophobic agent and pore blocker).

Many research studies have shown the potential of coatings to significantly improve the barrier properties of concrete surface to intrusive media (Pan et al. 2017; Jia et al. 2016; Liu and Hansen 2016; Pigino et al. 2012; Aguiar and Junior 2013). (Almusallam et al. 2003) demonstrated the ability of surface treatments (e.g., epoxy, polyurethane, and acrylic coatings) to decrease chloride penetrability of coated concrete specimens compared to uncoated concrete. Chloride ions infiltration into the concrete coated with epoxy, polyurethane, and acrylic coatings was approximately one-tenth that of the uncoated concrete.

Few research studies illustrated the role of coatings in protecting concrete elements from sodium sulfate attack. (Ibrahim et al. 1999) indicated that silane with an acrylic topcoat significantly reduced the reduction in compressive strength of concrete by 80% relative to that of uncoated concrete after being soaked in a 3.1% sodium sulfate solution for 11 months. In addition, (Aguiar et al. 2008) showed that applying epoxy on concrete specimens remarkably reduced mass loss of concrete by an average of 65% relative to that of uncoated concrete after being exposed to eight cycles of wetting-drying in a sodium sulfate solution (215 g/l).

Recent studies evaluated the performance of concrete superficially treated with nano-modified surface treatments (blended nanomaterials with polymers). (Li et al. 2018) stated that adding nano-silica and nano-titania up to a dosage of 4% to polyurethane, epoxy, and chlorinated rubber decreased the water absorption of concrete by an average of 16% relative to that of concrete coated with neat resins and increased the contact angle of concrete surface with water (wettability) by an average of 20%. (Scarfato et al. 2012) incorporated nano-montmorillonite clay at dosages of 2, 4, and 6% to two polymeric resins: Fluoline CP (a mixture of acrylic and vinylidene fluoride polymers) and Antipluviol S (a solution based on siloxane). The nano-modified composites with 4% nano-clay reduced the capillary absorption of concrete by an

average of 63% compared to that of concrete coated with neat resins. Moreover, (Woo et al. 2008) indicated that applying silane with a 5% nano-clay significantly decreased the chloride diffusivity of concrete by 69% relative to that of uncoated concrete. Similarly, (Leung et al. 2008) found that adding nano-clay (3%) to epoxy significantly reduced the chloride content in concrete specimens by 96% relative to that of specimens coated with neat epoxy after being exposed to spraying by a 5% sodium chloride solution combined with wetting-drying cycles.

A few research studies illustrated the positive impact of nano-modified surface treatments in improving the durability of concrete to sodium sulfate exposure. (Scarfato et al. 2012) stated that adding 4% nano-clay to polymeric coatings remarkably reduced relative mass loss of concrete by an average of 50% compared to that of concrete specimens coated with neat polymers after being exposed to sodium sulfate solution (215 g/l) combined with eight wetting-drying cycles. Moreover, (Hou et al. 2021) showed that applying silane combined with 0.3% graphene oxide nano sheets on concrete specimens reduced the amount of sulfate corrosion of concrete by around 80% compared to that of concrete specimens superficially treated with neat silane after being soaked in 10% sodium sulfate solution for 50 days. However, there is still dearth of information on the performance of concrete superficially treated with plain or nano-modified coatings under other types of sulfate solutions such as ammonium sulfate.

On the other hand, the durability of superficially treated concrete to sulfuric acid exposures was evaluated by several research studies (Elnaggar et al. 2019; Xu et al. 2018; Esfandi et al. 2004; Vipulanandan and Liu 2002; Fattuhi and Hughes 1983). (Fattuhi and Hughes 1983) found that applying water proofer on concrete specimens reduced the changes in weight by 50% relative to that of uncoated concrete after being immersed in a 1% sulfuric acid solution for 172 days. In addition, (Soroushian et al. 2009) demonstrated that adding water-repelling

additives to concrete specimens reduced the thickness loss by up to 50% relative to that of concrete without water-repelling admixtures after 90 days of immersion in a 3% sulfuric acid solution. In another study, (Xu et al. 2018) found that adding silane to mortar specimens decreased the compressive strength loss by an average of 37% relative to that of plain specimens after being soaked in a sulfuric acid solution (0.05 M) for 30 days. (Vipulanandan and Liu 2002) showed that applying glass-fiber mat-reinforced epoxy on concrete specimens significantly reduced the mass change by around 96% compared to that of uncoated concrete after being immersed in a 3% sulfuric acid solution for 23 days. In addition, (Almusallam et al. 2003) illustrated that mortar specimens superficially treated with polyurethane and epoxy were relatively intact (visual rating of 2), while uncoated plain specimens experienced significant damage (visual rating of 5) after being soaked in a 2.5% sulfuric acid solution for 60 days. In another research study, (De Muynck et al. 2009) found that concrete discs coated with epoxy and polyurea experienced negligible loss in thickness, while uncoated specimens lost around 0.8 mm of their initial thickness after 10 wetting-drying cycles in a 0.5% sulfuric acid solution. (Elnaggar et al. 2019) stated that applying asphaltic/polyurethane as a surface treatment on concrete specimens decreased the reduction in compressive strength by an average of 38% compared to that of uncoated concrete after being immersed in a 3% sulfuric acid solution for 28 days. (Merachtsaki et al. 2021) stated that applying a slurry containing 60% of magnesium hydroxide micro particles on concrete specimens reduced the change in hardness by 69% compared to that of uncoated concrete after 4 days of spraying by a sulfuric acid solution (0.2 M). Furthermore, (Özalp et al. 2023) indicated that applying polyurea on concrete reduced the mass loss by 79% compared to that of uncoated concrete after 28 days of immersion in 10% sulfuric acid solution.

A few research studies illustrated the effect of nano-modified surface treatments in enhancing the durability of concrete to acidic attack. For example, (Huang et al. 2021) indicated that concrete specimens superficially treated with nano-modified acrylic coating (modified with 0.15% graphene oxide nano sheets) experienced no mass loss after 30 days of immersion in organic acids, while uncoated specimens experienced 0.15% mass loss. However, there is still dearth of information on the performance of concrete superficially treated with nano-modified coatings under sulfuric acid exposures.

2.6. Closure

Several research studies have been conducted on ammonium sulfate and acidic attack on cement-based materials as discussed in the literature review. Sulfuric acid exposures have gained more attention compared to others (ammonium sulfate) and evolution of code provisions to this concrete durability issue has also been insufficient. Although, currently available research could explain the basic mechanisms of damage involved in these durability issues, many questions regarding the improvement of durability of concrete to ammonium sulfate and sulfuric acid environments still remain debated and unresolved. Without answering these questions, it would be impossible for the codes to put appropriate stipulations for concrete where risk of such attacks is involved. In obscurity of a reliable solution from conventional concrete with or without supplementary cementitious materials (SCMs) to resist such exposures, research is growing towards surface treatments to solve these durability issues. In addition, adding nanoparticles to neat surface treatments has a promising effect to improve the durability of concrete infrastructure. However, research on nano-modified surface treatments is still in its infancy and has mainly focused on the initial barrier properties of concrete. To date, there is dearth of information on the durability of concrete superficially treated with nano-modified coatings,

especially its resistance to ammonium sulfate and sulfuric acid exposures. Hence, this research program mainly aims at enhancing sulfate and acid resistance of concrete by treating concrete elements with nano-modified surface treatments, and thus contributing to updating current code provisions for these durability issues.

3. Experimental Program

This chapter depicts the materials, mixture constituents, aggressive exposures, and experimental procedures in this research project.

3.1. Concrete Mixtures

Two concrete mixtures were prepared representing low-porosity and high-porosity concrete, using general use (GU) cement and fly ash (Type F; FA) complying with CSA A3001 (CSA, 2013). The chemical and physical characteristics of the cement and fly ash are listed in **Table 3.1**. The binder content was kept constant at 400 kg/m^3 (75% GU + 25% fly ash) for both mixtures with two different water-to-binder ratios (*w/b*: 0.40 [low porosity mixture] and 0.60 [high porosity mixture]). These mixes represent a typical binder for new and deteriorated concrete substructures in Manitoba, Canada. For concrete with *w/b* of 0.4, the targeted workability (slump of 75–125 mm) was achieved by using a high-range water reducer (HRWR) based on polycarboxylic acid and complying with ASTM C494 (2017). However, for concrete with 0.6 *w/b*, the HRWA was not used as it was sufficiently flowable. In addition, a fresh air content of 6±1% was accomplished by using an air-entraining agent. A local natural gravel was used as coarse aggregate (maximum size of 9.5 mm), with a specific gravity and absorption of 2.65 and 2%, respectively. The fine aggregate used was well-graded river sand with a specific gravity of absorption, and fineness modulus of 2.53, 1.5% and 2.9, respectively. The proportions of the concrete mixtures and their 56-days compressive strength according to ASTM C39 (2021), are listed in **Table 3.2**. Concrete was mixed in a mechanical mixer to prepare cylinders (100 × 200 mm and 75 × 150 mm) and prisms (50 × 50 × 285 mm), which were demolded after 24 h

and cured in a standard moisture curing room (22±2°C and relative humidity (RH) ≥ 95%) for 56 days according to ASTM C192 (2015).

Table 3. 2: Chemical and physical properties of GU cement and Fly ash

Parameter	GU cement[a]	Fly ash[a]
Chemical analysis		
SiO_2 (%)	19.22	55.20
Al_2O_3 (%)	5.01	23.13
Fe_2O_3 (%)	2.33	3.62
CaO (%)	63.22	10.81
MgO (%)	3.31	1.11
SO_3 (%)	3.01	0.22
$Na_2Oeq.$ (%)	0.12	3.21
Physical properties		
Specific Gravity	3.15	2.12
Fineness (m^2/kg)	390	290

[a] The characteristics of the materials were provided by the manufacturer.

Table 3. 2: Proportions of concrete mixtures per cubic meter

Mix ID	Cement (kg)	Fly ash (kg)	Water (kg)	Coarse aggregate (kg)	Fine aggregate (kg)	HRWR (l)	Compressive strength at 56-days (MPa)
GU-FA0.4	300	100	160	1115	549	0.6	40 [0.9]
GU-FA0.6	300	100	240	975	480	--	25 [1.21]

[a] Values between brackets are the standard deviations for compressive strength results.

3.2. Surface treatments

Commercially available water-based colloidal silica [SiO_2<50%] (denoted as CS) was used as a surface treatment for concrete specimens. The nano silica particles in CS have purity higher than 99%, average specific surface area of 200 m^2/g, density of 2.56 g/cm^3, and an average diameter of 12 nm. In addition, two types of polymeric resins were used as a base resin for nanocomposite coatings: silane (denoted as S), and vinyl ester (denoted as VE). In the first chapter, halloysite nano-clay (denoted as NC) and nano-calcium carbonate (denoted as NCC) were used to formulate the nanocomposite coatings at contents of 2.5% and 5%. These symbols and numbers were used to represent coatings' IDs; for example, silane with 2.5% NC is denoted as SNC2.5%,

while vinyl ester with 5% nano-calcium carbonate is denoted as VENCC5%). The NC has purity higher than 90%, average specific surface area of 64.2 m^2/g, density of 2.53 g/cm^3, and a tube structure with average length, inner, and outer diameters of 2 μm, 20 nm, and 200 nm, respectively. The NCC (98% purity) has particle size of 50 nm, average specific surface area of 60 m^2/g, and density of 2.5 g/cm^3. In the second chapter, the same nanoparticles and nano-modified coatings were used with different symbols. Halloysite nano-clay (denoted as C) and nano-calcium carbonate (denoted as CC) were used to formulate the nanocomposite surface treatments at dosages of 2.5% and 5%. These symbols and numbers were used to represent coatings' IDs; for example, silane with 5% C is denoted as SC5%, while vinyl ester with 2.5% nano-calcium carbonate is denoted as VECC2.5%).

In case of CS, the amorphous silica was already dispersed in the water-based solution plus a dispersing agent by the manufacturer and the ready-to-use product was applied as a surface treatment for concrete specimens. For the silane nano-modified coatings, the nanoparticles (NC and NCC) were mixed with the neat silane using a single spindle mixer (homogenizer) at a speed of 18,000 rpm for six minutes to uniformly disperse the nanoparticles in the base resin to achieve homogenous dispersion without visible agglomerates/lumps. For the vinyl ester resin, after mixing the NC and NCC with the base resin (part A) using a single spindle mixer at a speed of 8,000 rpm for 5 minutes and 13,000 rpm for 2.5 minutes, respectively, the catalyst (part B) was added to the mixture and mixing continued at lower speed (600 rpm) for 1 minute. The procedures selected were based on trial batches to achieve homogenous nanocomposites and avoid reaching high temperatures during mixing (above 40^oC).

After curing period of concrete samples, specimens from each mixture were air dried for 48 hours, and then the surface was prepared by a wire brush and cleaned from debris by a

pressurized air before applying the coatings. For VE/nanocomposites, concrete surface was brushed by three successive layers at a time-interval of 10 minutes, for S/nanocomposites, three layers separated by 30 minutes were applied, while for CS, three layers were sprayed continuously without intervals as recommended by the respective manufacturers of the neat resins. The performance of concrete coated with nano-modified coatings was compared to uncoated specimens and specimens coated with the neat resins.

3.3. Testing procedures

3.3.1. Characterization of nanocomposites and penetrability of concrete

Transmission electron microscopy (TEM) and Environmental scanning electron microscopy (ESEM) were used on ultrathin film samples of nanocomposites to examine the quality of particle dispersion. Moreover, static contact angle measurements were conducted on concrete samples using contact angle goniometer to evaluate the effect of nano-modified coatings on the wettability of concrete surface (Sakr and Bassuoni 2021; Law and Zhao 2016). The threshold wettability angle (Θ) is 90^{o}, while if the value above and below this value, the surface is considered hydrophobic and hydrophilic, respectively. For each coating, five water droplets were placed on separate spots over the surface of coated samples and the average contact angle was determined.

To evaluate the barrier properties of coatings, the rapid chloride penetrability test (RCPT) was conducted on uncoated and coated concrete specimens according to ASTM C1202 (2022). Concrete disks (100 mm diameter and 50 mm thickness) were put between cathodic (3% NaCl solution) and anodic (0.3 N NaOH solution) compartments with applied potential difference of 60V DC for 6 hours. In addition to the passing charges (in coulombs) through the concrete, the penetration depth of the chloride ions into concrete was determined, as this depth correlates well

to the physical characteristics of pore structure of concrete (Bassuoni et al. 2006). Hence, after the RCPT, the specimens were axially split and sprayed with 0.1 M silver nitrate solution, to form a white layer of silver chloride, and then the average penetration depth of the white precipitation was determined by five measurements along the diameter of each half specimen.

3.3.2. Ammonium sulfate exposures

The durability of the coated concrete prisms against ammonium sulfate attack was evaluated by two exposures: a reference exposure following the general guidelines of ASTM C1012 (2018) in terms of continuous immersion, and a combined exposure involving ammonium sulfate and cyclic environments. These exposures were selected to stimulate the aggravated exposure of concrete elements (foundations, slabs, abutments) in agricultural zones comprising ammonium sulfate fertilizers under seasonal climatic changes, or concrete elements in industrial facilities producing ammonium-sulfate salts. The pH of the solution was within the range of 6.0–8.0, which was achieved by changing the ammonium sulfate solution after two months for all exposures.

In the reference exposure, concrete specimens were fully immersed in 10% ammonium sulfate solution for 120 days at room temperature. The solution-to-specimen volume ratio was kept constant at 3.0. In the combined exposure, coated concrete specimens were subjected to concurrent damage from the sulfate solution and cyclic environmental conditions. This combination represents field conditions for concrete elements in ammonium sulfate-rich environments under seasonal climatic changes (consecutive cold winters and hot summers) such as agricultural zones. Coated concrete specimens were initially immersed in 10% ammonium sulfate solution (pH of 6.0–8.0) at a temperature of 21±2°C for 5 days before being exposed to the cyclic environmental conditions. A winter season was simulated by 60 successive freezing–

thawing cycles according to the general procedure of ASTM C 666 (2017), Procedure A: freezing at -18±1°C for 7 hours followed by thawing in 10% ammonium sulfate solution (pH of 6.0–8.0) at 5±1°C for 3.5 hours, 45 minutes to drop the temperature to the minimum freezing temperature, and another 45 minutes to rise the temperature to the maximum thawing temperature. A summer season was simulated by four alternating wetting–drying cycles. Each cycle consisted of 4 days of immersion in 10% ammonium sulfate solution (pH of 6.0–8.0) at a temperature of 20±2°C and 55%±5% RH followed by 3 days of drying at 40±2°C and 35%±5% RH. The combined exposure lasted for 120 days, simulating two winter seasons alternating with two summer seasons.

Before the exposures, the initial mass and length were measured for all concrete specimens. During the exposures, specimens were extracted from the sulfate solution every month and left to dry at laboratory conditions for 30 minutes before visual inspection, recording changes in mass and length with time. The visual assessment was evaluated by visual ratings as listed in **Table 3.3**.

Table 3. 3: Visual rating for deterioration in concrete specimens

Visual Rating	Description
1	Intact specimen
2	Corners or edges damaged
3	Corners and edges deteriorated
4	Corners, edges and some surface deterioration
5	Significant disintegration of the specimens

3.3.3. Sulfuric acid exposures

The durability of the concrete cylinders against sulfuric acid attack was evaluated by two exposures: a reference exposure following the general guidelines of ASTM C1898 (2020) in terms of continuous immersion, and a W/D exposure involving sulfuric acid and cyclic environments. The volume ratio of solution-to-specimen was maintained constant at 2.0. These exposures were selected to evaluate the durability of concrete elements such as foundations (attack from groundwater containing sulfuric acid as a result of oxidization of pyrite used in backfill or as an aggregate in concrete), floors in chemical plants, retaining walls of basements near chemical factories and superstructures (attack from acid rains), which are vulnerable to chemical attack by sulfuric acid. The pH of the solution was within the range of -0.6 to 0.6, which was achieved by changing the sulfuric acid solution after five weeks of both the full immersion and W/D exposures.

In the reference exposure, concrete specimens were fully immersed in 5% (by volume) sulfuric acid solution for 10 weeks at room temperature. In the W/D exposure, concrete specimens were subjected to concurrent damage from the acidic solution and cyclic environmental conditions. This combination represents field conditions for concrete elements exposed to acidic environments under seasonal climatic changes such as septic tanks and sewage pipelines with variable wastewater levels. Concrete specimens were initially immersed in 5% sulfuric acid solution (pH of -0.6 to 0.6) at a temperature of 21±2°C for 4 days before being exposed to the cyclic environmental conditions. The seasonal climatic changes were simulated by ten alternating wetting–drying (W/D) cycles. Each cycle consisted of 4 days of immersion in 5% sulfuric acid solution (pH of -0.6 to 0.6) at 55%±5% RH and a temperature of 20±2°C and followed by 3 days of drying at 35%±5% RH and 40±2°C.

Before both exposures, the initial appearance and mass were detected for all concrete specimens. During the exposures, specimens were extracted from the acidic solution every week and left to dry at laboratory conditions for 30 minutes before visual inspection, recording change of mass with time. The visual assessment was evaluated by visual ratings as listed in **Table 3.3**.

3.3.4. Thermal, microstructural, and mineralogical analyses

To distinguish the implicit mechanisms of deteriorations in both exposures, the deterioration in microstructure of damaged specimens was studied by thermal, microscopy, and mineralogical analyses. To quantify the reaction products in the deteriorated specimens, differential scanning calorimetry (DSC) (**Fig 3.1**) on powder specimens extracted from the surface (0-5 mm from the exposed surface) of some specimens was executed. These powder samples were prepared from extracted fracture pieces of specimens (not including coarse aggregates), which were grinded to fine powder passing from sieve #200 (75 μm). In addition, un-exposed samples after 56 days of curing were tested by the DSC for comparison with the exposed specimens. The powder specimens were heated up to 550°C with a ramp temperature of 10°C/min in the DSC tests. The results from DSC were confirmed by microscopy analysis. Fracture concrete specimens were prepared from the exposed surface (up to 5 mm depth) to be observed by scanning electron microscopy (SEM) (**Fig 3.2**) accompanied with energy-dispersive X-ray analysis (EDX). The specimens were coated with a thin layer of carbon before conducting the analysis to have a conductive surface and to enhance the quality of sample imaging. To supplement the observations from the SEM, the reaction compounds in the deteriorated cementitious matrix were studied by X-ray diffraction (XRD, Cu-Kα) (**Fig 3.3**). Sampling interval of 0.01° 2θ and scan speed of 2°/min were used for all the specimens tested by XRD.

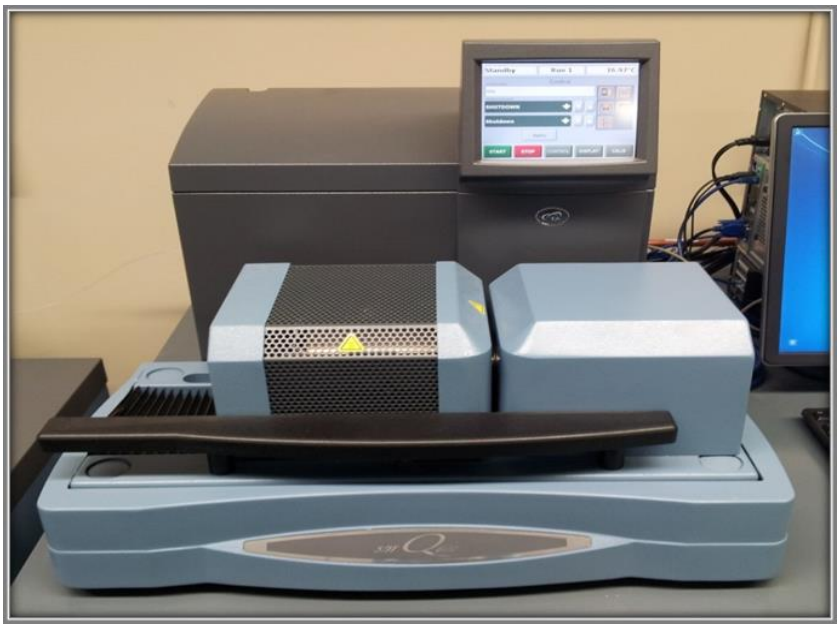

Figure 3. 1: DSC instrument by which the thermal analysis was conducted.

Figure 3. 2: SEM chamber where the fracture specimens were mounted for observation.

Figure 3. 3: XRD instrument by which the mineralogical analysis was conducted.

4. Phase I: Results and Discussion for Ammonium Sulfate Attack

4.1. Results

4.1.1. Dispersion of Nanoparticles in Polymers

Transmission electron microscopy (TEM) images were used to qualitatively assess dispersion of nano-silica in colloidal silica and nano-calcium carbonate and nano-clay in silane, because of the low viscosity of theses resins. Nano-silica particles were homogeneously dispersed in the colloidal silica as shown in **Fig. 4.1(a)**. Nano-calcium carbonate particles were well dispersed in silane as for example depicted in **Fig. 4.1(b)**. Comparatively, nano-clay particles formed an interwoven or a lath-like structure spreading in the silane resin [e.g., **Fig. 4.1(c)**]. For the vinyl ester nanocomposites, the environmental scanning electron microscopy (ESEM) was used to evaluate dispersion of nanoparticles, because of its higher viscosity. **Figure 2** shows ESEM images of the vinyl ester nanocomposites at a loading ratio of 5% by mass. Nano-calcium carbonate patches were less visible in the vinyl ester matrix, likely due to encapsulation in the high viscosity resin, as depicted in **Fig. 4.2(a)**; comparatively, **Fig. 4.2(b)** shows that nano-clay particles, represented by spots, were randomly dispersed in the vinyl ester matrix.

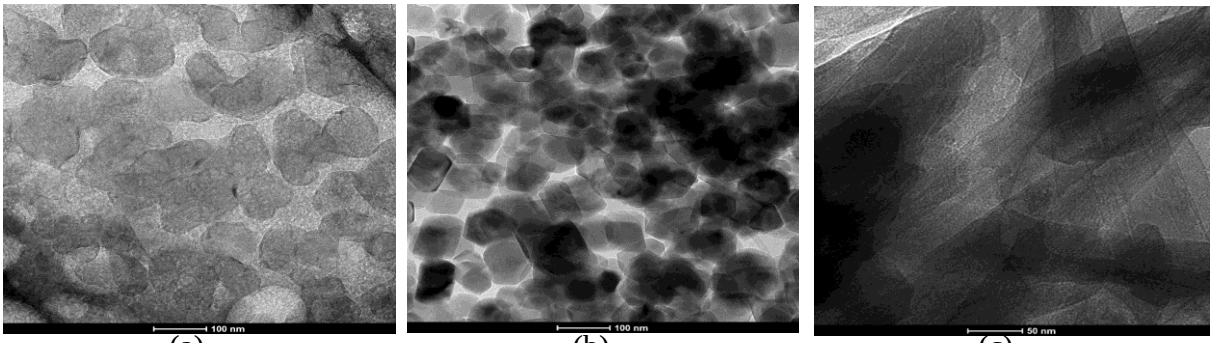

(a) (b) (c)

Figure 4. 1. Exemplar TEM images of: (a) colloidal silica, (b) silane/nano-calcium carbonate at 5% loading ratio, and (c) silane/nano-clay composites at 5% loading ratio.

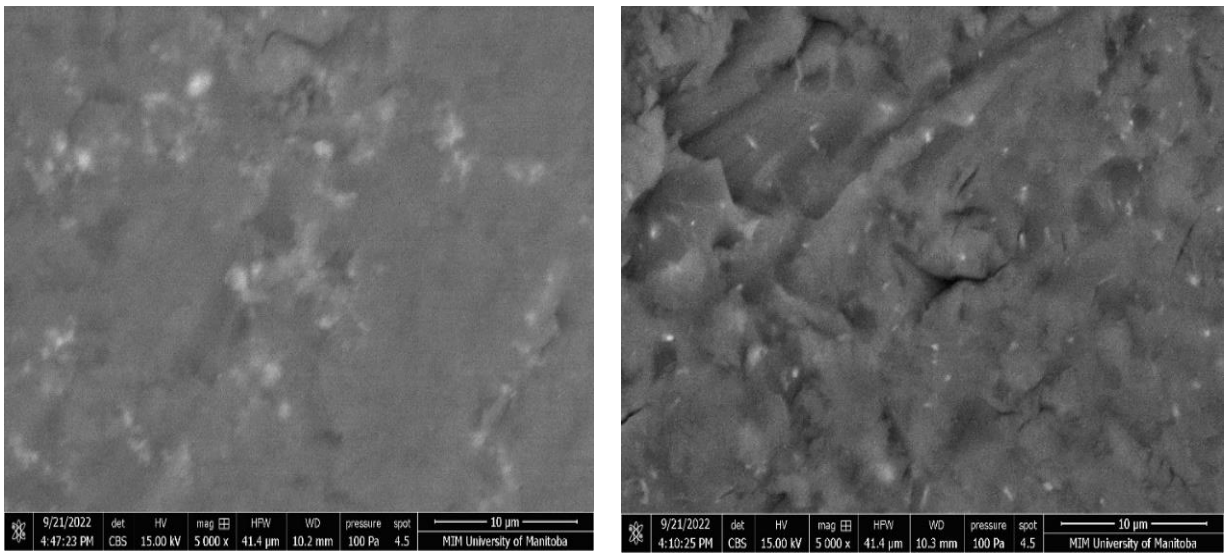

(a) (b)

Figure 4. 2. Exemplar ESEM images of: (a) vinyl ester/nano-calcium carbonate, and (b) vinyl ester/nano-clay composites at 5% loading ratio.

4.1.2. Wettability of Coated Concrete

Contact angle measurements were used as an indication of the degree of wettability (i.e., hydrophobicity) of the surface of coated concrete specimens. Contact angle is a function of the surface energy of the contact surface (depending on heterogeneity and roughness) and surface tension of the wetting liquid. A stronger interface between solid and liquid results in a low contact angle (i.e., droplet spreading out) and vice versa, while hydrophobic surfaces show a contact angle of at least 90^{o} (i.e., droplet tends to a spherical shape) (Chau et al. 2009). Uncoated concrete specimens, regardless of the *w/b*, had zero contact angle due to the spreading and penetration of fluid, indicating a hydrophilic nature of the bare concrete surface. Comparatively, applying surface treatments resulted in higher contact angles with fluid, which was demonstrated by water droplets having more rounded shapes on the surface, as depicted in **Fig. 4.3**. For instance, applying colloidal silica on concrete specimens at both *w/b* resulted in a wettable concrete surface (average angle 64^{o}). This could be attributed to the hydrophilic nature of the

nano-silica particles (Xu and Zhang 2021) combined with its high specific surface area (more than three times that of NC and NCC), resulting in stronger interaction with water and in turn lower contact angles.

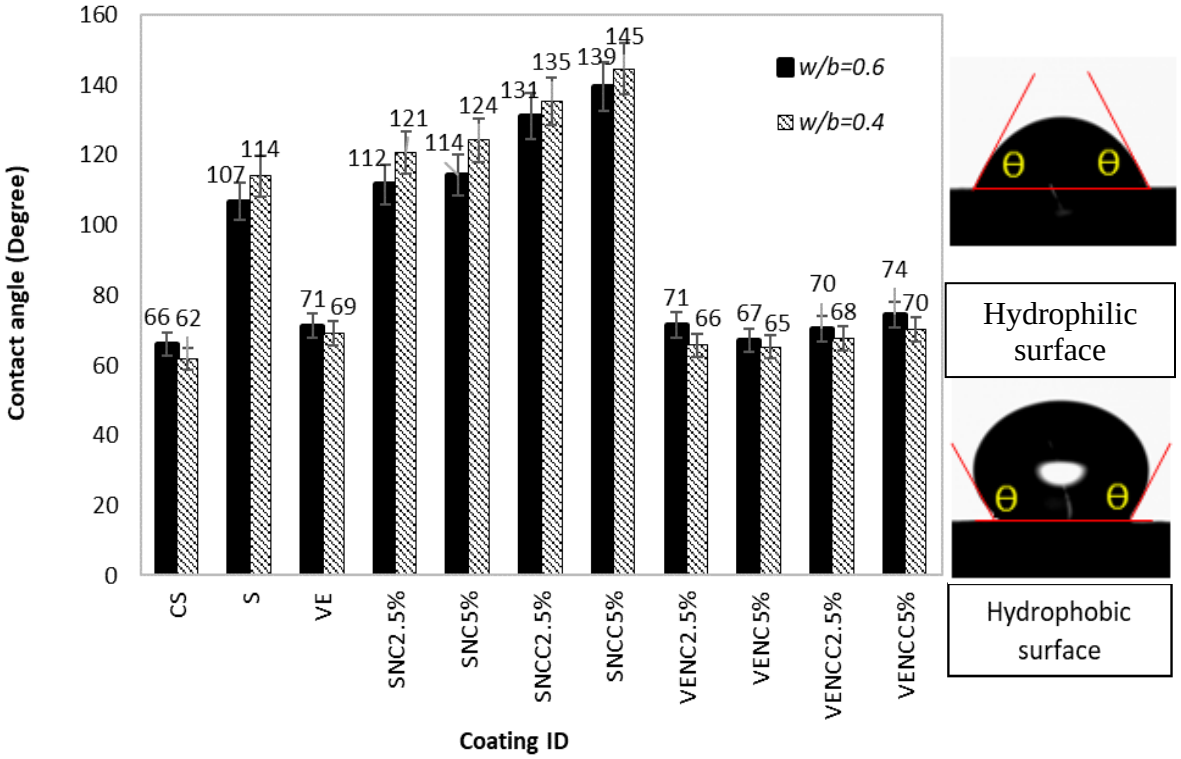

Figure 4. 3. Contact angle of concrete surface treated with various coatings.

For silane (hydrophobic agent) and silane/nanocomposites, reducing the *w/b* improved the water repellency of a coated surface, as the ranges of contact angles were 107 to 139^{o} and 114 to 145^{o} for concrete with *w/b* of 0.6 and 0.4, respectively. This trend might be attributed to the denser pore structure of concrete with *w/b* of 0.4, resulting in deposition of more silane on the surface, and consequently higher water repellency. Adding nanoparticles to neat silane systematically enhanced the resistance of the coated concrete to wettability at both *w/b*. For instance, at *w/b* of 0.4, concrete specimens coated with SNC2.5% and SNC5% had increased contact angles by 6% and 9%, respectively compared to that of neat silane (114^{o}). Higher degree

of hydrophobicity was observed for the silane/nano-calcium carbonate composites. For example, at *w/b* of 0.4, the contact angle was increased by 27% for concrete superficially treated with SNCC5% relative to that of specimens coated with neat silane. For both types of nanoparticles, it seems that the layout of nanoparticles on/into the concrete surface pores (barrier effect), led to further deposition of silane at the surface which increased the resistance to wettability.

On the other hand, applying vinyl ester and vinyl ester/nanocomposites on concrete specimens with different *w/b* resulted in comparable contact angles. Vinyl ester has a high dynamic viscosity [approximately 600 that of water [1 mPa·s] at room temperature], which resulted in forming a membrane on the surface of concrete causing angles between 65-74^{o} indicating that it is not hydrophobic. The modification of vinyl ester by nanoparticles, which were mostly encapsulated by the high viscosity layer as indicated by the TEM, did not increase the hydrophobicity of this isolating coating, since the contact angles obtained were in a close range (i.e., **Fig. 4.3**). For instance, specimens with *w/b* of 0.4 coated with vinyl ester/nano-calcium carbonate composites had an average contact angle of 69^{o}, which was similar to that of the neat vinyl ester.

4.1.3. Penetrability of Concrete

The RCPT results are listed in **Table 4.1**. The penetration depths and penetrability classes were directly related to passing charges. For untreated and superficially treated concrete, reducing the *w/b* resulted in lower penetrability regardless of the type of surface treatment, which complies with the well-documented impact of *w/b* on the concrete penetrability (Mehta and Monteiro 2014). At a *w/b* of 0.6, applying colloidal significantly reduced the penetrability (Moderate Class) of concrete compared to that of uncoated specimens (Over follow - OVF). In addition, applying silane and vinyl ester on concrete specimens remarkably reduced the penetration depth

of concrete specimens to different extents of 35 mm (High Class) and 2 mm (Very Low Class), respectively compared to the uncoated specimens. Adding nanoparticles to the neat resins further reduced the transport characteristics into concrete. For silane/nano-clay composites, specimens coated with SNC2.5% and SNC5% exhibited a reduction in penetration depth by 51% (Very Low Class) relative to that of specimens coated with neat silane. Similarly, applying SNCC2.5% and SNCC5% reduced the penetration depth by an average of 54% (Very Low Class) compared to that of specimens treated with neat silane. Superior reduction in penetrability was observed in the case of vinyl ester/nanocomposites. For example, concrete specimens superficially treated with vinyl ester/nano-calcium carbonate composites experienced a decrement in the penetration depth by an average of 75% (Negligible Class) compared to that of specimens coated with neat vinyl ester.

Indeed, superficially treated concrete specimens with a *w/b* of 0.4 had lower penetration depths (0 to 12 mm) relative to that of counterpart specimens with a *w/b* of 0.6 (range of penetration depth from 0 to 29 mm). Concrete specimens coated with colloidal silica had a reduction in the penetration depth by 25% (Low Class) compared to that of uncoated specimens. In addition, applying neat silane and vinyl ester on concrete specimens reduced the penetration depth by 44% (Low Class) and 94% (Very Low Class), respectively relative to that of uncoated specimens. The trends of nanocomposite surface treatments were similar to that of counterpart specimens with a *w/b* 0.6 as listed in **Table 4.1.**

Table 4. 1: RCPT results for uncoated and coated concrete specimens

Coating ID	Mixture ID					
	GU-FA0.6			GU-FA0.4		
	Charges passed[a] (Coulombs)	Penetration depth[a] (mm)	Penetrability class (ASTM C1202)[17]	Charges passed[a] (Coulombs)	Penetration depth[a] (mm)	Penetrability class (ASTM C1202)
Uncoated	OVF[b]	--	--	2326	16	Moderate
CS	3814	29	Moderate	1849	12	Low
S	4485	35	High	1576	9	Low
VE	268	2	Very low	211	1	Very low
SNC2.5%	641	17	Very low	307	3	Very low
SNC5%	750	17	Very low	336	3	Very low
SNCC2.5%	488	15	Very low	378	4	Very low
SNCC5%	726	17	Very low	596	6	Very low
VENC2.5%	63	0	Neg.	10	0	Neg.
VENC5%	153	2	Very low	66	1	Neg.
VENCC2.5%	74	1	Neg.	34	0	Neg.
VENCC5%	44	0	Neg.	23	0	Neg.

[a] The range of standard deviations for the passing charges and penetration depths are from 4 to 506 Coulombs and from 0.6 to 4 mm, respectively.
[b]OVF designates current overflow due to very high porosity which led to stopping the RCPT before 6 hours.

4.1.4. Visual Assessment

After 120 days of exposure to 5% ammonium sulfate solution, concrete specimens experienced noticeable features of deterioration such as softening, cracking, and disintegration, depending on the *w/b* and type of coatings. Under both exposures, uncoated concrete specimens (UC) with a *w/b* of 0.6 were totally disintegrated (visual rating of 5), while concrete with a *w/b* of 0.4 (visual rating of 4) experienced swelling and map cracking without breakage of the specimens after 120 days (e.g., **Fig. 4.4)**.

(a) [5] (b) [4]

(c) [5] (d) [4]

Figure 4. 4. Examples of uncoated **concrete** specimens: (a) UC-*w/b* 0.6-full immersion exposure, (b) UC-*w/b* 0.4-full immersion exposure, (c) UC-*w/b* 0.6-combined exposure, and (d) UC-*w/b*=0.4 combined exposure. (Note: numbers between brackets represent the final visual rating).

Under both exposures, the coated concrete performed better than that of uncoated concrete. In the full immersion exposure, the concrete specimens coated with colloidal silica experienced swelling and intensive map cracking on the surface without any scaling. Comparatively, concrete specimens coated with silane experienced less damage with surface softening and spalling along the edges combined with minor deterioration near the ends (**Fig. 4.5**). Overall, the neat silane and nano-modified silane coatings showed comparable performance in this exposure with visual ratings between 2 and 3. Generally, concrete specimens coated with neat vinyl ester were intact, except some peeling along the edges, which was also observed for the nano-modified vinyl ester composites (visual ratings of 1 to 2) [**Fig. 4.5**].

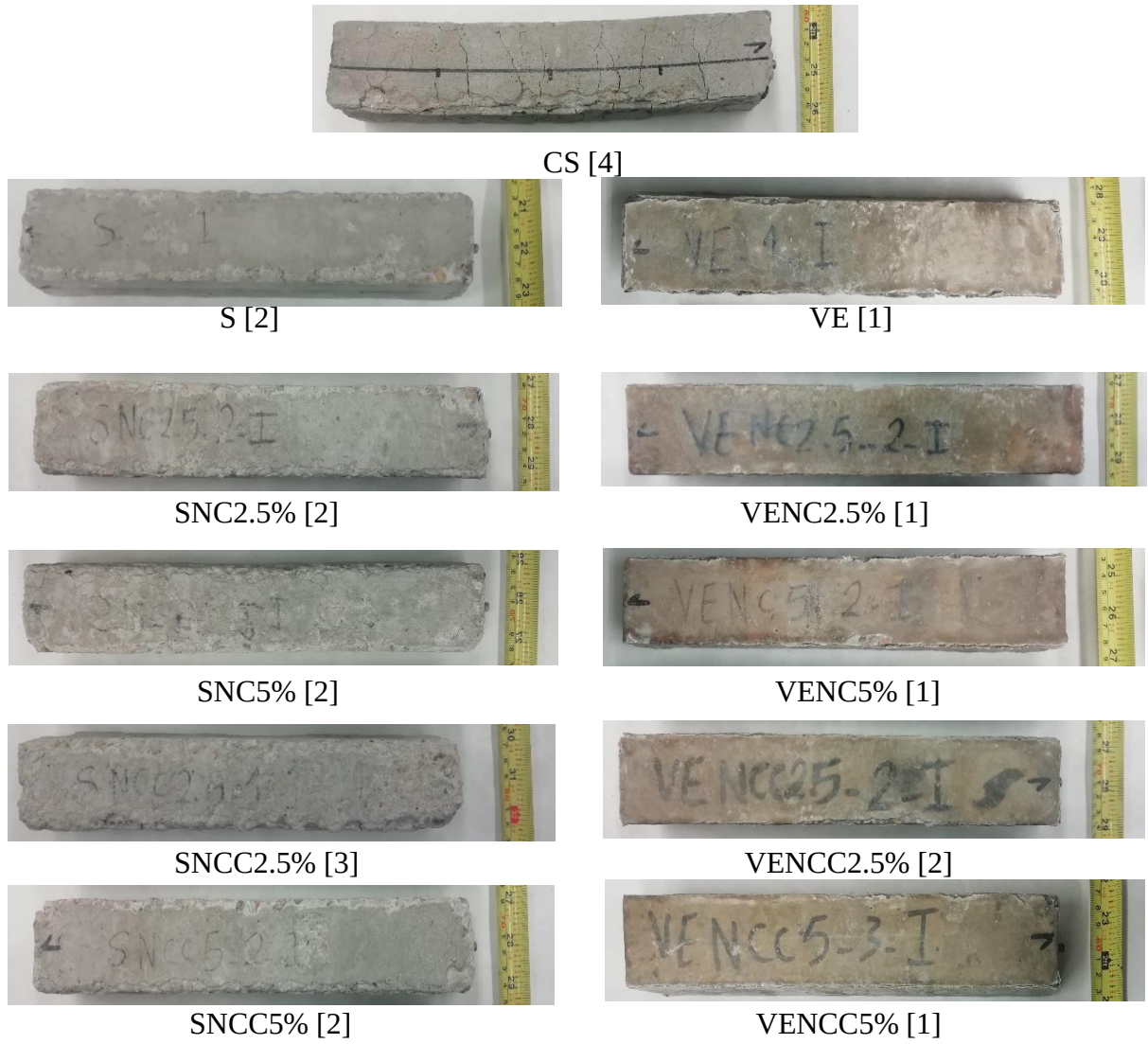

Figure 4. 5. Examples of coated concrete specimens (GU-FA0.6) after 120 days in full immersion exposure. (Note: numbers between brackets represent the final visual rating).

The deterioration of concrete specimens was more aggravated under the combined exposure (e.g., **Fig. 4.6**). The concrete specimens coated with colloidal silica (visual rating of 5) totally disintegrated after 120 days in the combined exposure similar to uncoated concrete. Concrete specimens coated with the neat silane and nano-modified silane experienced softening, moderate surface scaling and crumbling near the end of the specimens (**Fig. 4.6)**, with visual ratings ranging between 3 and 4. The specimens coated with vinyl ester coatings (neat and nano-

modified) (visual ratings between 2 to 3) experienced some peeling and crumbling near the ends but remained intact (**Fig. 4.6)**. However, the visual assessment observations alone could not decisively distinguish the level of protection among specimens coated with different surface treatments, and other assessment parameters are thus needed.

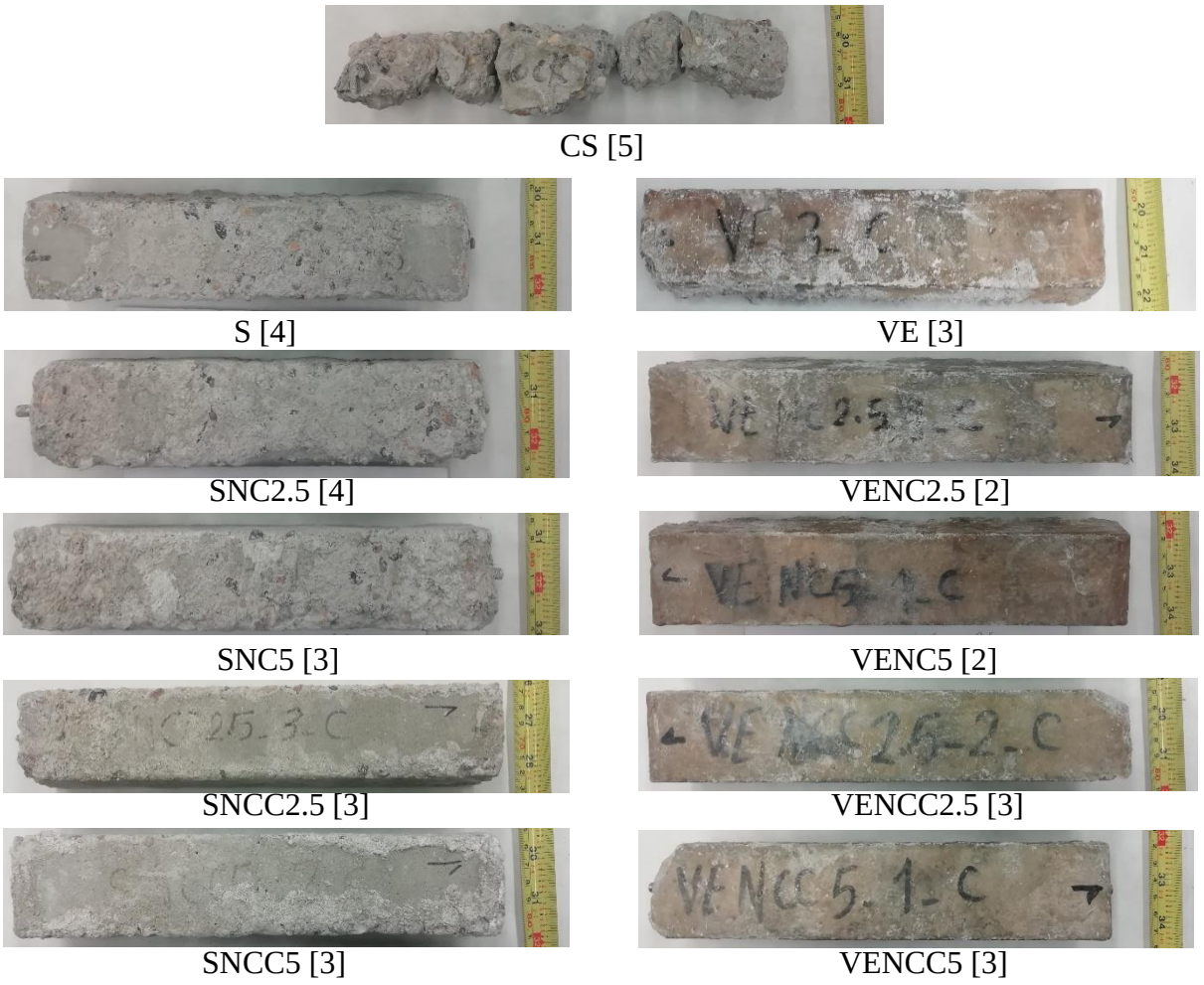

Figure 4. 6. Examples of coated concrete specimens (GU-FA0.6) after 120 days in the combined exposure. (Note: numbers between brackets represent the final visual rating).

4.1.5. Mass Change

The mass change of specimens during the full immersion exposure is listed in **Table 4.2**. All specimens experienced an increase in mass, which could be attributed to initial solution absorption, deposition of chemical reaction products within the surface layer of specimens, cracking, direct uptake of solution and eventual disintegration of some specimens. The degree of deterioration was significantly affected by the *w/b* and type of coatings. Uncoated concrete specimens with the higher *w/b* (0.6) completely disintegrated at the end of the full immersion exposure, while uncoated concrete specimens with a *w/b* of 0.4 experienced 3% mass gain without crumbling (**Fig. 4.4**). In addition, the mass gain of specimens was generally discounted with the application of coatings, complying with the visual observations (**Fig. 4.5**).

For coated concrete specimens with a *w/b* of 0.6, concrete specimens coated with colloidal silica experienced the highest cumulative mass gain (11%) by the end of the full immersion exposure, which was much higher than the cumulative mass gain of all other coated specimens. Silane and vinyl ester coatings effectively protected the concrete from the ammonium sulfate solution (visual ratings of 2 and 1, respectively; **Fig. 4.5**); they experienced mass gain of 5% and 4%, respectively, while the uncoated specimens were disintegrated after 120 days in the full immersion exposure. Moreover, applying both nanoparticles to the neat reins further improved the protective effect for coatings. For the silane/nano-clay coatings (SNC2.5% and SNC5%), the cumulative mass gain of specimens at the end of exposure was reduced by 18% and 14%, respectively, compared to that of the concrete specimens coated with neat silane. For the silane/nano-calcium carbonate coatings the reduction in mass gain was comparable (32%) at both dosages. For the vinyl ester nanocomposites, applying both dosages of nanoparticles consistently reduced the mass gain relative to that of the specimens coated with neat vinyl ester.

For instance, at 120 days, VENC5% and VENCC5% specimens had reduced cumulative mass gain by 23% and 20%, respectively compared to that of VE specimens.

Table 4. 2: Cumulative mass change (%) of uncoated and coated concrete specimens in the full immersion exposure

Coating ID	Days			
	30	**60**	**90**	**120**
		GU-FA0.6		
Uncoated	+4.6	+3.5	+10.2	--*
CS	+2.6	+7.8	+10.0	+11.3
S	+1.4	+1.3	+5.0	+4.9
VE	+1.8	+1.4	+3.2	+4.0
SNC2.5%	+1.3	+0.6	+3.6	+4.0
SNC5%	+1.3	+1.1	+4.8	+4.2
SNCC2.5%	+1.6	+1.4	+5.5	+3.3
SNCC5%	+1.1	+1.4	+4.0	+3.4
VENC2.5%	+1.7	+1.4	+2.6	+3.2
VENC5%	+1.4	+1.1	+2.5	+3.1
VENCC2.5%	+1.9	+1.4	+3.3	+3.7
VENCC5%	+1.9	+1.4	+2.7	+3.2
		GU-FA0.4		
Uncoated	+2.0	+1.6	+4.6	+3.3
CS	+2.1	+5.0	+4.2	+5.6
S	+1.1	+1.2	+4.2	+3.3
VE	+0.7	+0.4	+1.5	+1.5
SNC2.5%	+0.8	+0.6	+2.7	+1.8
SNC5%	+1.1	+0.9	+4.3	+1.8
SNCC2.5%	+1.4	+1.0	+3.9	+3.2
SNCC5%	+0.7	+0.6	+2.9	+2.2
VENC2.5%	+0.6	+0.4	+1.1	+1.3
VENC5%	+0.5	+0.4	+1.0	+1.0
VENCC2.5%	+0.4	+0.3	+1.0	+1.2
VENCC5%	+0.3	+0.2	+0.8	+1.0

Note: (-) refers to mass loss and (+) refers to mass gain.
Note: the standard deviations for the cumulative mass change range from 0.1 to 2.2%.
*Specimens were disintegrated at this time.

Table 4. 3: Cumulative mass change (%) of uncoated and coated concrete specimens in the combined exposure

Coating ID	Days			
	30	**60**	**90**	**120**
			GU-FA0.6	
Uncoated	+3.7	-12.6	-9.7	--*
CS	-6.2	-2.2	--*	--*
S	-1.1	-6.3	-4.7	-14.4
VE	+1.7	-3.6	-2.0	-13.4
SNC2.5%	-1.0	-5.3	-4.1	-9.5
SNC5%	-0.8	-4.7	-2.9	-9.7
SNCC2.5%	-1.1	-4.0	-2.4	-8.2
SNCC5%	-1.1	-3.3	-2.1	-6.3
VENC2.5%	+1.0	-3.5	-1.4	-10.5
VENC5%	+0.5	-3.3	-1.6	-9.8
VENCC2.5%	+1.6	-0.9	-0.4	-9.6
VENCC5%	+2.4	-2.2	-1.5	-9.7
			GU-FA0.4	
Uncoated	+1.0	-1.7	-0.3	-9.8
CS	-0.3	+1.4	-1.1	-2.1
S	-0.2	-2.6	-1.3	-9.1
VE	+0.7	-1.2	-0.7	-6.6
SNC2.5%	-0.2	-2.8	-1.9	-6.0
SNC5%	0.0	-2.6	-1.9	-8.1
SNCC2.5%	-0.1	-3.2	-1.1	-4.8
SNCC5%	-0.1	-2.5	-0.9	-6.4
VENC2.5%	+0.3	-1.0	-0.4	-2.3
VENC5%	+0.4	-0.2	-0.1	-2.9
VENCC2.5%	+0.2	-0.5	-0.2	-3.8
VENCC5%	+0.2	-0.5	-0.5	-3.8

Note: (-) refers to mass loss and (+) refers to mass gain.

Note: the standard deviations for the cumulative mass change range from 0.1 to 7.6%.

*Specimens were disintegrated at this time.

Coated concrete specimens with a *w/b* of 0.4 had lower mass gain (1 to 6%) relative to that of counterpart specimens with a *w/b* of 0.6 (range of mass gain from 3 to 11%). Again, concrete specimens coated with colloidal silica had the highest cumulative mass gain (5.6%) in the 0.4 *w/b* group. Applying neat silane on concrete specimens with a *w/b* of 0.4 resulted in a comparable cumulative mass gain to that of uncoated specimens. Comparatively, applying neat vinyl ester on concrete reduced the cumulative mass gain by 55% compared to that of uncoated specimens. The trends of nanocomposite coatings were similar to that of counterpart specimens with a *w/b* 0.6, and vinyl ester nanocomposites had the lowest cumulative mass gain (average of 1%) at the end of the full immersion exposure.

The combined exposure was more aggravated relative to the full immersion one as most specimens showed mass losses at 60 days [**Table 4.3**] (*i.e.*, one winter and one summer seasons) due to loss of surface and crumbling resulting from combining the ammonium sulfate solution with cyclic environments. By the end of the combined exposure, superficially treated concrete specimens experienced mass loss in the range of 2% to 14% depending on the *w/b* and type of coating. Uncoated and colloidal silica specimens with a *w/b* of 0.6 completely disintegrated by 120 days.

For concrete specimens with a *w/b* of 0.6, the silane and vinyl ester coatings effectively protected the specimens from complete disintegration (mass losses of 14% and 13%, respectively). Applying SNC2.5% and SNC5% on concrete specimens further reduced the cumulative mass loss by around 34% compared to that of the counterpart specimens coated with neat silane. Similarly, for the silane/nano-calcium carbonate composites (SNCC2.5% and SNCC5%), their specimens had reduced cumulative mass losses by 43% and 56%, respectively, compared to that of the concrete specimens coated with neat. For the vinyl ester/nano-clay

composites, applying VENC2.5% and VENC5% reduced the cumulative mass losses by approximately 25% compared to that of concrete specimens coated with neat vinyl ester. Concrete specimens coated with VENCC2.5% and VENCC5% experienced an average reduction in the cumulative mass loss by 28% compared to that of concrete specimens coated with the neat vinyl ester.

For concrete specimens with a *w/b* of 0.4, uncoated and silane coated specimens had a comparable mass loss at the end of the combined exposure. Comparatively, specimens coated with the neat vinyl ester and colloidal silica reduced the cumulative mass losses by 33% and 79%, respectively compared to that of uncoated specimens. Concrete specimens coated with neat silane and silane nanocomposites had cumulative mass losses in the close range of 5 to 9%. For the vinyl ester nanocomposites, applying VENC2.5% and VENC5% on concrete specimens reduced the cumulative mass loss by 65% and 56%, respectively, compared to that of concrete specimens coated with neat vinyl ester. Similarly, concrete specimens superficially treated with VENCC2.5% and VENCC5% experienced a reduction in cumulative mass loss by 42% compared to that of concrete specimens coated with neat vinyl ester.

4.1.6. Length Change

The length change of concrete specimens during the full immersion exposure is listed in **Table 4.4.** The cumulative expansion of all specimens was caused by a combination of factors, including early solution absorption and deposit of reaction products, and aggravation of this process by cracking. Complying with the visual assessment and mass change results, uncoated concrete specimens with the higher *w/b* (0.6) experienced high expansion at 60 days, resulting in their disintegration before the end of the full immersion exposure (120 days), while uncoated

concrete specimens with a *w/b* of 0.4 showed less rate of expansion with time and sustained swelling pressure up to 120 days without disintegration (**Fig. 4.4**).

Table 4. 4: Cumulative length change (%) of uncoated and coated concrete specimens in the full immersion exposure

Coating ID	Days			
	30	60	90	120
	GU-FA0.6			
Uncoated	+0.080	+0.621	--*	--*
CS	+0.046	+0.401	--*	--*
S	+0.015	+0.021	+0.031	+0.606
VE	+0.021	+0.019	+0.054	+0.059
SNC2.5%	+0.019	+0.029	+0.044	+0.172
SNC5%	+0.015	+0.019	+0.072	+0.494
SNCC2.5%	+0.010	+0.008	+0.082	+0.453
SNCC5%	+0.015	+0.015	+0.048	+0.133
VENC2.5%	+0.019	+0.013	+0.021	+0.040
VENC5%	+0.019	+0.017	+0.015	+0.040
VENCC2.5%	+0.019	+0.013	+0.021	+0.025
VENCC5%	+0.019	+0.019	+0.025	+0.038
	GU-FA0.4			
Uncoated	+0.027	+0.031	+0.317	--*
CS	+0.035	+0.106	+1.239	--*
S	+0.012	+0.015	+0.033	+0.094
VE	+0.014	+0.010	+0.021	+0.039
SNC2.5%	+0.011	+0.009	+0.031	+0.040
SNC5%	+0.011	+0.015	+0.029	+0.071
SNCC2.5%	+0.012	+0.010	+0.031	+0.054
SNCC5%	+0.013	+0.010	+0.029	+0.036
VENC2.5%	+0.013	+0.008	+0.015	+0.019
VENC5%	+0.010	+0.008	+0.012	+0.015
VENCC2.5%	+0.008	+0.004	+0.012	+0.015
VENCC5%	+0.015	+0.010	+0.017	+0.021

Note: (-) refers to shrinkage and (+) refers to expansion.
Note: the standard deviations for the cumulative length change range from 0.001 to 0.523%.
* Specimens were extremely expanded and could not be measured on the length comparator.

For coated concrete specimens with a *w/b* of 0.6 specimens coated with colloidal silica experienced extreme expansion (not measurable by the limits of the length comparator) after 90 days similar to that of the uncoated specimens, which conformed to the highest mass gain for this group of specimens. Conversely, silane and vinyl ester coatings significantly reduced the cumulative expansion of concrete specimens to 0.606% and 0.059%, respectively at 120 days. For silane/nano-clay composites, applying SNC2.5% and SNC5% on concrete specimens reduced the cumulative expansion by 72% and 18%, compared to that of neat silane specimens. For the silane/nano-calcium carbonate composites, the concrete specimens coated with SNCC2.5% and SNCC5% experienced a systematic reduction in the cumulative expansion by 25% and 78%, respectively compared to that of concrete specimens coated with neat silane, conforming to the mass change trends. For the vinyl ester nanocomposites, applying VENC2.5% and VENC5% reduced the length change relative to that of the specimens coated with neat vinyl ester by an average of 32% at the end of full immersion exposure. Similarly, the vinyl ester/nano-calcium carbonate composites (VENCC2.5% and VENCC5%) experienced a reduction in the cumulative expansion by an average of 47%, relative to that of specimens coated with neat vinyl ester.

As expected, less expansion was observed in concrete specimens with a *w/b* of 0.4. Concrete specimens coated with colloidal silica significantly expanded (1.239%) after 90 days of exposure. Again, applying neat silane and vinyl ester on concrete specimens with a *w/b* of 0.4 reduced the cumulative length change by approximately 93% and 97%, respectively compared to that of uncoated specimens after 120 days. Complying with the mass change results, the trends of silane nanocomposite coatings for specimens with a *w/b* of 0.4 were similar in the sense that nano-clay and nano-calcium carbonate were more efficient in suppressing the expansion of

specimens (average reduction of 41% and 53%, respectively), compared to that of neat silane. For the vinyl ester nano-modified coatings, applying VENC5% and VENCC2.5% on concrete with a *w/b* of 0.4 resulted in the lowest cumulative length change (average of 0.015%) compared to all other coated specimens.

During the combined exposure, uncoated specimens and specimens coated with colloidal silica experienced expansion, but less than that of the full immersion exposure, while the others experienced length change varying from shrinkage to expansion (**Table 4.5)**. The reduction in expansion or shrinkage could be attributed to the drying portion of the combined exposure. Similar to the previous trends, the *w/b* and coatings had a significant effect on the degree of length change. Uncoated concrete specimens with the higher *w/b* (0.6) experienced high expansion at 90 days and eventually disintegrated at the end of the combined exposure, while uncoated concrete specimens with a *w/b* of 0.4 yielded 0.040% expansion without disintegration (**Fig. 4.4**).

The trends of coated concrete were comparable to the ones observed in the full immersion exposure, in terms of the effect of *w/b* and coatings. For example, for concrete specimens with a *w/b* of 0.6, applying neat silane and vinyl ester significantly reduced the cumulative expansion of concrete specimens to 0.027% and 0.065% compared to that of uncoated specimens, which disintegrated after significant expansion. Addition of nanoparticles to these resins further reduced the length change. For example, applying SNC2.5% and SNC5% on concrete specimens (visual rating of 4 and 3, respectively) reduced cumulative length change of concrete specimens by 70%, compared to that of concrete specimens coated with neat silane.

Table 4. 5: Cumulative length change (%) of uncoated and coated concrete specimens in the combined exposure

Coating ID	Days			
	30	**60**	**90**	**120**
	GU-FA0.6			
Uncoated	+0.031	+0.050	+0.274	--*
CS	+0.048	+0.119	--*	--*
S	-0.006	-0.019	+0.012	+0.027
VE	+0.019	+0.008	+0.025	+0.065
SNC2.5%	-0.004	-0.017	+0.006	+0.008
SNC5%	-0.004	-0.010	+0.008	+0.008
SNCC2.5%	-0.002	-0.017	+0.011	+0.013
SNCC5%	-0.002	-0.017	+0.004	+0.010
VENC2.5%	+0.017	+0.006	+0.017	+0.040
VENC5%	+0.011	+0.002	+0.017	+0.034
VENCC2.5%	+0.017	+0.008	+0.023	+0.055
VENCC5%	+0.008	+0.006	+0.011	+0.054
	GU-FA0.4			
Uncoated	+0.017	+0.004	+0.021	+0.040
CS	+0.013	+0.040	+0.050	+0.055
S	+0.002	-0.013	+0.006	+0.013
VE	+0.013	+0.004	+0.017	+0.019
SNC2.5%	+0.000	-0.013	+0.002	+0.010
SNC5%	+0.002	-0.015	+0.004	+0.010
SNCC2.5%	+0.000	-0.014	+0.004	+0.012
SNCC5%	+0.000	-0.013	+0.006	+0.006
VENC2.5%	+0.000	+0.002	+0.002	+0.011
VENC5%	+0.002	+0.000	+0.002	+0.008
VENCC2.5%	+0.006	+0.000	+0.006	+0.008
VENCC5%	+0.002	+0.000	+0.000	+0.008

Note: (-) refers to shrinkage and (+) refers to expansion.
Note: the standard deviations for the cumulative length change range from 0.001 to 0.049%.
* Specimens were extremely expanded and could not be measured on the length comparator.

4.2. Discussion

4.2.1. Mechanisms of Damage

In the full immersion exposure (pH 6.0–8.0), the damage process was driven by the acidic action of ammonium ions, which led to consumption of portlandite, and production of gypsum [**Eqs. 4.1**-**4.2**, (Marchand et al. 2001; Nagele et al. 1984)], as for example depicted in **Fig. 4.7**, resulting in softening, mass gain, and expansion of specimens, especially for uncoated specimens. Moreover, direct dissolution of calcium silicate hydrate (C-S-H) was possible, converting to hydrous silica, gypsum, and gaseous NH_3 [**Eq. 4.3**, (Marchand et al. 2001; Nagele et al. 1984)]. The relative phase formation can be detected by a semi-quantitative method based on the enthalpy concept (integration of heat flow peaks over temperature), as the enthalpy of each phase is directly related to its amount (Brown 1998) as for example shown in **Fig. 4.7** for gypsum enthalpy. The low solubility and high stability of gypsum, even at low pH levels below 1 (Mahmud Amin 2017), could retain it in the pore structure of concrete surface. Hence, continual precipitation of gypsum, as shown by the large amounts retained on the surface of specimens (**Fig. 4.7**), contributed to expansive pressures in the matrix, resulting in softening, map cracking and disintegration in some cases, as for example depicted in **Figs. 4.4 and 4.5**. Indeed, surface cracking provided direct paths for infiltration of additional ammonium sulfate solution, and precipitation of more gypsum, which led to significant mass gain (**Table 4.2**) and swelling (**Table 4.4)**.

$$NH_4^+ \leftrightarrow NH_3 + H^+ \qquad \text{(Eq. 4.1)}$$

$$Ca(OH)_2 + (NH_4)_2SO_4 \rightarrow CaSO_4.2H_2O + 2NH_3 \qquad \text{(Eq. 4.2)}$$

$$xCa.SiO_2.aq + x(NH_4)_2SO_4 + xH_2O \rightarrow SiO_2.aq + xCaSO_4.2H_2O + 2xNH_3 \quad \text{(Eq. 4.3)}$$

$$SO_4^{-2} + 2Ca^{+2} + Ca_4\,Al_2(OH)_{12}.SO_4.6H_2O \rightarrow Ca_6\,Al_2(OH)_{12}(SO_4)_3.26H_2O \quad \text{(Eq. 4.4)}$$

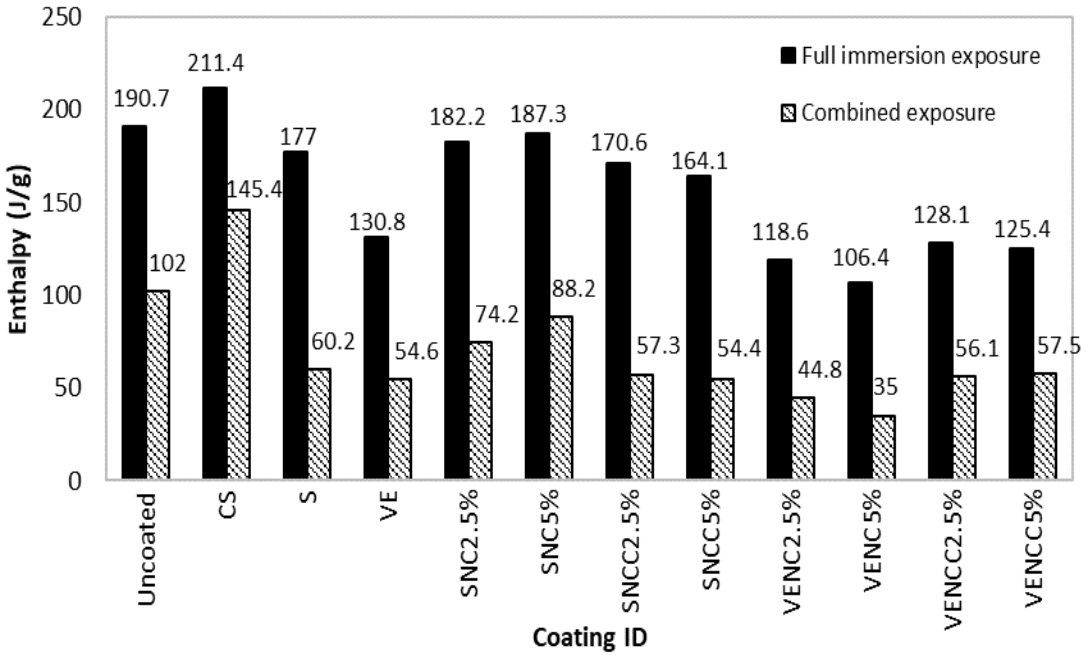

Figure 4. 7. Enthalpy of gypsum (dehydration range of 120-135°C) in uncoated and coated specimens (*w/b* of 0.6) after 120 days in full immersion and combined exposures. (Note: accuracy of enthalpy determination is ±3%).

In the combined exposure, the ammonium sulfate deleterious effects on concrete were amplified by the freezing-thawing and wetting-drying cycles. Gypsum precipitation in the convective zone of specimens was substantially less than that in the full immersion exposure. For example, uncoated concrete specimens (*w/b* of 0.6) in the combined exposure had 47% less gypsum compared to that in the uncoated specimens exposed to full immersion (**Fig. 4.7).** This could be due to the synergistic effects of ammonium sulfate and cyclic environments. During the freezing-thawing (-18 to +5°C) portion of the combined exposure, the cold temperatures

decelerated the kinetics of chemical interactions between the solution and the paste (**Eqs. 4.1-4.4**). On the other hand, continual penetration of the solution during the thawing and wetting cycles, especially through uncoated concrete surfaces, promoted the degree of critical saturation, and decomposition of the matrix, and precipitation of sulfate reaction products within the surface of concrete specimens, resulting in large tensile stresses in the confined pore space, surface micro-cracking, and eventually significant mass loss of specimens with cyclic environments, which was the dominant damage manifestation in this exposure (**Table 4.2)**. The synergistic effects of partial shrinkage during the drying cycles and cumulative surface scaling of concrete contributed to lower net expansion of the specimens in the combined exposure (**Table 4.5**) relative to that of specimens in the full immersion exposure (**Table 4.4**).

Alternating cyclic environments induced micro-cracks (e.g., **Fig. 4.8**) in the cementitious matrix providing direct pathways for the ingress of ammonium sulfate solution, thus aggravating the kinetics of specimens' deterioration. In the combined exposure, formation of gypsum and ettringite clusters [**Eqs. 4.2-4.4** (Bassuoni and Nehdi 2009)] was observed as a result of the solution interaction with the paste (e.g., **Figs. 4.9-4.11**), but this did not necessarily lead to higher expansion of specimens relative to that in the full immersion exposure, as explained earlier. Secondary ettringite formation was promoted in the combined exposure, due to the effect of wetting-drying cycles (Stark and Bollmann 1999). With changing the moisture conditions during the wetting-drying cycles, recrystallization and precipitation of secondary ettringite into large crystals was possible [e.g., **Fig. 4.11(a)**] due to Ostwald Ripening (crystallization of large crystals at the expense of smaller crystals to attain thermodynamic stability) (Boistelle and Astier 1988). In addition, incidental formation of thaumasite was observed [e.g., **Fig. 4.11(b)]**. The conducive conditions for thaumasite formation are the coexistence of sulfates, calcium silicate,

moisture, and carbonates (from aggregate used in the mixtures) at low temperatures (below 15^{o}C), which occurred during the cold cycles herein. Also, formation of thaumasite is readily possible from precursor ettringite formation and its interaction with carbonate and calcium silicate [indirect route]. Thaumasite maintained its stability during the wetting-drying cycles, as it is thermally stable up to 80-90°C (Rahman and Bassuoni 2014). The coexistence of gypsum and ettringite with incidental thomasite formation indicated that those concrete specimens were vulnerable to significant deterioration under the combined exposure, as indicated by the results.

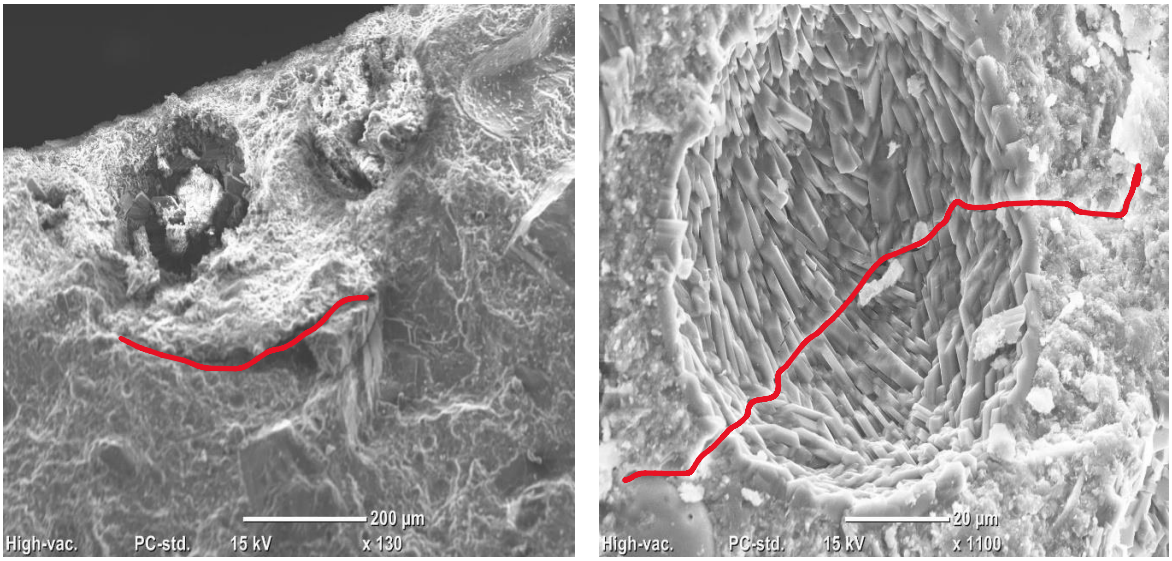

Figure 4. 8. Micro-cracks in uncoated concrete specimens (*w/b* of 0.6) after 120 days in the combined exposure: (a) sub parallel crack close to concrete surface, and (b) micro-crack crossing a void filled with gypsum crystals.

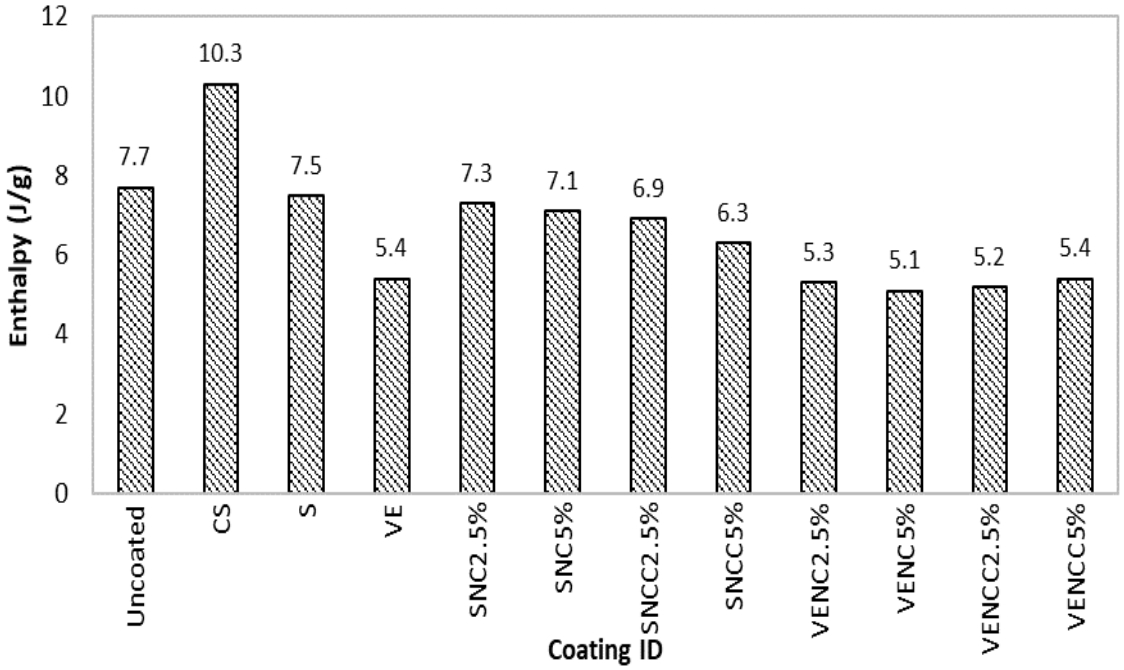

Figure 4. 9. Enthalpy of ettringite (average dehydration temperature 90°C) in uncoated and coated specimens (*w/b* of 0.6) after 120 days in the combined exposure. (Note: accuracy of enthalpy determination is ±3%).

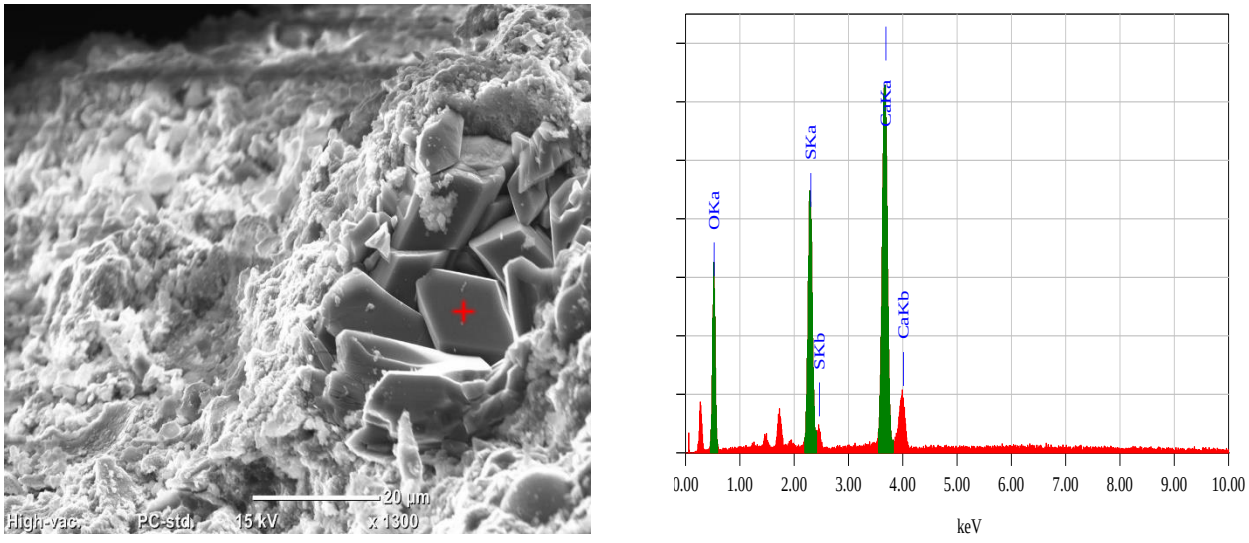

Figure 4. 10. Gypsum crystals filling a void near the concrete surface of uncoated concrete (*w/b* of 0.6) after the combined exposure and associated EDX.

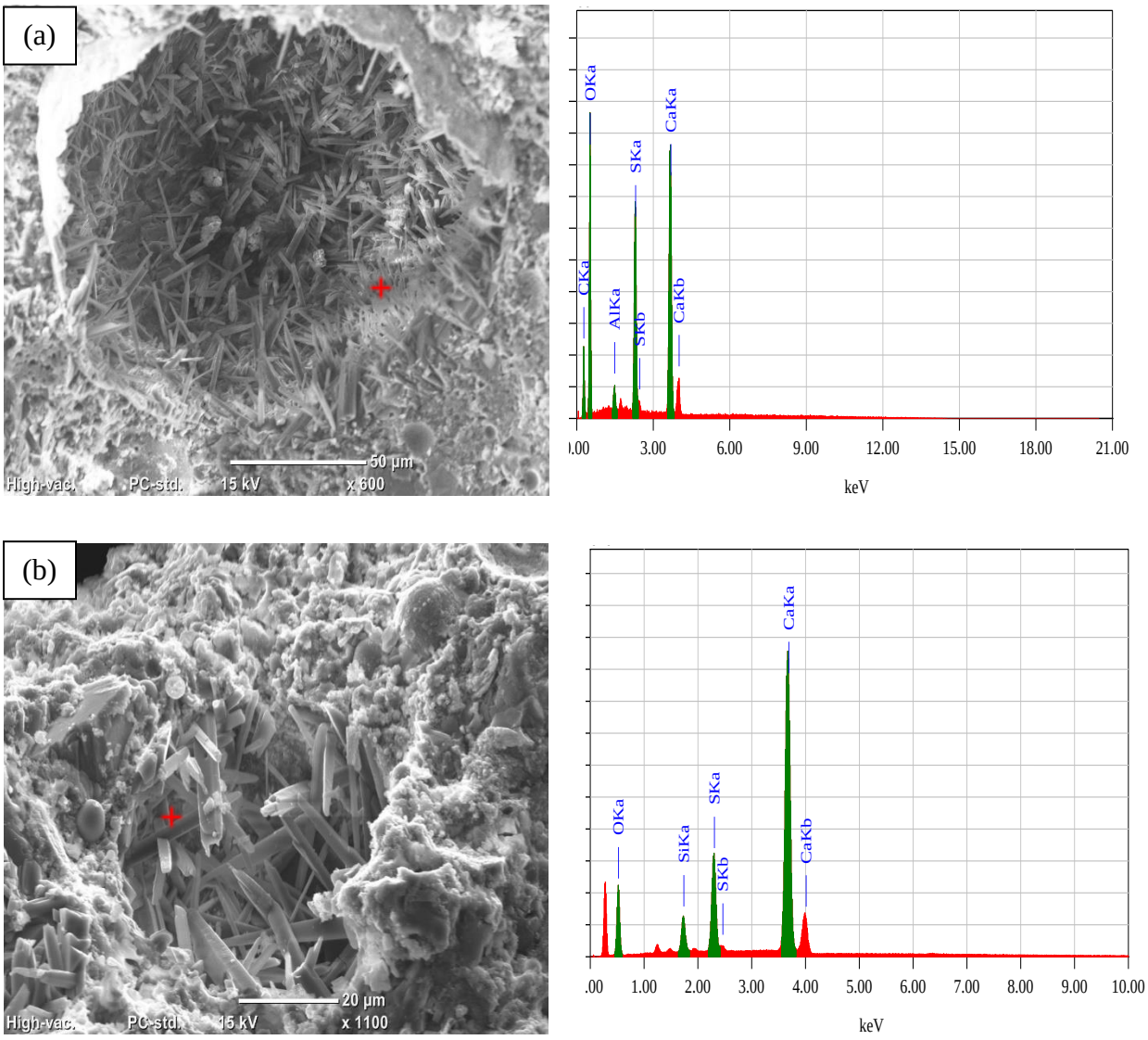

Figure 4. 11. Uncoated concrete specimens (*w/b* of 0.6) after the combined exposure: (a) ettringite clusters filling an air void with associated EDX, and (b) incidental thaumasite formation with EDX.

4.2.2. Effect of water-to-binder ratio

Overall, the effect of *w/b* conformed to the results observed in previous research studies, in terms of the favorable effect of *w/b* reduction on improving the durability of cement-based materials

(Bassuoni and Rahman 2016). For uncoated and coated concrete specimens, decreasing the *w/b* from 0.6 to 0.4 resulted in discounting the initial penetrability of concrete (e.g., **Table 4.1**), regardless of the type of coating, which conformed to its well-documented effect at refining the pore structure of concrete [physical defense] (ACI 201.2R). For example, after 120 days in both exposures, uncoated concrete specimens with a *w/b* of 0.4 experienced map cracking and softening, while counterpart specimens with a *w/b* of 0.6 totally disintegrated (**Fig**. **4.4**). According to the RCPT results (**Table 4.1**), reducing the *w/b* led to concrete with significantly lower penetrability, due to densification of the pore structure, which discounted the ingress of ammonium sulfate solution and hence decreasing the degree of deterioration, as indicated by mass and length change results (**Tables 4.2-4.5**) during both exposures and formation of less amounts of reaction products. For example, the enthalpy of gypsum and ettringite was reduced by an average of 10% in concrete with a *w/b* of 0.4 compared to that in counter concrete with a 0.6 *w/b* after both exposures. Hence, reducing the *w/b* was a key parameter for enhancing the resistance of uncoated and coated concrete specimens to the ammonium sulfate exposures, which led to lower rates of deterioration. The effect of different coatings is discussed in the succeeding sections.

4.2.3. Effect of Colloidal Silica

Applying colloidal silica as a surface treatment on hardened concrete specimens resulted in improving the initial resistance of concrete to penetration of fluids relative to uncoated concrete specimens, as indicated by the RCPT. This occurred due to the deposition of colloidal silica particles on the concrete surface (**Fig. 4.12**). Partial amounts of colloidal silica particles could react with portlandite to produce C-S-H (pozzolanic activity), densifying the pore structure of concrete, as indicated by the consumption of portlandite in specimens coated with colloidal silica

relative to that of uncoated specimens (**Fig. 4.13**). However, these processes did not adequately protect the concrete surface from the ammonium sulfate exposures.

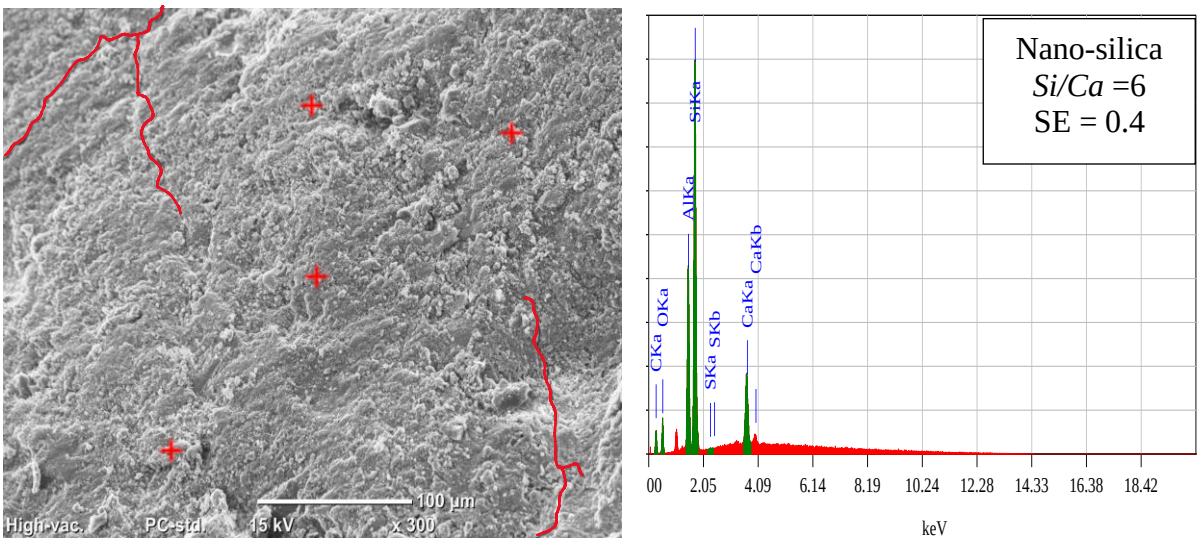

Figure 4. 12. Precipitation of condensed nano-silica particulates on the surface of unexposed concrete coated with CS (*w/b* of 0.6) with shrinkage micro-cracks on the surface and associated EDX for nano-silica particles. (Note: SE refers to the standard error for the average ratio of the marked location).

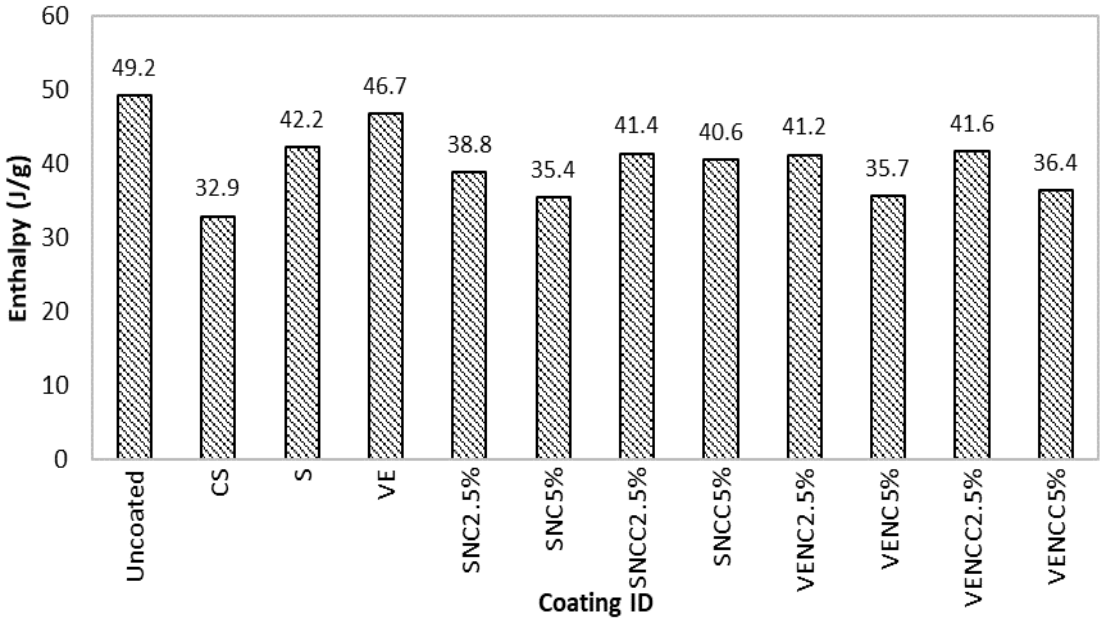

Figure 4. 13. Enthalpy of portlandite (dehydration range of 400-450°C) in uncoated and coated specimens (*w/b* of 0.6) after 56 days of curing. (Note: accuracy of enthalpy determination is ±3%).

Concrete specimens coated with colloidal silica generally had high rates of mass/length change, and in some cases disintegrated similar to uncoated concrete. This corresponded to the highest enthalpy of gypsum at the end of the full immersion and combined exposures (211.4 and 145.4 J/g, respectively; **Fig. 4.7**) and ettringite (10.3 J/g; **Fig. 4.9**). This could be attributed to the precipitation of condensed silica particles, with ultra-high surface area (average of 200 m^2/g) on the surface of concrete specimens (**Fig. 4.12),** which have hydrophilic nature (**Fig. 4.3**), thus imbibing ammonium sulfate solution into the concrete surface. This layer also comprised shrinkage micro-cracks during the drying period (48 hours before exposures), likely due to the evaporation of dispersing solution, which acted as direct entry paths for the ammonium solution. In addition, significant reduction of portlandite within the underlying surface of these specimens made this C-S-H rich zone directly vulnerable to decalcification by the 10% ammonium sulfate solution forming large amounts of gypsum and ettringite, and thus deterioration of these specimens.

4.2.4. Effect of Silane/Nanocomposites

Applying neat silane to concrete specimens generally improved the durability of concrete at both *w/b* to the full immersion and combined exposures compared to the uncoated specimens. This could be attributed to the water-repelling effect of silane; it can infiltrate into the pore structure of concrete due to its small particle size (from 10 nm to a few micrometers) and react with alkaline species and water in the matrix producing active hydrophobic ingredients precipitating in the pores (Moon and Lee 2017). This was substantiated by the DSC results of cured specimens before exposures, as the silane coated specimens had less portlandite (42.2 J/g) than that in the uncoated specimens [49.2 J/g] (**Fig. 4.13**). Accordingly, the wettability (**Fig. 4.3)** and penetrability (**Table 4.1**) of specimens coated with silane had been effectively reduced.

Further improvement in the concrete performance under both exposures was observed for concrete specimens coated with silane/nanocomposites (**Tables 4.2-4.5)**. The enhanced performance of concrete specimens treated with silane/nano-clay composites, at both dosages, could be mainly attributed to the added barrier effect due to the layout of the nano-clay particles, which was observed as an interwoven structure by TEM (**Fig. 4.1**), depositing on the surface of concrete (**Fig. 4.14)**. Hence, the net effect of the silane/nano-clay coatings led to increasing hydrophobicity (contact angles of at least 112°; **Fig. 4.3**) and fortifying the surface layer of concrete, as indicated by the reduced penetrability of these specimens (very low penetrability, **Table 4.1**), which efficiently reduced the ingress of the solution into the specimens and discounted the rate of damage relative to that of the specimens coated with neat silane. In addition, the nano-clay appeared to induce additional pozzolanic reactivity in the cementitious matrix with dosage, since the portlandite content was further reduced (e.g., 16% reduction with SNC5% as shown in **Fig. 4.13**) relative to the specimens coated with neat silane. This could be attributed to the high alumino-silicate content of halloysite (more than 80%), which promoted the pozzolanic activity to produce additional cement gel. This could be the reason for precipitating more gypsum (average of 5% and 35% in the full and combined exposures, respectively; **Fig. 4.7**) in the surface layer of concrete specimens coated silane/nano-clay composites relative that in specimens coated with neat silane. However, this did not coincide with more degradation of the specimens, due to the dominant synergistic effects of silane (hydrophobicity) and nano-clay (fortifying surface barrier).

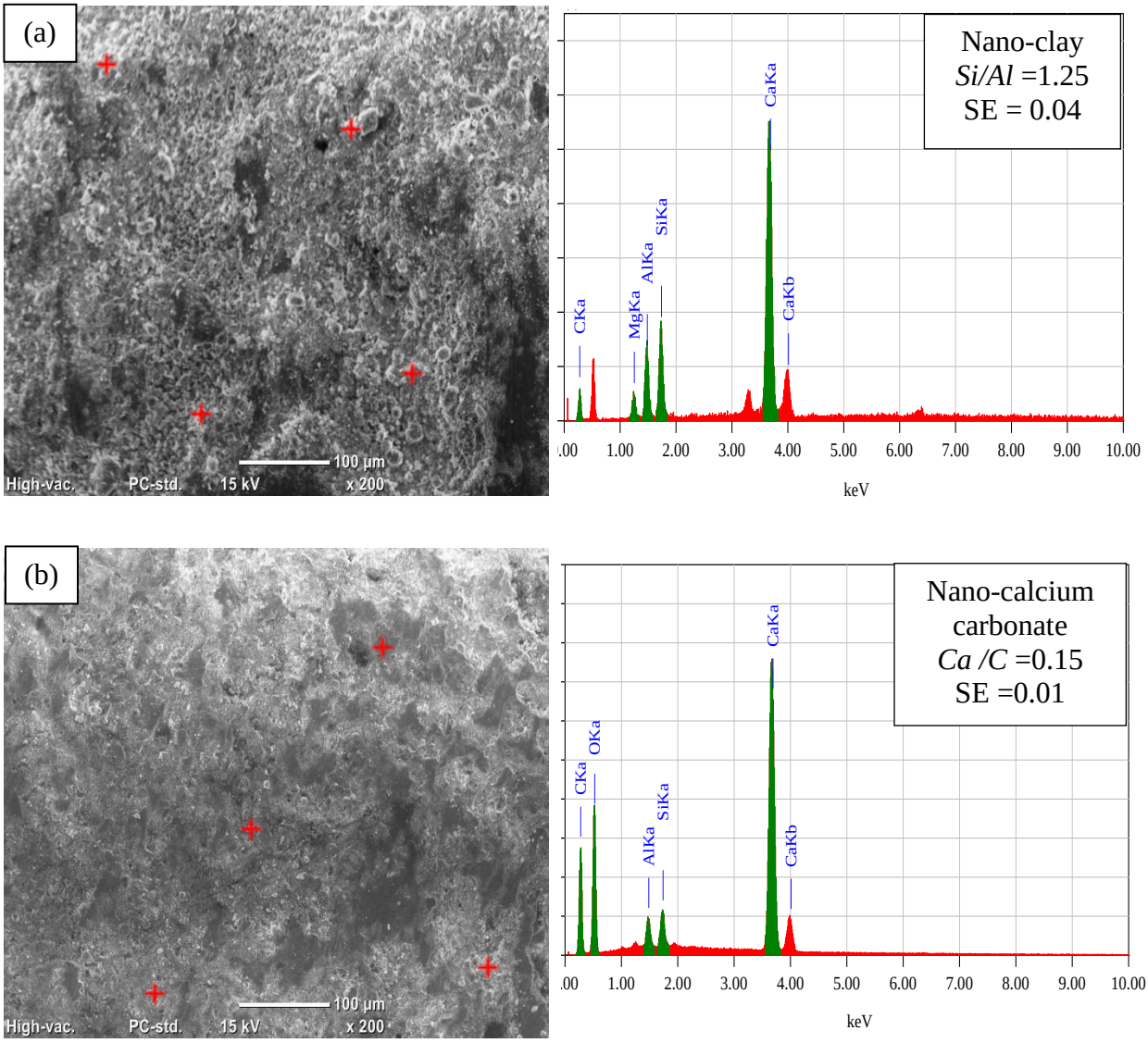

Figure 4. 14. Unexposed concrete specimens (*w/b* of 0.6) coated with: (a) SNC5% with associated EDX, and (b) SNCC5% with associated EDX. (Note: SE refers to the standard error for the average ratio of the marked location).

Likewise, silane/nano-calcium carbonate coatings improved the performance of treated concrete specimens relative to that of neat silane under both exposures. This might be attributed to the physical filler effect of nano-calcium carbonate (cubic crystals with a mean particle size of 50 nm) depositing on/into the surface layer of concrete (**Fig. 4.14)**, which conformed to reduced wettability (increased roughness) by an average of 24% (**Fig. 4.3**) and penetrability

(densification; very low class, **Table 4.1**) of these treated surfaces with increasing the nano-calcium carbonate dosage, relative to that treated with neat silane. In addition**,** nano-calcium carbonate has a basic nature, acting as a neutralizing or sacrificial buffer, at both dosages, to the acidic effect of the ammonium ions forming additional gypsum (**Eq. 4.5**) to that described in **Eqs. 4.1-4.3**, which contributed to decelerating the deterioration of concrete specimens by consuming part of the attacking solution in this process. As gypsum precipitation at the surface is much faster than the rate of ingress of sulfate ions into the specimens (Bouchelaghem 2010, Jahani et al. 2001).

$$CaCO_3 + (NH_4)_2SO_4 + H_2O \rightarrow CaSO_4.2H_2O + 2NH_3 + CO_2 \quad \text{(Eq. 4.5)}$$

However, the additionally formed gypsum on the surface of concrete might readily leach out to the solution, as for example indicated by the 9% average reduction, in the enthalpy of gypsum in the SNCC5% specimens relative to that in silane coated specimens (**Fig. 4.7**) at the end of exposures. These specimens showed reduced ettringite enthalpy by 16% compared to that of specimens coated with neat silane (**Fig. 4.9)**. Furthermore, the calcium carbonate particulates could react with portlandite (**Fig. 4.13;** marginal reduction of portlandite in SNCC2.5% and SNCC2.5% compared to S) and aluminate in the cement paste forming calcium carbo-aluminate hydrate according to (Dhandapani et al. 2021) by the following chemical reaction:

$$3CaO.Al_2O_3 + CaCO_3 + Ca(OH)_2 + 5H_2O \rightarrow 4CaO.Al_2O_3.CaCO_3.6H_2O \quad \text{(Eq. 4.6)}$$

This compound was found in the XRD analysis on the surface of specimens coated with nano-calcium carbonate particles, as for example shown in **Fig. 4.15.** It is an insoluble phase and

may contribute to further decelerating the rate of infiltration of ammonium sulfate solution in the cementitious matrix. This complies with previous studies that showed that the resistance of concrete to ammonium sulfate solutions was enhanced by using portland limestone cement in concrete instead of ordinary portland cement (Amin and Bassuoni 2018).

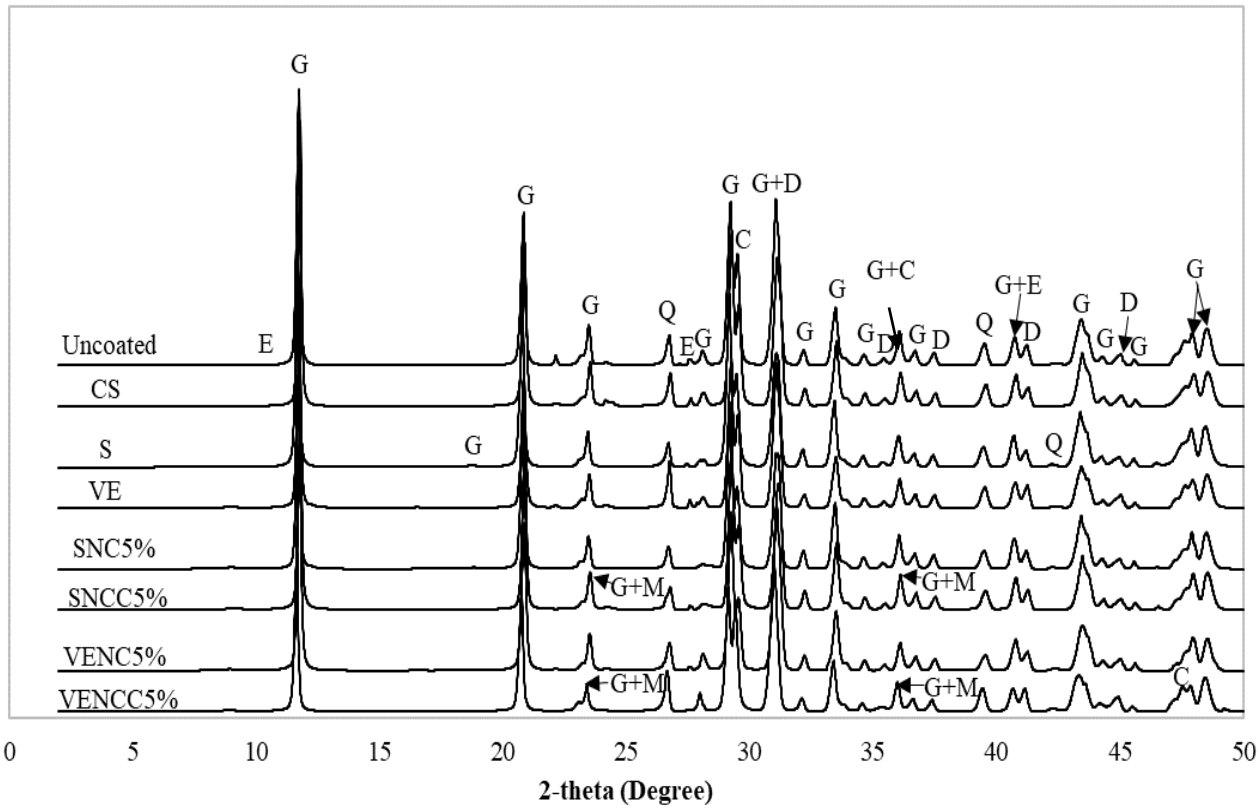

Figure 4. 15. XRD patterns of uncoated and coated specimens (*w/b* of 0.6) after 120 days of the full immersion exposure (Note: E = ettringite, G = gypsum, M = mono-carboaluminate, Q = quartz, C = calcite, D = dolomite).

4.2.5. Effect of Vinyl ester/Nanocomposites

Applying neat vinyl ester on concrete specimens generally enhanced the durability of concrete at both *w/b* to the full immersion and combined exposures. This could be attributed to membrane layer formed on the surface of concrete at a thickness ranging from 100 to 150 µm, due to the high viscosity of this resin [approximately 600 mPa·s] [**Fig**. **4.16(a)**]. Although, this membrane is not hydrophobic (**Fig. 4.3**), it significantly reduced the penetrability (very low, **Table 4.1**) of

concrete compared to that of uncoated concrete and concrete coated with silane. In addition, this layer was highly stable in the ammonium sulfate exposures and preserved adequate bonding with the concrete surface during both exposures as depicted in **Figs**. **4.16(b-c)**.

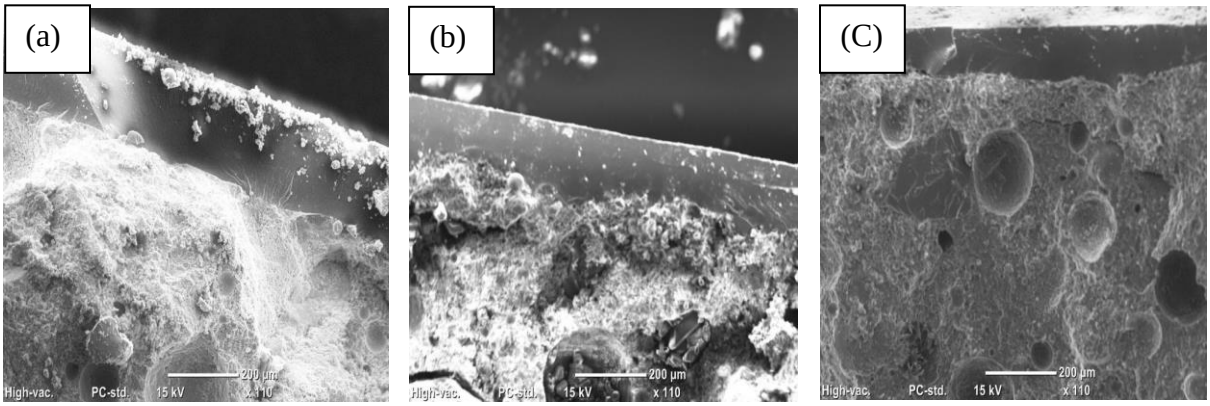

Figure 4. 16. Coated concrete specimens (*w/b* of 0.6) with vinyl ester: (a) unexposed, (b) after the full immersion exposure, and (c) after the combined exposure.

Similar to silane/nanocomposites, further improvement in the performance of concrete under both exposures was observed for concrete specimens coated with vinyl ester/nanocomposites (**Tables 4.2-4.5)**, with generally comparable performance of the nano-clay and nano-calcium carbonate particulates. The enhanced performance of concrete specimens treated with vinyl ester/nano-clay composites could be mainly attributed to the added barrier (physical) effect of the nano-clay particles dispersed in the resin (**Fig. 4.2**), which slightly increased with dosage. Moreover, the SEM analysis illustrated that the surface of concrete specimens coated with vinyl ester/nano-clay coatings had a continuous membrane of encapsulating NC particles [e.g., **Fig. 4.17(a)**]. In addition, the nano-clay particles in contact with concrete substrate stimulated a pozzolanic reaction with the cementitious matrix as discussed in the preceding section, since the portlandite content was further reduced (e.g., 24% reduction with VENC5% as shown in **Fig. 4.13**) relative to the specimens coated with neat vinyl ester. Hence, the net effect of the vinyl ester/nano-clay coatings led to enhancing the barrier

properties of the concrete surface, as indicated by the reduced penetrability of these specimens (**Table 4.1**), which discounted the ingress of the ammonium sulfate solution into the specimens and in turn the rate of damage relative to that of the specimens coated with neat vinyl ester. This conformed to the DSC results after both exposures; for example, lower enthalpy of gypsum (**Fig. 4.7**) in the full immersion and combined exposures (106.4 and 35 J/g, respectively) was found in the specimens coated with VENC5%, compared to that of specimens coated with neat vinyl ester (enthalpy of 130.8 and 54.6 J/g, respectively).

Vinyl ester/nano-calcium carbonate coatings enhanced the performance of superficially treated concrete specimens relative to that of neat vinyl ester under both exposures. SEM analysis substantiated that these specimens coated had a continuous vinyl ester membrane encapsulating nano-calcium carbonate particles, except for some surface clusters [**Fig. 4.17(b)**]. In addition to the vinyl ester protection and bonding to concrete substrate, the additive effects of nano-calcium carbonate (physical filler, neutralizing buffer), resulted in lower penetrability (**Table 4.1**) and higher stability of these coatings relative to that of vinyl ester; consequently, the results of mass and length change were reduced for these specimens relative to that of vinyl ester coated specimens.

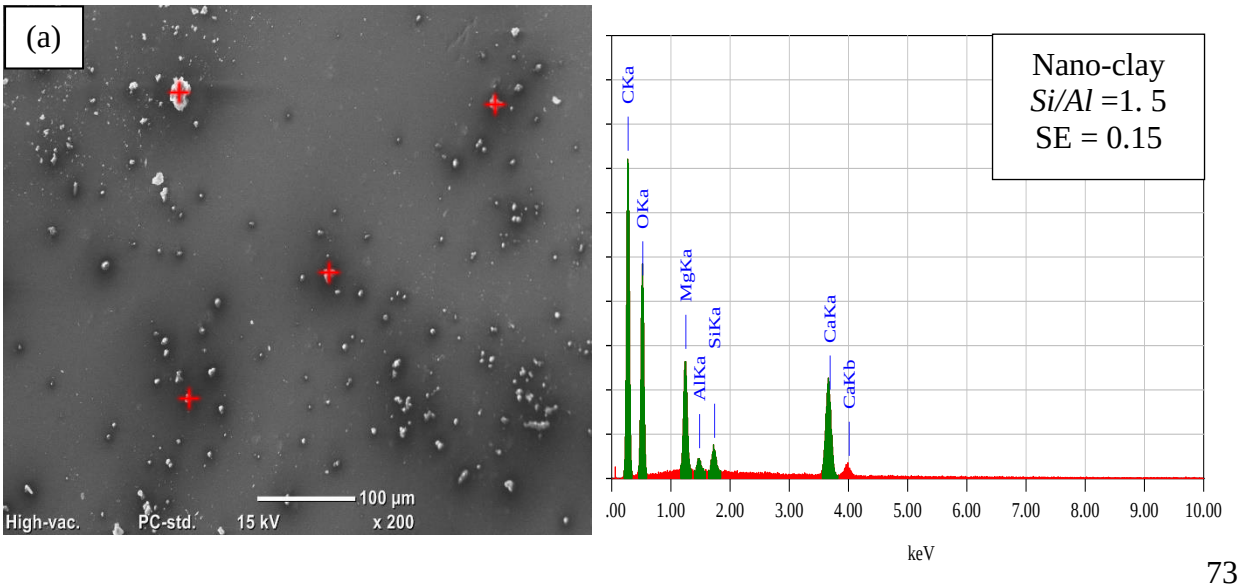

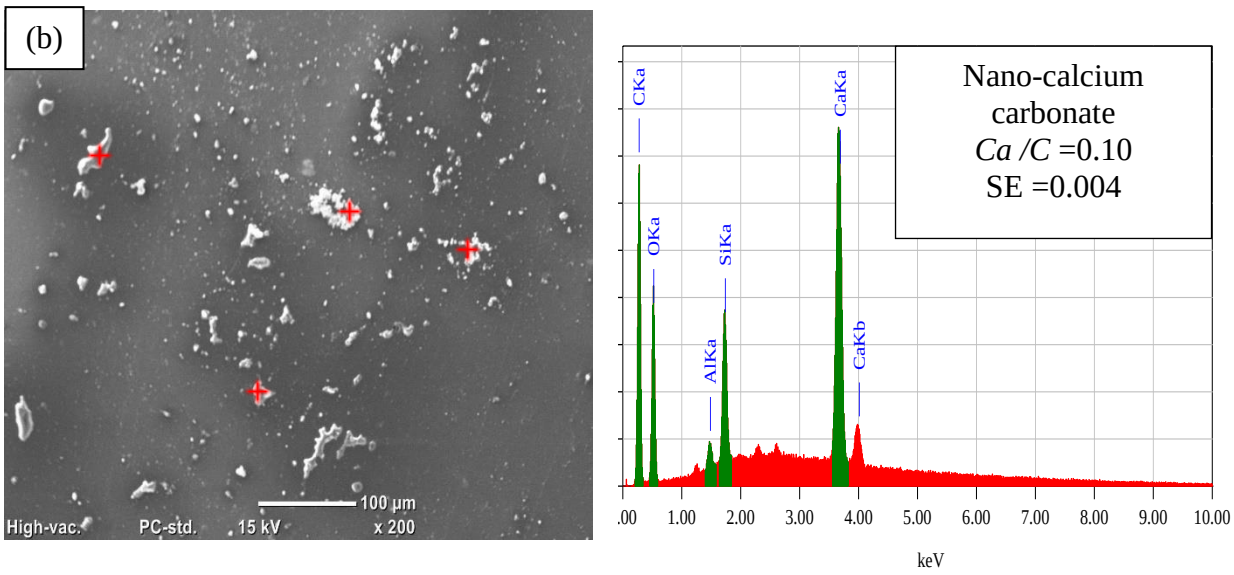

Figure 4. 17. Unexposed concrete specimens (*w/b* of 0.6): (a) coated with VENC5% with EDX, and (b) coated with VENCC5% with EDX. (Note: SE refers to the standard error for the average ratio of the marked location).

5. Phase II: Results and Discussion for Sulfuric Acid Attack

5.1. Results

5.1.1. Dispersion of Nanoparticles in Polymers

As the surface treatments and mixture designs are the same in this chapter, the results of TEM and ESEM described in the previous section (Section 4.1.1) were also relevant here and further discussion was excluded from this chapter to avoid redundancy.

5.1.2. Wettability of Coated Concrete

As the nano-modified coatings and mixture designs are the same in this chapter, the results of wettability test described in the previous section (Section 4.1.2) were also relevant here and further explanation was excluded from this chapter to avoid redundancy.

5.1.3. Penetrability of Concrete

As the surface treatments and mixture designs are the same in this chapter, the results of RCPT described in the previous section (Section 4.1.3) were also relevant here and further discussion was excluded from this chapter to avoid redundancy.

5.1.4. Visual Assessment

Concrete specimens experienced noticeable signs of (softening, swelling, loss of surface, and exposure of aggregates) depending on the *w/b* and type of coatings. The deterioration of concrete specimens was slower under the W/D exposure, but the trends of uncoated and coated concrete specimens were generally similar in terms of performance. Under both exposures, uncoated concrete specimens (UC) with *w/b* of 0.4 experienced more deterioration (visual ratings of 4 and 3), compared to concrete with *w/b* of 0.6 (visual rating of 3 and 2) [e.g., **Fig. 5.1**]. Similarly, the

concrete specimens coated with colloidal silica experienced softening and intensive surface loss (visual ratings of 4 and 3) under both exposures [e.g., **Fig. 5.2**].

(a) [4] (b) [3] (c) [3] (d) [2]

Figure 5. 1. Examples of uncoated concrete specimens: (a) UC-*w/b* 0.4-full immersion exposure, (b) UC-*w/b* 0.6-full immersion exposure, (c) UC-*w/b* 0.4-combined exposure, and (d) UC-*w/b* 0.6-combined exposure. (Note: numbers between brackets represent the final visual rating).

Under both exposures, concrete specimens coated with silane experienced surface softening and notable surface loss of the entire specimens (**Figs. 5.2 and 5.3**). Overall, the neat silane and nano-modified silane coatings showed comparable performance with visual ratings between 3 and 5. Comparatively, concrete specimens coated with neat or nano-modified vinyl ester had the best performance under both exposures maintaining large areas of intact coating (visual ratings of 2 to 3) [**Figs. 5.2** and **5.3**]. They only experienced localized peeling towards the ends and at some spots combined with surface loss, which was also observed for the nano-modified vinyl ester composites. However, the visual assessment could not decisively distinguish the level of preservation among specimens coated with different coatings, and other evaluation parameters (mass change) are thus needed.

Figure 5. 2. Examples of coated concrete specimens (GU-FA0.4) after 10 weeks in the full immersion exposure. (Note: numbers between brackets represent the final visual rating).

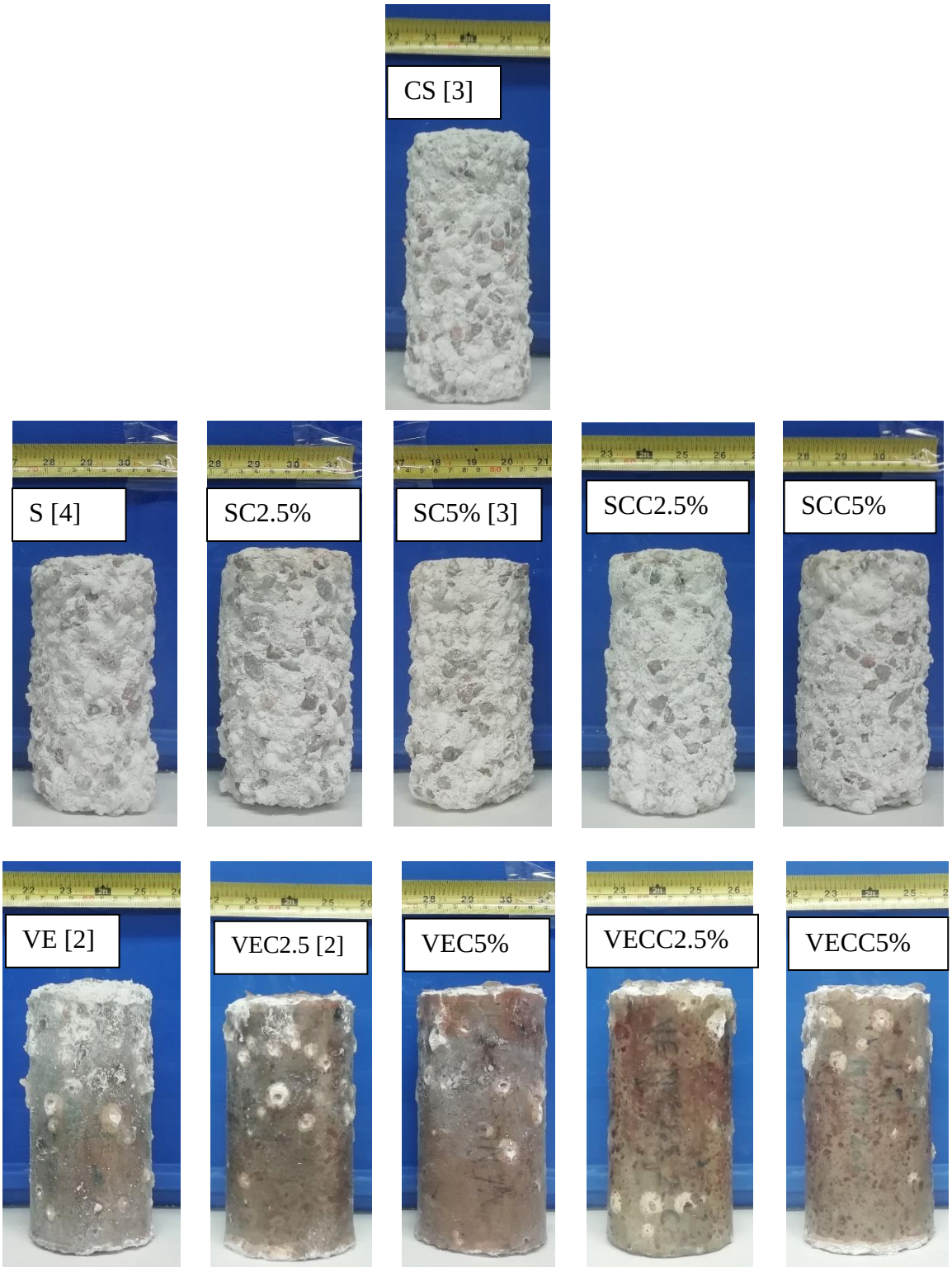

Figure 5. 3. Examples of coated concrete specimens (GU-FA0.4) after 10 weeks in the W/D exposure. (Note: numbers between brackets represent the final visual rating).

5.1.5. Mass Change

The mass change of specimens during the full immersion exposure is illustrated in **Figs. 5.4-5.5**. At a *w/b* of 0.4, uncoated specimens and specimens coated with colloidal silica, silane and silane/nanocomposites experienced continual mass loss during this exposure reaching high loss values between 18 to 35%. On the other hand, counterpart specimens with a *w/b* of 0.6 experienced mass gain (6 to 8%) for four weeks followed by high rates of mass loss, but the ultimate cumulative losses were small (maximum 4%) after 10 weeks considering the initial mass gain of specimens. Concrete specimens treated with colloidal silica showed comparable mass change results to that of uncoated specimens at both *w/b*.

Blending silane with nano-clay and nano-calcium carbonate particles comparably reduced the surface damage of the specimens (**Fig. 5.4**). For example, at a *w/b* of 0.4 specimens coated with silane/nanocomposites had an average mass loss reduction of 38% compared to that of specimens coated with neat silane, which had the highest cumulative mass loss of 35%. Similarly, at a *w/b* of 0.6, applying silane/nanocomposites on concrete significantly reduced the cumulative mass change by an average of 76% relative to that of the uncoated specimens.

Concrete specimens coated with vinyl ester and vinyl ester/nanocomposites with *w/b* of 0.4 had mass gain up to five weeks, followed by marginal mass losses with a maximum cumulative value less than 3%. Similarly, counterpart specimens with *w/b* of 0.6 had continual, but marginal mass gain (less than 1%), conforming to the preservation of the vinyl ester coatings (**Figs. 5.2** and **5.3**). These coatings had the best overall performance under the full immersion exposure. For example, at a *w/b* of 0.4, specimens coated with vinyl ester and vinyl ester/nano-clay (VEC5%) had reduced mass losses by an average of 98%, compared to that of uncoated specimens (mass loss of 18%). Applying vinyl ester/nanocomposites further improved the

performance of neat vinyl ester to different extents for concrete with *w/b* of 0.6. For example, at a *w/b* of 0.6, applying VEC5% and VECC 2.5% on concrete specimens reduced the cumulative mass change by 45% and 55%, respectively compared to that of specimens coated with neat vinyl ester.

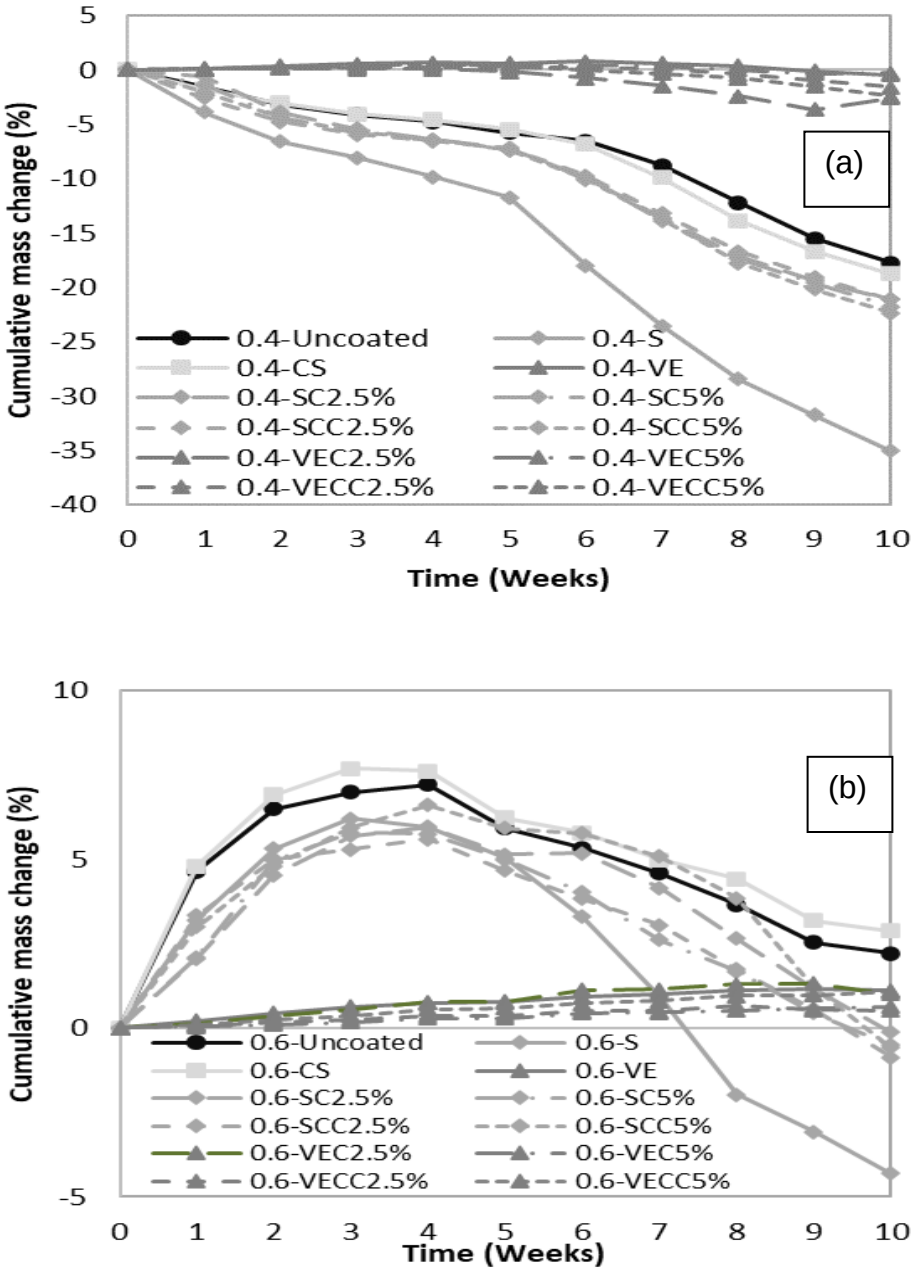

Figure 5. 4. Mass change of concrete specimens over time in the full immersion exposure: (a) GU-FA-0.4, and (b) GU-FA-0.6.

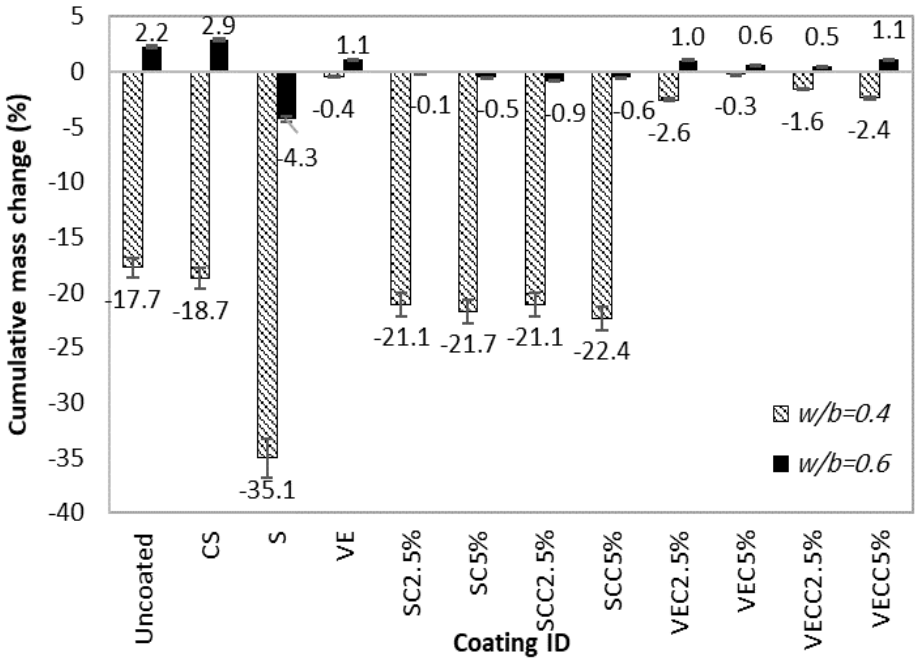

Figure 5. 5. Cumulative mass change of concrete specimens after 10 weeks in the full immersion exposure.

The mass change of specimens during the combined exposure is demonstrated in **Fig. 5.6, 5.7**. Specimens with *w/b* of 0.4 experienced continual mass loss during the exposure, which could be attributed to precipitation of voluminous reaction products leading to softening, spalling, and surface scaling. On the other hand, uncoated concrete and specimens coated with CS with *w/b* of 0.6 experienced mass gain for two weeks of the exposure followed by mass loss till the end of exposure. Concrete specimens (*w/b* of 0.6) coated with neat silane and silane/nanocomposites experienced similar trend of mass gain for the first five and seven weeks, respectively followed by mass loss. This mass gain might be due to initial solution absorption, deposition of chemical reaction products within the surface layer of specimens, and direct uptake of solution. On the other hand, concrete specimens coated with VE and VE/nanocomposites with *w/b* of 0.6 experience slight mass gain and showed mass loss during the exposure based on the *w/b* and type of coatings. Uncoated concrete specimens with lower *w/b* (0.4) significantly deteriorated (mass loss of 12.9%) at the end of the combined exposure, while uncoated concrete

specimens with *w/b* of 0.6 experienced 2.5% mass gain (**Fig. 5.1**). In addition, the mass change of specimens was discounted with the application of VE coatings, complying with the visual observations (**Fig. 5.3**).

Concrete specimens treated with CS had a slight reduction in cumulative mass loss by 5% relative to that of the uncoated specimens in the 0.4 *w/b* group. For coated concrete specimens with *w/b* of 0.4, neat silane and silane/nano-clay coatings failed to protect concrete from sulfuric acid attack. These specimens experienced higher cumulative mass change relative to that of uncoated specimens at the end of the exposure (**Fig. 5.7**). However, silane/nano calcium carbonate slightly reduced the deterioration of concrete specimens relative to the uncoated specimens. For instance, applying SCC2.5% and SCC5% reduced the cumulative mass loss by an average of 5% compared to that of uncoated specimens. On the other hand, applying vinyl ester on specimens effectively protected the concrete from the sulfuric acid solution (visual rating of 2; **Fig. 5.3**). These specimens experienced a cumulative mass loss of 0.6%, while the uncoated specimens experienced a cumulative mass loss of 12.9% after 10 weeks of the combined exposure. Adding nano particulates to the neat resin at a dosage of 5% resulted in a comparable performance relative to that of the neat vinyl ester.

Indeed, coated concrete specimens with *w/b* of 0.6 had lower mass change (-2 to 0.7%) relative to that of counterpart specimens with *w/b* of 0.4 (range of mass change from -19.9 to -0.6%). Applying neat silane on concrete specimens with *w/b* of 0.6 resulted in a higher cumulative mass change at the end of exposure. However, applying SC2.5% and SC5% reduced the cumulative mass change by 80 and 30%, respectively compared to that of uncoated specimens. In addition, applying silane/nano-calcium carbonate coatings on concrete specimens reduced the cumulative mass change by an average of 65% compared to that of uncoated

specimens. On the other hand, applying neat vinyl ester on concrete reduced the cumulative mass change by 60% compared to that of uncoated specimens after 10 weeks of exposure. Applying VE/nanocomposites on concrete specimens resulted in a comparable performance relative to that of the specimens treated with neat vinyl ester. Concrete specimens coated with CS had an increment in cumulative mass change by 50% relative to that of the uncoated specimens in the 0.6 *w/b* group.

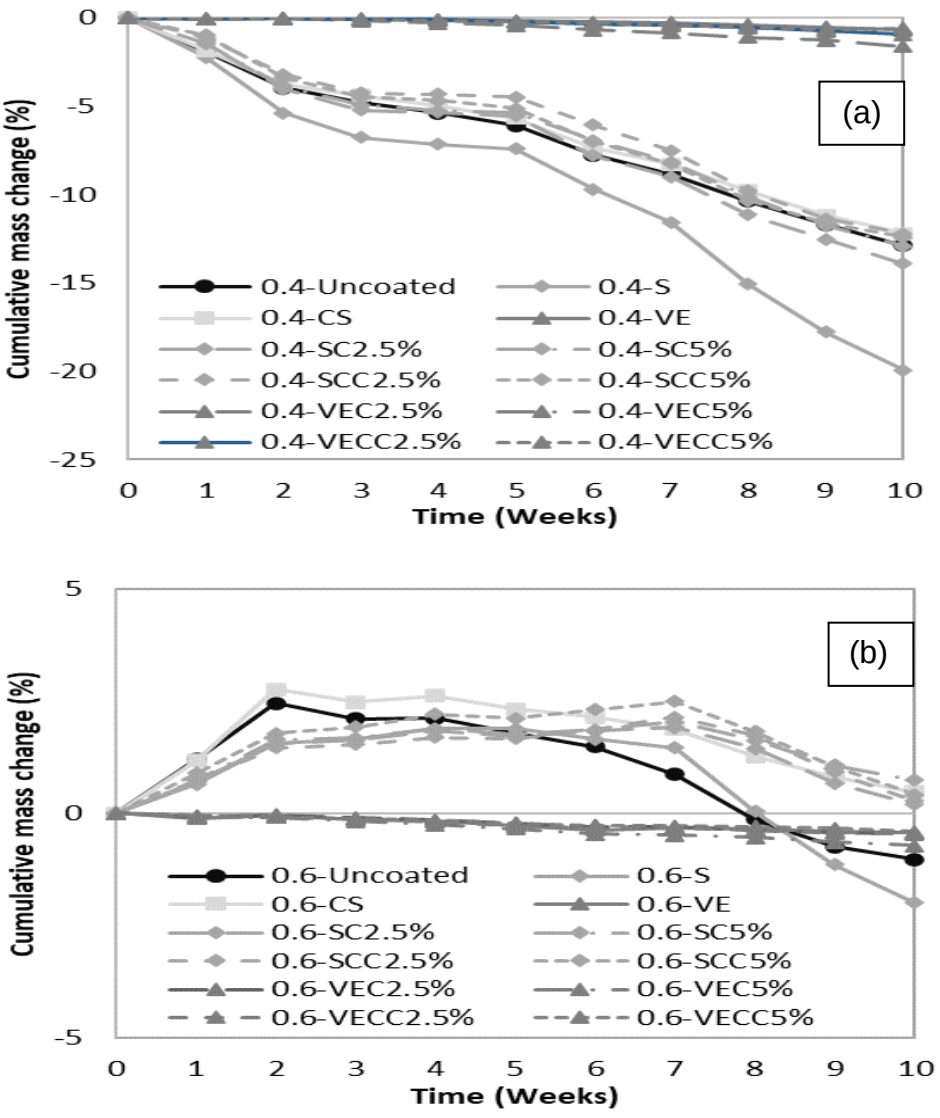

Figure 5. 6. Mass change of concrete specimens over time in the W/D exposure: (a) GU-FA-0.4, and (b) GU-FA-0.6.

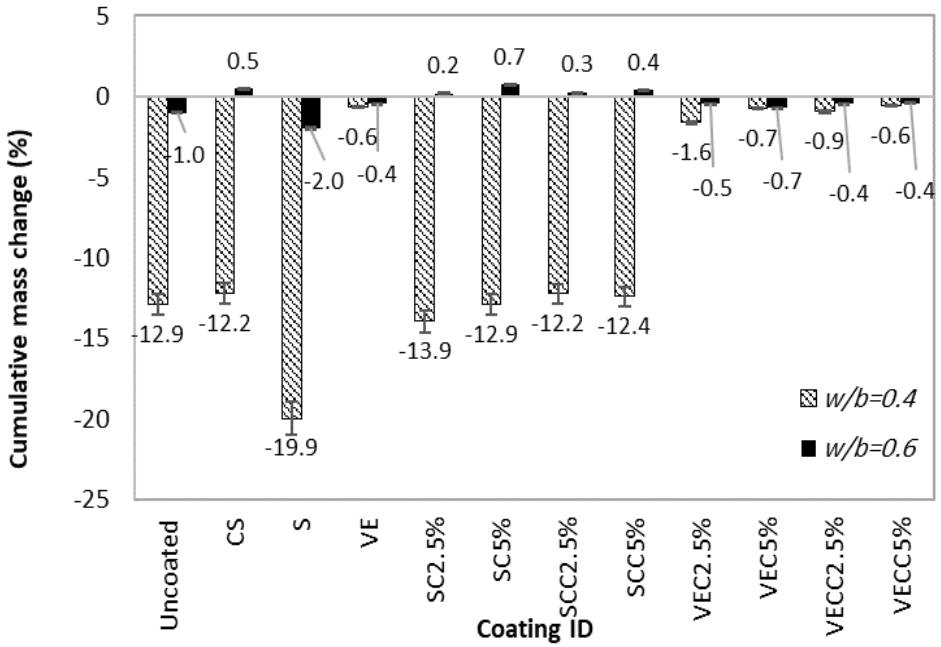

Figure 5. 7. Cumulative mass change of concrete specimens after 10 weeks in the W/D exposure.

5.2. Discussion

5.2.1. Mechanisms of Damage

The detrimental effect of sulfuric acid attack on concrete is more severe than that of ammonium sulfate attack, which could be attributed to the combined effects of sulfate ions attack, and dissolution effect of hydrogen ions (Attiogbe and Rizkalla 1988). In the full immersion exposure, paste deterioration due to sulfuric acid attack can generally be described by the following chemical reactions (Monteny et al. 2000):

$$Ca(OH)_2 + H_2SO_4 \rightarrow CaSO_4.2H_2O \qquad \text{(Eq.5.1)}$$

$$Ca.SiO_2.2H_2O + H_2SO_4 \rightarrow CaSO_4 + Si(OH)_4 + H_2O \qquad \text{(Eq.5.2)}$$

$$3CaO.Al_2O_3.12H_2O + 3(CaSO_4.2H_2O) + 14\,H_2O \rightarrow 3CaO.Al_2O_3.3CaSO_4.32H_2O \qquad \text{(Eq.5.3)}$$

Gypsum is the major reaction product, from the decomposition of main paste components CH and C-S-H, manifested on the concrete surface, as for example depicted in **Figs. 5.8-5.9,** which led to softening and volume expansion [factor of 2.2 relative to the initial volume of its reactants (Monteny et al. 2001)], inducing high tensile stresses in the matrix, and consequently spalling of concrete (**Figs. 5.1-5.2)**. If not leached away, the precipitation of gypsum on the concrete surface might slow down the infiltration rate of sulfuric acid solution due to surface sealing.

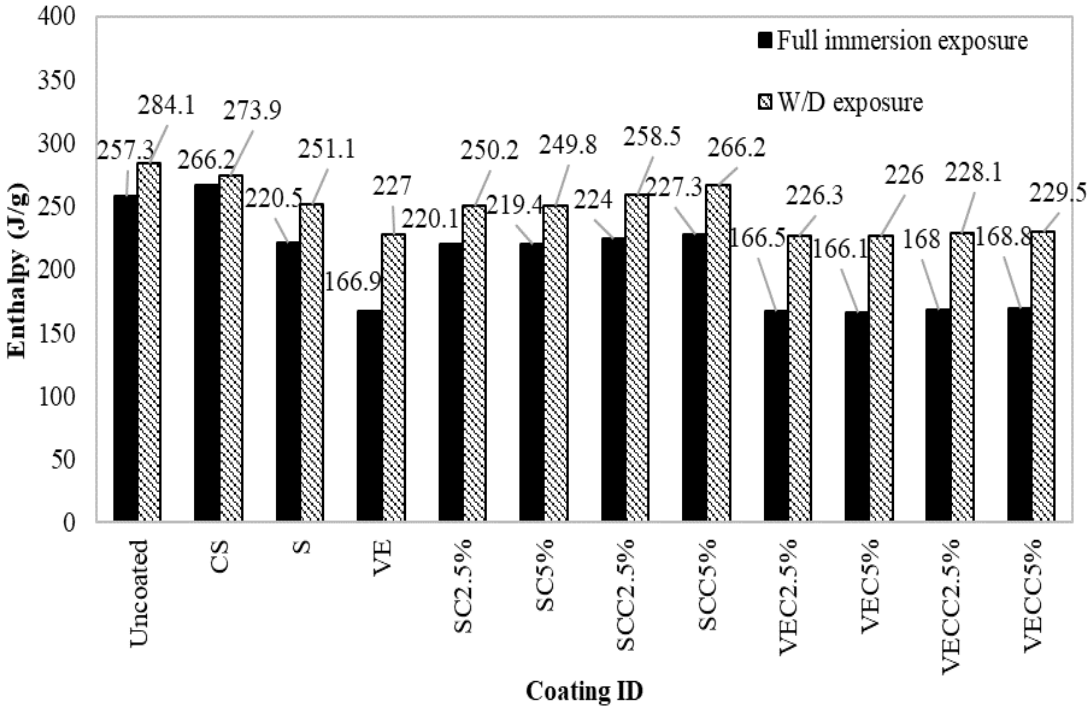

Figure 5. 8. Enthalpy of gypsum (dehydration range of 120-135°C) in uncoated and coated specimens (*w/b* of 0.4) after 10 weeks in the full immersion and W/D exposures. (Note: accuracy of enthalpy determination is ±3%).

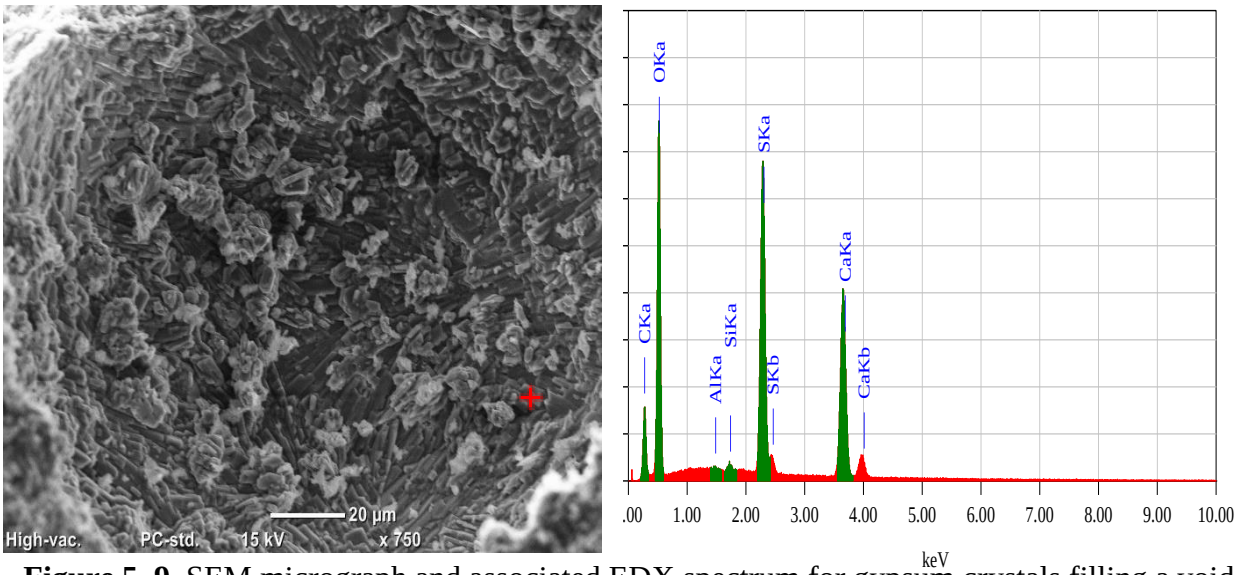

Figure 5. 9. SEM micrograph and associated EDX spectrum for gypsum crystals filling a void near the concrete surface of uncoated concrete (*w/b* of 0.6) after the full immersion exposure.

In addition, the reaction between calcium aluminate phases in the paste and gypsum can lead to forming ettringite in deeper regions where the pH is greater than 9, as depicted in **Figs 5.10-5.11,** which has a significant volume increment [up to a factor of 7 relative to the initial volume of its reactants (Monteny et al. 2000)], thus resulting in more micro-cracking (e.g., **Fig. 5.12**). Indeed, these cracks provide direct paths for infiltration of additional sulfuric acid solution, formation of additional reaction products, and thus significant damage and mass loss (**Figs. 5.1, 5.2 and 5.5**). The precipitated crystals of gypsum and ettringite were also confirmed by the mineralogical analysis by XRD as shown in **Fig. 5.13**. The calcite and dolomite peaks originated from the fraction of carboniferous aggregate, which is contained in the coarse aggregate of concrete, while the quartz peaks occurred as a result of using sand, siliceous coarse aggregate, and fly ash in all the concrete mixtures.

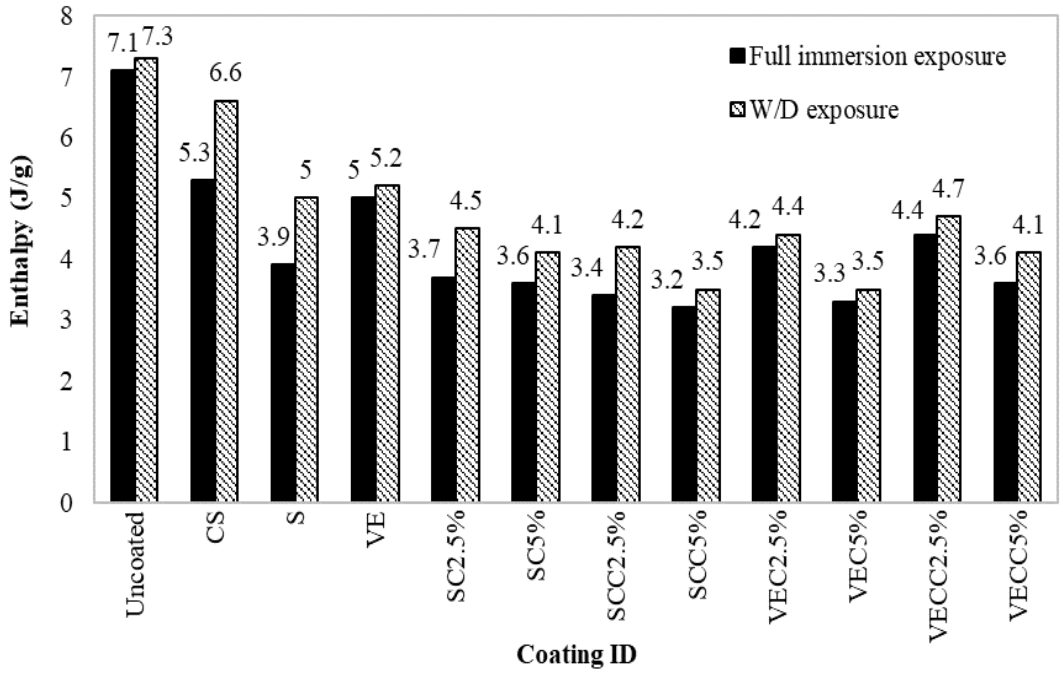

Figure 5. 10. Enthalpy of ettringite (dehydration peak at 90°C) in uncoated and coated specimens (*w/b* of 0.4) after 10 weeks in full immersion and W/D exposures. (Note: accuracy of enthalpy determination is ±3%)

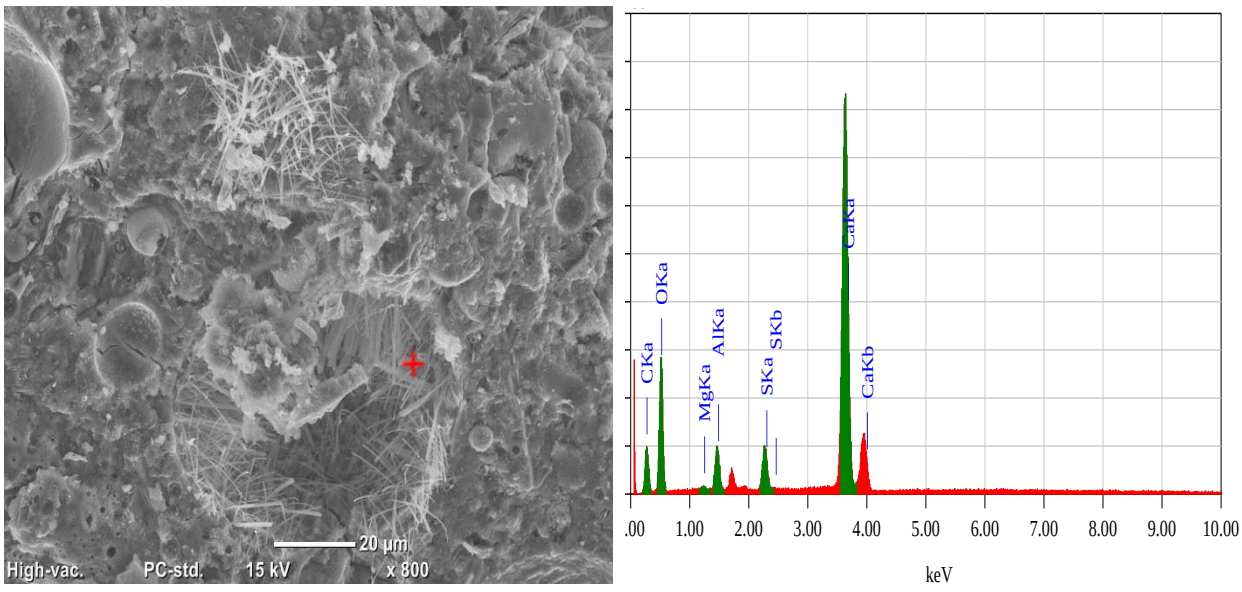

Figure 5. 11. SEM micrograph and associated EDX spectrum for ettringite crystals away from the concrete surface of uncoated concrete (*w/b* of 0.4) after the W/D exposure.

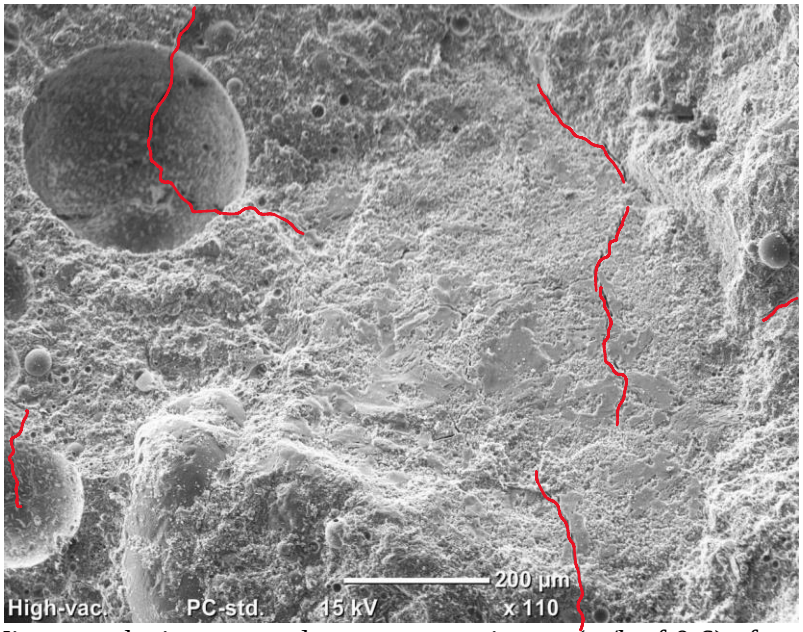

Figure 5. 12. Micro-cracks in uncoated concrete specimens (*w/b* of 0.6) after 10 weeks in the full immersion exposure.

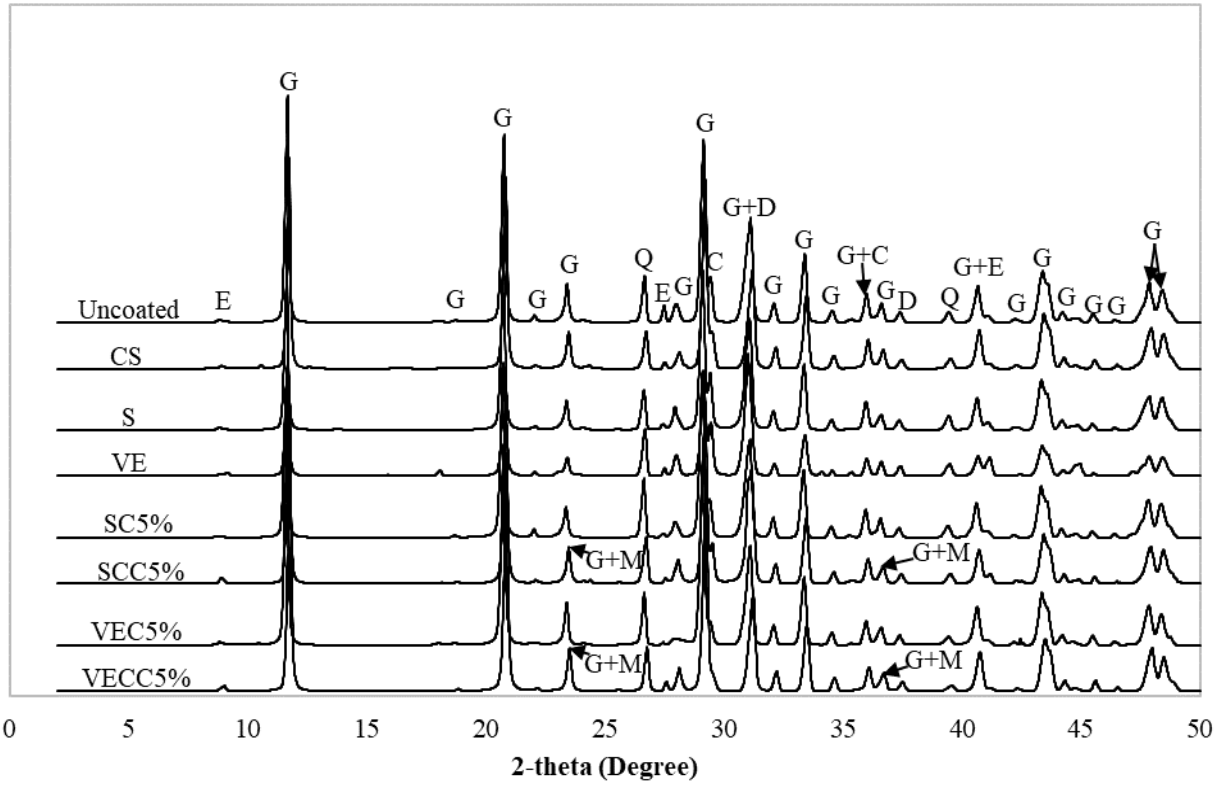

Figure 5. 13. XRD patterns of uncoated and coated specimens (*w/b* of 0.4) after 10 weeks of the full immersion exposure (Note: E = ettringite, G = gypsum, M = mono-carboaluminate, Q = quartz, C = calcite, D = dolomite).

In the W/D exposure, the sulfuric acid deleterious effects on concrete were impacted by the W/D cycles. The reduction in exposure time to the sulfuric acid solution led to less damage manifestations and cumulative mass change (**Figs. 5.1, 5.3, and 5.7**). Similar trends were observed in previous studies (Irico et al. 2020; Gu et al. 2018) Unlike the full immersion exposure, in which continual attack of the paste occurred associated with continual formation and leaching of gypsum. The W/D exposure allowed for additional intrusion of sulfuric acid solution by capillary suction after the drying periods, in which gypsum formation was not accompanied by leaching. Hence, more gypsum built up within the surface zone of concrete was after the W/D exposure (**Fig. 5.8**), which acted as a passivating layer or buffer, reducing the rate of solution ingress, and thus discounting the rate of deterioration of concrete. On the other hand, secondary ettringite formation might be promoted in the W/D exposure, due to the effect of wetting-drying cycles (Stark and Bollmann 1999). With changing the moisture conditions during the W/D cycles, recrystallization and precipitation of secondary ettringite into large crystals might be possible due to Ostwald Ripening (crystallization of large crystals at the expense of smaller crystals to attain thermodynamic stability) (Boistelle and Astier 1988). However, the precipitated amounts of ettringite after the W/D exposure was marginally higher than that of the full immersion exposure (**Fig. 5.10**), and it did not exacerbate the deterioration of concrete specimens in this exposure.

5.2.2. Effect of water-to-binder ratio

Overall, reducing the *w/b* decreased the penetrability of concrete specimens as indicated by the RCPT results (**Table 4.1**), due to refining the matrix pore structure complying with the well-known effect of *w/b* reduction at reducing concrete penetrability (Mehta and Monteiro 2014). For example, (Sakr et al. 2019), reported that decreasing the *w/b* from 0.6 to 0.4 for similar concrete

significantly reduced the total intrusion by 45% by mercury intrusion porosimetry; as the threshold pore diameter remarkably reduced from 0.3 to 0.075 µm. However, after the sulfuric acid exposures herein, concrete specimens with a *w/b* of 0.4 experienced higher mass loss relative to that of the specimens with a *w/b* of 0.6 (**Figs. 5.5 and 5.7**), with corresponding increase in the amount of reaction products (approximately 4% and 38% for gypsum and ettringite, respectively. Similar trends were also observed in previous studies (Hewayde et al. 2007; Jirasit et al. 1999; Fattuhi and Hughes 1988a,b).

This trend could be attributed to the increased paste volume vulnerable to decomposition in the concrete with a lower *w/b* relative to that of concrete with high *w/b* (Fattuhi and Hughes 1988b). In addition, concrete with a *w/b* of 0.4 has denser microstructure than that of concrete with a *w/b* of 0.6; the higher volume of paste with smaller pore sizes directly interacted with the sulfuric solution with limited intrusion into the matrix (**Table 4.1**). Consequently, the surface layer continually decomposed precipitating gypsum crystals as depicted in **Fig. 5.14(a)**, which could be easily detached from the concrete surface to the solution causing, leaving behind an underlying layer of sound paste ready for interaction with the acid [e.g., **Fig. 5.14(b)**]. It was also stated that the internal core of concrete may have a dense microstructure in an acidic medium due to continual hydration of the cementitious matrix, reduction in calcium-to-silicate ratio and polymerisation of C-S-H (Macías et al. 1999). This progressive layer by layer attack of concrete led to remarkable deterioration and loss of cross-section as depicted in **Fig. 5.1**. On the other hand, concrete with a *w/b* of 0.6, possessing a porous and coarse microstructure, could absorb the acidic solution significantly into the concrete (**Table 4.1**), which reacted into the cementitious matrix forming accumulating gypsum crystals in the coarse pore structures (**Fig. 5.9),** resulting in significant swelling of the concrete specimens (**Fig. 5.1)**, and internal cracking (**Fig. 5.12**).

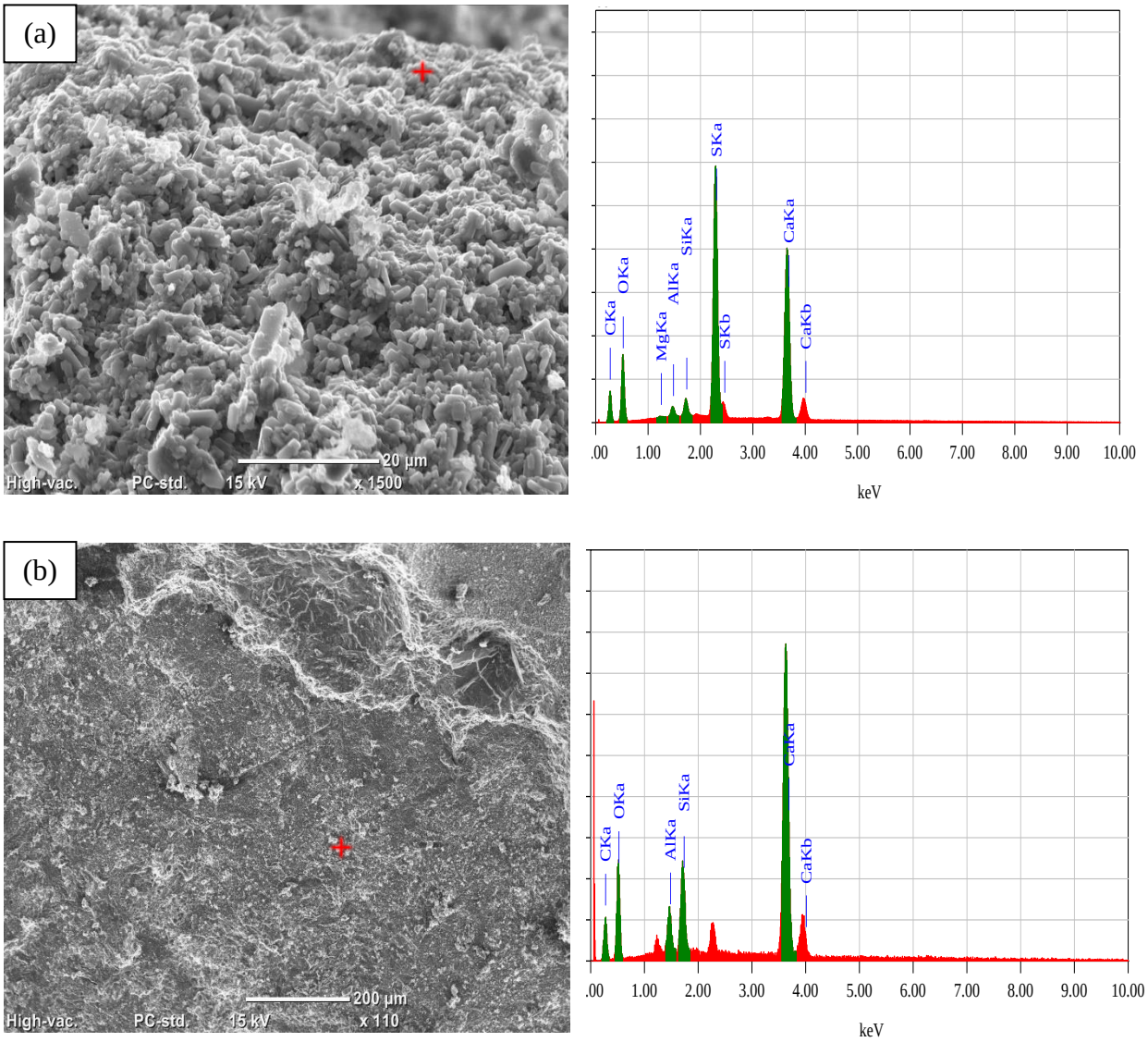

Figure 5. 14. SEM micrograph and associated EDX spectrum for uncoated concrete (*w/b* of 0.4) after the full immersion exposure: (a) gypsum crystals covering the surface of concrete specimens, and (b) a dense core with C-S-H in the concrete specimens.

5.2.3. Effect of Colloidal Silica

Albeit specimens coated with colloidal silica had better resistance to infiltration of fluids compared to uncoated specimens (RCPT; **Table 4.1**), both groups of specimens performed comparably under the sulfuric acid exposures (**Figs. 5.1-5.7**). On one hand, partial amounts of

colloidal silica agglomerates on the concrete surface (**Fig. 5.15**) could stimulate pozzolanic reactivity with calcium hydroxide to precipitate C-S-H, thus refining the pore structure of concrete surface and in turn reducing its penetrability. This was suggested by the notable depletion of calcium hydroxide (approximately 33%) in the surface of specimens coated with colloidal silica compared to that of uncoated specimens (**Fig. 5.16**).

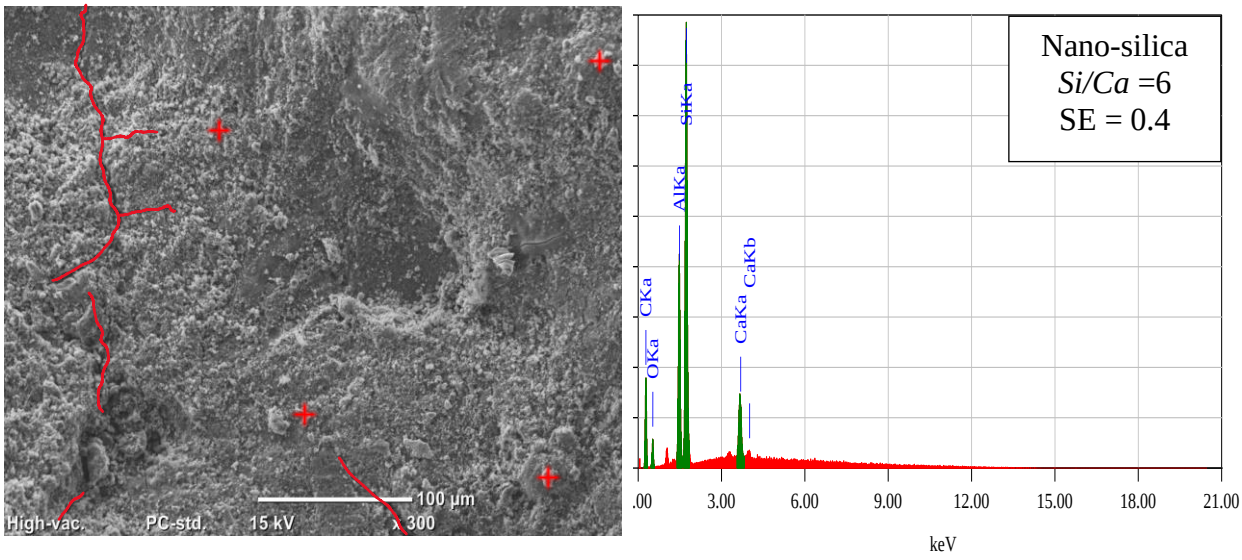

Figure 5. 18. Precipitation of condensed nano-silica particles on the surface of unexposed concrete coated with CS (*w/b* of 0.6) with shrinkage micro-cracks on the surface and associated EDX for nano-silica particles. (Note: SE refers to the standard error for the average ratio of the marked location).

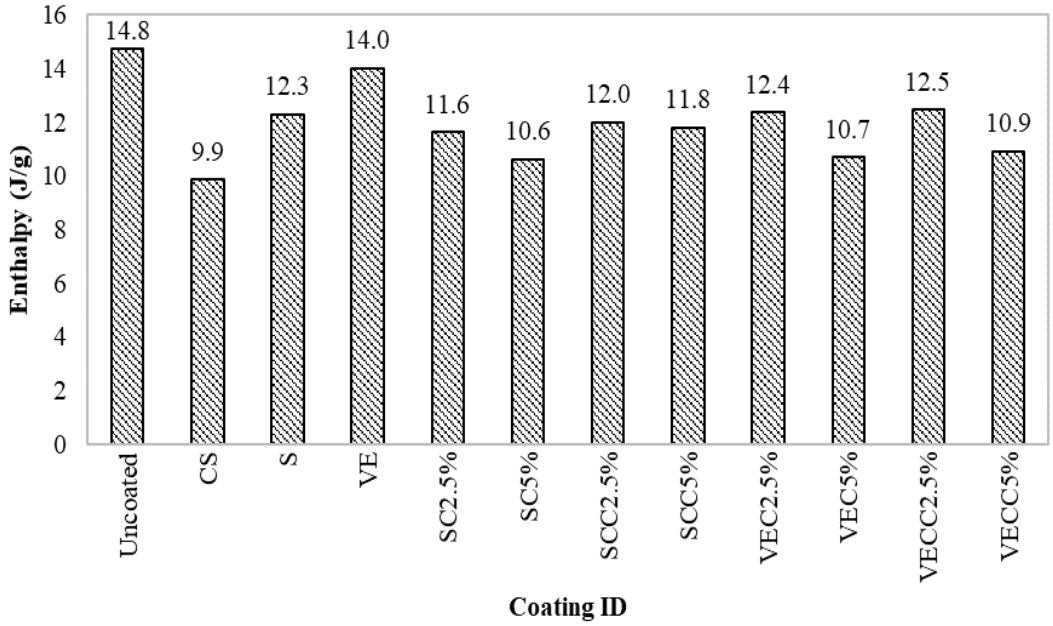

Figure 5. 15. Enthalpy of portlandite (dehydration range of 400-450°C) in uncoated and coated specimens (*w/b* of 0.4) after 56 days of curing. (Note: accuracy of enthalpy determination is ±3%).

On the other hand, this initial reduction in penetrability did not provide continual protection for concrete with time under the sulfuric acid solution, since the enthalpy of ettringite and gypsum in these specimens were close to that of uncoated specimens (7.1 and 7.3 J/g, and 257.3 and 284.1 J/g, respectively) by the end of both exposures [**Figs. 5.8** and **5.10**]. This might be due to the precipitation of a condensed silica layer, with ultra-high surface area (175-225 m^2/g) on the concrete surface (**Fig. 5.15),** which have affinity for water **(Fig. 4.3**), thus readily absorbing the sulfuric acid solution into the concrete surface. The continuity of this layer was also interrupted by micro-cracks, likely due to shrinkage form volatilization of dispersing agent during the drying period (two days before exposures), serving as localized entries for the sulfuric acid solution to the concrete surface. Moreover, the remarkable decrement of calcium hydroxide, and hence rich in cement gel, directly susceptible to decalcification by the sulfuric acid solution, precipitating gypsum leaching out to the solution. Hence, the deterioration of concrete gradually processed to interior layers (unaffected by colloidal silica) in a manner similar to that of uncoated concrete.

5.2.4. Effect of Silane/Nanocomposites

Silane can penetrate into the pore network of concrete surface due to its low viscosity and small particle size (nano- to micro-meter) and interact with portlandite in the hardened paste forming an active hydrophobic compound (Moon and Lee 2017). Also, it was indicated that silanol groups might form and react with portlandite in the cementitious matrix precipitating C-S-H (Chen et al. 2020) resulting in refined microstructure with reduced penetrability. This was demonstrated by the DSC results at 56 days, as the surface of specimens coated with silane had

relatively less portlandite (12.3 J/g) than that in the uncoated specimens [14.8 J/g] (**Fig. 5.16**). The aforementioned interactions were confirmed by the enhancement in RCPT results (**Table 4.1**) and contact angle measurements (**Fig. 4.3**) relative to that of uncoated concrete. However, the precipitated cement gel increased the volume fraction of the paste comprising less portlandite, and thus it was vulnerable to chemical deterioration by sulfuric acid (**Eq. 5.3**) transforming into gypsum and hydrous silica gel. The latter is metastable and could disintegrate at low pH levels [less than 6] (Alexander et al. 2013; Gaze and Crammond 2000; Hobbs and Taylor 2000). The pH of the solution in the current study was less than 1.0, which might have resulted in rapid decomposition of the silane coated surface, thus opening entry paths for infiltration of more sulfuric acid solution. Furthermore, silane could not bridge these new surface pathways after its initial application (ACI 515.2R). The aforementioned patterns led to inferior performance of concrete specimens superficially treated with neat silane compared to that of other specimens.

Relative to specimens coated with neat silane, notable improvement in the concrete performance under both acidic exposures was observed in concrete specimens superficially treated with silane/nanocomposites (**Figs. 5.2-5.7),** with generally comparable performance of the nano-calcium carbonate and nano-clay. However, comparable gypsum quantities were observed (in the full and W/D exposures; **Fig. 5.8**) in the surface layer of specimens superficially treated with SC5% and specimens coated with neat silane. The improved performance of concrete specimens coated with silane/nano-clay composites, could be due to the physical barrier effect due to the intermingling of the nano-clay particulates (**Fig. 4.1**), deposited on the concrete surface [**Fig. 5.17(a**)], and consequently discounting the rate of solution ingress. Hence, the additive effect of the silane/nano-clay composites led to increasing the hydrophobicity (**Fig.**

4.3) and densifying the concrete surface layer, as demonstrated by the reduction in initial penetrability of these specimens (RCPT, **Table 4.1**). In addition, nano-clay particulates was found to be stable in acidic environments (Roghanian and Banthia 2019). Moreover, the nano-clay particles (alumino-silicate content of more than 80%) appeared to have some level of pozzolanic activity in the paste, since the portlandite was relatively decreased (**Fig. 5.16**) compared to the specimens superficially treated with neat silane. However, this did not coincide with more deterioration of the concrete specimens, due to the dominant synergistic effects of silane (hydrophobicity) and nano-clay (surface barrier).

For silane/nano-calcium carbonate surface treatment, nano-calcium carbonate (mean particle size of 50 nm) acted as a filler in the concrete surface layer [**Fig 5.17(b)]**, which conformed to reduced penetrability (**Table 4.1**) and increased roughness/contact angle (**Fig. 4.3**) compared to that of specimens coated with neat silane. Moreover**,** it acting as a neutralizing zone to sulfuric acid precipitating additional gypsum (**Eq. 5.4**), which contributed to decelerating the rate of deterioration of concrete.

$$CaCO_3 + H_2SO_4 + H_2O \rightarrow CaSO_4.2H_2O + CO_2 \qquad \text{(Eq. 5.4)}$$

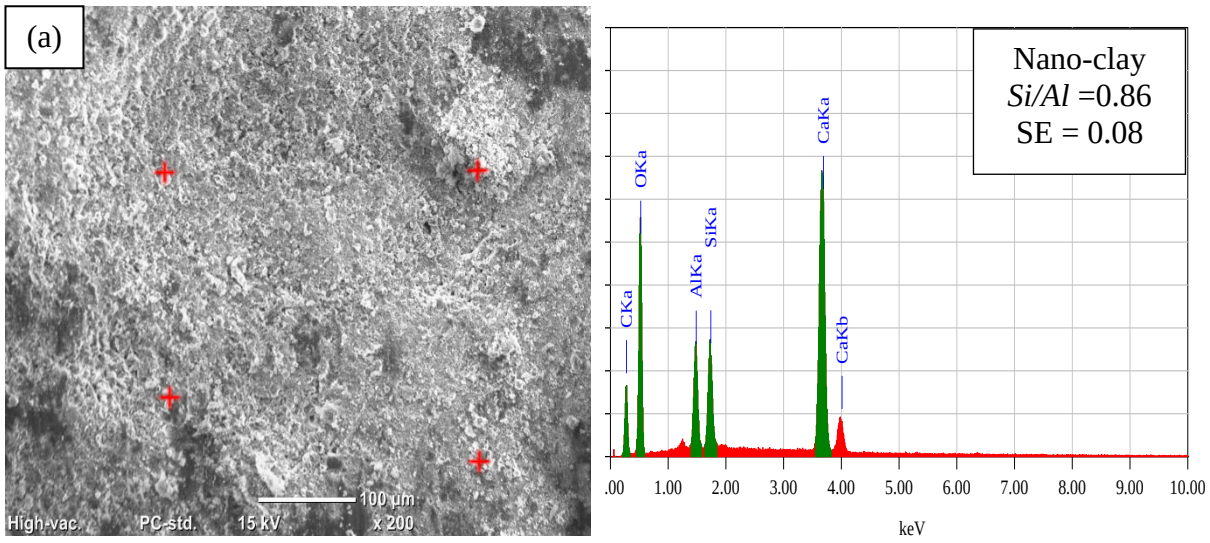

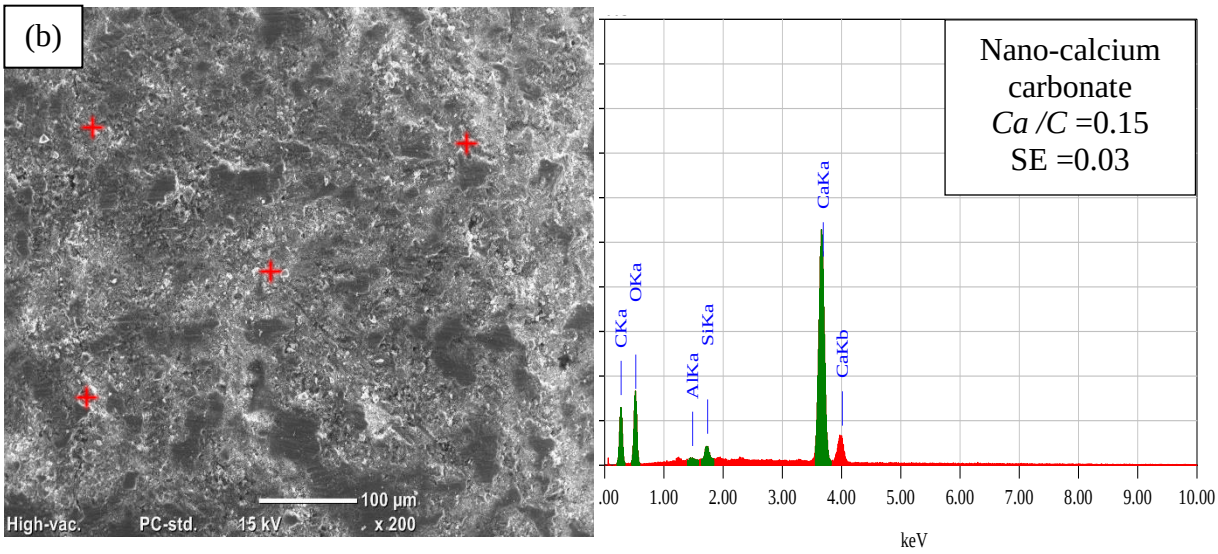

Figure 5. 16. Unexposed concrete specimens (*w/b* of 0.6) coated with: (a) SC5% with associated EDX, and (b) SCC5% with associated EDX. (Note: SE refers to the standard error for the average ratio of the marked location).

If not washed away, the additional gypsum on the concrete surface might act as a passivating layer reducing the infiltration rate of the sulfuric acid solution, as for example demonstrated by the 5% average increase, in the enthalpy of gypsum in the specimens coated with SCC5% compared to that in specimens coated with neat silane (**Fig. 5.8**). Therefore, the ettringite enthalpy was reduced in these specimens by an average of 24% relative to that of specimens treated with neat silane (**Fig. 5.10)** by the end of both exposures. Furthermore, the nano-calcium carbonate particles could interact with portlandite and aluminate in the cementitious matrix forming insoluble mono carbo-aluminate hydrate phases following (Eq. 5.5) (Dhandapani et al. 2021), as detected in the XRD analysis in the surface layer of these specimens **Fig. 5.13**. Hence, it might further contribute to deceleration in the rate of penetration of the acidic solution in the concrete specimens. This trend complied with previous research studies that demonstrated that the durability of concrete to sulfuric acid exposures was improved by using portland limestone cement (limestone filler content of 13% by mass) in the concrete mixtures instead of ordinary portland cement [limestone filler content of less than 5% by mass]

(Amin and Bassuoni 2017). In addition, using limestone as an aggregate enhanced concrete durability to sulfuric acid attack (Chang et al. 2005).

$$3CaO.Al_2O_3 + CaCO_3 + Ca(OH)_2 + 5H_2O \rightarrow 4CaO.Al_2O_3.CaCO_3.6H_2O \quad \text{(Eq. 5.5)}$$

5.2.5. Effect of Vinyl ester/Nanocomposites

Applying high viscosity neat vinyl ester as a surface treatment on concrete specimens generally improved the durability of concrete at both *w/b* to the full immersion and W/D exposures. This could be due to the formation of an isolating membrane on the concrete surface at an average thickness of approximately 150 µm [**Fig**. **5.18(a)**]. While the membrane is not hydrophobic (**Fig. 4.3**), it significantly reduced the concrete penetrability (RCPT, **Table 4.1**) relative to that of uncoated specimens and specimens coated with neat silane. In addition, this membrane was chemically stable in the acidic exposures and maintained high degree of bonding with the surface of concrete during both exposures as substantiated by the SEM analysis in [**Figs**. **5.18(b-c)**].

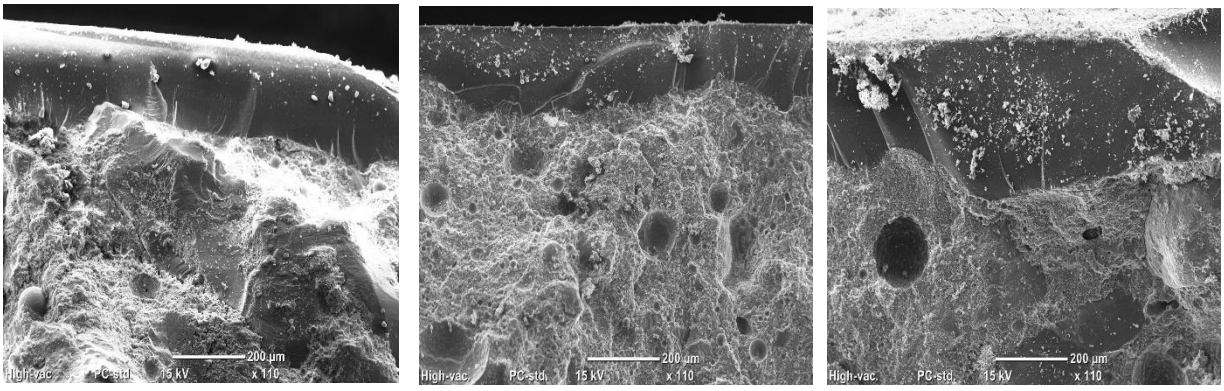

(a) (b) (c)

Figure 5. 17. Concrete specimens (*w/b* of 0.4): (a) coated with VE before exposures, (b) coated with VE after the full immersion exposure, and (c) coated with VE after the W/D exposure.

Comparable visual features and mass change (**Figs. 5.2-5.7)** were observed for concrete specimens coated with vinyl ester/nanocomposites relative to that of specimens coated with plain

vinyl ester, highlighting the dominant effect of this resin in enclosing the nanoparticles and resisting the sulfuric acid attack. For instance, comparable enthalpy of gypsum (**Fig. 5.8**) in the full immersion and W/D exposures (166.1 and 226 J/g, respectively) was found in the specimens superficially treated with VEC5%, relative to that of specimens superficially treated with neat vinyl ester (enthalpy of 166.9 and 227 J/g, respectively). SEM demonstrated that the concrete specimens superficially treated with vinyl ester/nano-clay composites had a continuous polymeric film [e.g., **Fig. 5.19 (a)**]. Vinyl ester/nano-clay composites had the added barrier (physical) effect of the nano-clay dispersed in the polymer (**Fig. 4.2**), which marginally increased with dosage. Moreover, the nano-clay particulates in contact with concrete surface induced a pozzolanic interaction with the portlandite in the paste, as the enthalpy was further reduced (e.g., 24% reduction with VEC5% relative to VE; **Fig. 5.16**). Hence, the net effect of the vinyl ester/nano-clay coatings resulted in improving the barrier properties of concrete, as demonstrated by the reduction in penetrability of these specimens (**Table 4.1**), which reduced the rate of infiltration of the acidic solution into the specimens.

Similarly, concrete specimens coated with vinyl ester/nano-calcium carbonate composites exhibited a comparable performance to that of specimens coated neat vinyl ester under W/D exposure. Again, SEM substantiated that the specimens coated with these nanocomposites had a continuous polymeric film, with sporadic clusters of nano-calcium carbonate appearing at the surface [**Fig. 5.19 (b)**]. Beside the dominance of vinyl ester protection mechanism and bonding to concrete surface, the additional effects of nano-calcium carbonate particles (physical filler), led to lower penetrability of concrete coated with these surface treatments (**Table 4.1**) compared to that of specimens coated with neat vinyl ester. Should any discontinuity occur in this coating under field conditions, it is projected that the existence of nano-calcium carbonate would have

the added chemical benefit of neutralizing the sulfuric acid and in turn slowing the rate of concrete deterioration.

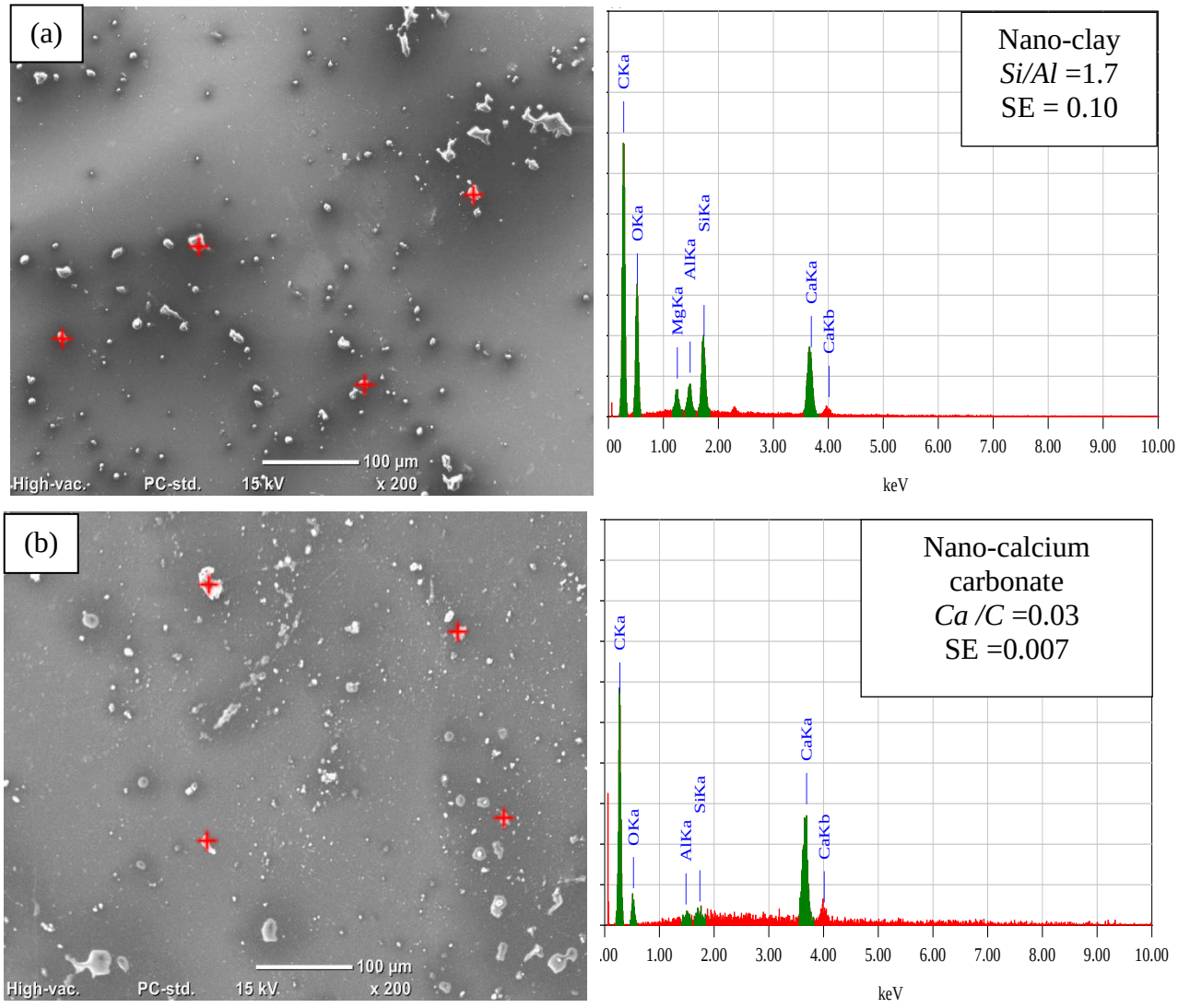

Figure 5. 18. Unexposed concrete specimens (*w/b* of 0.6) coated with: (a) VEC5% with associated EDX, and (b) VECC5% with associated EDX. (Note: SE refers to the standard error for the average ratio of the marked location).

6. Summary, Conclusions and Recommendations

6.1. Summary

In this thesis, two experimental phases were conducted to comprehend the behaviour of superficially treated concrete exposed to aggressive sulfate (ammonium sulfate) and acidic environment (sulfuric acid) under two exposures. For both exposures, specimens from two concrete mixtures with a *w/b* of 0.4 and 0.6 were superficially treated with different coatings and tested. The exposure conditions for the ammonium sulfate exposures were full immersion and combined exposures (F/T and W/D) in 10% ammonium sulfate solutions for 120 days. The sulfuric acid exposure was shorter (10 weeks) due to the nature of the solution, and in comparison, the specimens were exposed to full immersion and W/D exposures in a 5% sulfuric acid solution. The degradation of these specimens was evaluated by visual assessment, mass and length change. To elucidate the mechanisms of deterioration, the alteration of microstructure in the damaged specimens was studied by thermal, microscopy, and mineralogical analyses. The conclusions are given in the subsequent sections.

6.2. Conclusions for the Ammonium Sulfate Exposures

Based on the high concentration of ammonium sulfate solution, exposure duration, testing procedures, and the types of surface treatments used in this thesis, the following conclusions can be drawn:

- The combined exposure was more aggressive to concrete specimens than the full immersion exposure, due to the concomitant effects of acid-sulfate attack and cyclic environments, which provoked progressive scaling as well as ettringite and thaumasite formation.

- The durability of uncoated and coated concrete specimens under severe ammonium sulfate exposures was significantly improved by reducing the water-to-binder ratio (*w/b*) to 0.4, due densification of the microstructure of the paste and in turn reducing the penetrability of concrete to the solution. However, since the paste components were directly vulnerable to decomposition by ammonium sulfate, surface coatings were still needed to effectively combat the damage process.
- While the application of colloid silica as a surface treatment to hardened concrete led to improving the initial resistance of concrete to penetration of fluids relative to uncoated concrete, it did not adequately protect the concrete surface from the ammonium sulfate exposures. The hydrophilic nature and shrinkage micro-cracks in the colloidal silica layer facilitated the ingress of ammonium sulfate solution into the underlying surface (low portlandite and high C-S-H), which was directly vulnerable to decomposition forming large amounts of gypsum and ettringite.
- Relative to the neat silane, the resistance of concrete surface to both exposures was notably improved by applying the silane/nano composites as surface treatments with comparable performance for the two dosages of nanoparticles (2.5 and 5%). This was mainly attributed to the combined effects of hydrophobicity and fortifying the surface with nano-clay (lath like barrier) or nano-calcium carbonate (filler and neutralizing buffer).
- Relative to the neat vinyl ester, concrete specimens superficially treated with vinyl ester/ nanocomposites exhibited superior performance under both exposures, with a comparable performance for the two dosages of nanoparticles (2.5 and 5 %). This was ascribed to the polymeric membrane formed on the concrete surface, which had strong bonding and chemical stability, in addition to the physical and chemical functionalities of nano-clay and

nano-calcium carbonate. which might be attributed to the membrane layer of VE combined with the physical and chemical functionality of the nano particulates.

- The results of this study showed that silane and vinyl ester nanocomposites are viable surface treatments to protect and maintain concrete elements from aggressive ammonium sulfate exposures. Yet, field investigations are highly recommended for future research to confirm these laboratory observations.

6.3. Conclusions for the Sulfuric Acid Exposures

Based on the high concentration of sulfuric acid solution, exposure duration, testing procedures, and the types of surface treatments used in this thesis, the following conclusions can be drawn:

- The combined (W/D) exposure was less aggressive to concrete specimens than the full immersion exposure, due to the reduction in exposure time to the solution and built up of gypsum within the surface layer, which decelerated the rate of deterioration.
- While the 0.4 *w/b* led to densification of the microstructure of the paste and in turn reducing the penetrability of concrete, the higher paste volume was vulnerable to continual decomposition by sulfuric acid solution. For concrete with a *w/b* of 0.6, the solution penetrated deeply into concrete, forming reaction products depositing in the coarse microstructure, which was associated with internal cracking and swelling. In either case, surface coatings were still needed to effectively combat the damage process.
- While the application of colloid silica as a surface treatment to hardened concrete led to improving the initial resistance of concrete to penetration of fluids relative to uncoated concrete, it did not adequately protect the concrete surface from the sulfuric acid exposures. The hydrophilic nature and shrinkage micro-cracks in the colloidal silica layer facilitated the

ingress of sulfuric acid solution into the underlying surface (low portlandite and high C-S-H), which was directly vulnerable to decomposition forming large amounts of gypsum and ettringite.

- Relative to the neat silane, the resistance of concrete surface to both exposures was notably improved by applying the silane/nanocomposites as surface treatments with comparable performance for the two dosages of nanoparticles (2.5 and 5%). This was mainly attributed to the combined effects of hydrophobicity and fortifying the surface with nano-clay (lath-like and stable barrier) or nano-calcium carbonate (filler and neutralizing buffer).
- Relative to the neat vinyl ester, concrete specimens superficially treated with vinyl ester/ nanocomposites exhibited comparable performance under both exposures, with a comparable performance for the two dosages of nanoparticles (2.5 and 5 %). The dominant effect of the encapsulating vinyl ester membrane, chemical stability and high degree of bonding to concrete, were key to protecting concrete surface.
- The results of this study showed that vinyl ester and vinyl ester/nanocomposites are viable surface treatments to protect and maintain concrete elements from aggressive sulfuric acid exposures. Yet, field investigations are highly recommended for future research to confirm these laboratory observations.

6.4. Recommendations for Future Work

The results presented in this thesis provide useful directions for the extension of this research program. The following are recommendations for further work:

- Developing a standard test method for ammonium sulfate and sulfuric acid exposures with cyclic environmental conditions on concrete.
- Repeating the ammonium sulfate and sulfuric acid exposures on the same surface treatments with very slow and gradual increase in concentration from a very mild to a harsh exposure to stimulate field conditions.
- Due to the complexity of the deterioration mechanisms of ammonium sulfate attack on concrete, modeling of these interrelated patterns may be helpful for better understanding of this durability issue and thus is recommended for future research.
- Investigating the effect of other types of surface treatments with different application procedures on the performance of concrete in the ammonium sulfate and sulfuric acid exposures.

7. References

ACI 201.2R. (2016). “Guide to durable concrete.” Report by ACI Committee 201, MI: American Concrete Institute, Farmington Hills, USA.

ACI 515.2R. (2013). “Guide to selecting protective treatments for concrete.” Report by ACI Committee 515, MI: American Concrete Institute, Farmington Hills, USA.

Aguiar, J. B., Camões, A., and Moreira, P. M. (2008). Coatings for concrete protection against aggressive environments. Journal of Advanced Concrete Technology, 6(1), 243–250.

Aguiar, J. B., and Júnior, C. (2013). Carbonation of surface protected concrete. Construction and Building Materials, 49, 478–483.

Akman, M. S., and Guner, A. (1984). “The applicability of Sonreb method on damaged concrete.” Matériaux et Construction, 17(3), 195–200.

Alani, A. M., and Faramarzi, A. (2014). “An evolutionary approach to modelling concrete degradation due to sulphuric acid attack.” Applied Soft Computing Journal, 24, 985–993.

Alexander, M., Bertron, A., and De Belie, N. (2013). “Performance of cement-based materials in aggressive aqueous environments.” Springer Netherlands.

Alexander, M. G., and Fourie, C. (2011). “Performance of sewer pipe concrete mixtures with portland and calcium aluminate cements subject to mineral and biogenic acid attack.” Materials and Structures, 44, 313–330.

Allahverdi, A., and Škvára, F. (2005). “Sulfuric acid attack on hardened paste of geopolymer cements-Part 1. Mechanism of corrosion at relatively high concentration.” Ceramics − Silikáty, 49(4), 225–229.

Allahverdi, A., and Škvára, F. (2000). “Acidic corrosion of hydrated cement-based materials materials part 2. Kinetics of the phenomenon and mathematical models.” Ceramics - Silikaty, 44(4), 152–160.

Almusallam, A. A., Khan, F. M., Dulaijan, S. U., & Al-Amoudi, O. S. B. (2003). Effectiveness

of surface coatings in improving concrete durability. Cement and Concrete Composites, 25(4–5), 473–481.

Amin, M, and Bassuoni, M. T. (2018). Performance of concrete with blended binders in ammonium-sulphate solution. Journal of Sustainable Cement-Based Materials, 7(1), 15–37.

Amin, Mahmud, and Bassuoni, M. T. (2018). Response of concrete with blended binders and nanoparticles to sulfuric acid attack. Magazine of Concrete Research, 70(12), 617–632.

Amin, M. (2017). Performance of Concrete with Blended Binders in Sulfuric Acid and Ammonium Sulphate Solutions.

Ariffin, M. A. M., Bhutta, M. A. R., Hussin, M. W., Mohd Tahir, M., and Aziah, N. (2013). "Sulfuric acid resistance of blended ash geopolymer concrete." Construction and Building Materials, 43, 80–86.

ASTM C39. (2021). "Standard Test Method for Compressive Strength of Cylindrical Concrete Specimens." ASTM International, West Conshohocken, PA, USA.

ASTM C192. (2015). "Standard Practice for Making and Curing Concrete Test Specimens in the Laboratory." ASTM International, West Conshohocken, PA, USA.

ASTM C494. (2017). "Standard Specification for Chemical Admixtures for Concrete." ASTM International, West Conshohocken, PA, USA.

ASTM C666. (2017). "Standard test method for resistance of concrete to rapid freezing and thawing." West Conshohocken, PA, USA.

ASTM C1012. (2018). "Standard test method for length change of hydraulic-cement mortars exposed to a sulfate solution." ASTM International, West Conshohocken, PA, USA.

ASTM C1202. (2022). "Standard Test Method for Electrical Indication of Concrete's Ability to Resist Chloride Ion Penetration." ASTM International, West Conshohocken, PA, USA.

ASTM C1898 20. (2020). Standard Test Methods for Determining the Chemical Resistance of Concrete Products to Acid Attack. ASTM International, Stage II, 9–10.

Attiogbe, E. K., and Rizkalla, S. H. (1988). “Response of concrete to sulfuric acid attack.” ACI Materials Journal, 85, 481–488.

Aydın, S., Yazıcı, H., Yiğiter, H., and Baradan, B. (2007). “Sulfuric acid resistance of high-volume fly ash concrete.” Building and Environment, 42, 717–721.

Bassuoni, M. T., and Nehdi, M. L. (2007). “Resistance of self-consolidating concrete to sulfuric acid attack with consecutive pH reduction.” Cement and Concrete Research, 37, 1070–1084.

Bassuoni, M. T., and Nehdi, M. L. (2012). “Resistance of self-consolidating concrete to ammonium sulphate attack.” Materials and Structures, 45, 977–994.

Bassuoni, M. T., Nehdi, M. L., and Amin, M. (2007) “Self-compacting concrete: using limestone to resist sulfuric acid.” Proceedings of the ICE - Construction Materials, 160(CM3), 113-123.

Bassuoni, M. T., and Nehdi, M. L. (2009). Durability of self-consolidating concrete to sulfate attack under combined cyclic environments and flexural loading. Cement and Concrete Research, 39(3), 206–226.

Bassuoni, M. T., Nehdi, M. L., and Greenough, T. (2006). “Enhancing the reliability of evaluating chloride ingress in concrete using the ASTM C 1202 rapid chloride penetrability test.” Journal of ASTM International, 3, 13 p.

Bassuoni, M. T., and Rahman, M. M. (2016). Response of concrete to accelerated physical salt attack exposure. Cement and Concrete Research, 79, 395–408.

Baxi, C., and Patel, S. K. (1998). “Concrete exposed to calcium ammonium nitrate.” In: Gjorv, O.E., Sakai, K., Banthia, N. (eds.) Concrete under severe conditions 2: environment and loading, London, 76-83.

Beddoe, R. E., and Dorner, H. W. (2005). “Modelling acid attack on concrete: Part I. The essential mechanisms.” Cement and Concrete Research, 35(12), 2333–2339.

Bouchelaghem, F. (2010). “A numerical and analytical study on calcite dissolution and gypsum precipitation.” Applied Mathematical Modelling, 34, 467-480.

Boistelle, R., and Astier, J. P. (1988). Crystallization mechanisms in solution. Journal of Crystal Growth, 90(1–3), 14–30.

BRE Special Digest 1. (2005). "Concrete in aggressive ground: Third edition." Building Research Establishment (BRE), Watford, UK..

Brown. M.E. (1998). "Handbook of thermal analysis and calorimetry". Elsevier.

BS EN 206-1 (2005). "Concrete-specification: performance, production and conformity." British Standard European Norm, Gaylard & sons, London, UK: BSI.

BS EN 1504-2 (2004). "Products and systems for the protection and repair of concrete structures. Definitions, requirements, quality control and evaluation of conformity. Surface protection systems for concrete." British Standard European Norm, London, UK.

BS EN 1504-10 (2003). "Products and systems for the protection and repair of concrete structures. Definitions. Requirements. Quality control and evaluation of conformity. Site application of products and systems and quality control of the works." British Standard European Norm, London, UK.

Chang, Z. T., Song, X. J., Munn, R., and Marosszeky, M. (2005). "Using limestone aggregates and different cements for enhancing resistance of concrete to sulphuric acid attack." Cement and Concrete Research, 35, 1486 – 1494.

Chintalapudi, K., and Pannem, R. M. R. (2022). Enhanced chemical resistance to sulphuric acid attack by reinforcing Graphene Oxide in Ordinary and Portland Pozzolana cement mortars. Case Studies in Construction Materials, 17(September), e01452.

Chau, T. T., Bruckard, W. J., Koh, P. T. L., and Nguyen, A. V. (2009). A review of factors that affect contact angle and implications for flotation practice. Advances in Colloid and Interface Science, 150(2), 106–115.

Chen, B., Shao, H., Li, B., & Li, Z. (2020). Influence of silane on hydration characteristics and mechanical properties of cement paste. Cement and Concrete Composites, 113, 103743.

Cohen, M.D., and Bryant Mather, B. (1991). “Sulfate attack on concrete: Research needs.” ACI Materials Journal, 88(1), 62–69.

CSA A23.1-19/A23.2-19. (2019). “Concrete materials and methods of concrete construction/Methods of test and standard practices for concrete.” Canadian Standards Association, Mississauga, ON, Canada.

CSA A3001. (2013). “Cementitious materials for use in concrete.” Canadian Standards Association, Mississauga, ON, Canada.

Dashti, J., and Nematzadeh, M. (2020). Compressive and direct tensile behavior of concrete containing Forta-Ferro fiber and calcium aluminate cement subjected to sulfuric acid attack with optimized design. Construction and Building Materials, 253, 118999.

Dhandapani, Y., Santhanam, M., Kaladharan, G., & Ramanathan, S. (2021). Towards ternary binders involving limestone additions—A review. Cement and Concrete Research, 143, 106396.

De Belie, N., Monteny, J., Beeldens, A., Vincke, E., Van Gemert, D., and Verstraete, W. (2004). “Experimental research and prediction of the effect of chemical and biogenic sulfuric acid on different types of commercially produced concrete sewer pipes.” Cement and Concrete Research, 34, 2223–2236.

De Muynck, W., De Belie, N., & Verstraete, W. (2009). Effectiveness of admixtures, surface treatments and antimicrobial compounds against biogenic sulfuric acid corrosion of concrete. Cement and Concrete Composites, 31(3), 163–170.

DIN 4030-2. “Assessment of water, soil and gases for their aggressiveness to concrete — Part 2: Collection and examination of water and soil samples.” Germany.

Donatello, S., Palomo, A., and Fernández-Jiménez, A. (2013). “Durability of very high volume fly ash cement pastes and mortars in aggressive solutions.” Cement and Concrete Composites, 38, 12-20.

Dorner, H.W. (2000). “Acid resistance of high-performance concrete.” In G. C. for R. Concrete (Ed.), 38th research colloquium, Munich, 77–86.

Dorner, H.W., and Beddoe, R. E. (2002). “Prognosis of concrete corrosion due to acid attack.” In 9th Internat. Conf. Durability of Building Materials, Brisbane.

Tazawa, E. I., Morinaga, T., and Kawai, K. (1994). “Deterioration of concrete derived from metabolites of microorganisms.” 3rd CANMET/ACI international conference durability of concrete. American Concrete Institute. In ACI (Ed.), France, 1087–1098.

Elnaggar, E. M., Elsokkary, T. M., Shohide, M. A., El-Sabbagh, B. A., & Abdel-Gawwad, H. A. (2019). Surface protection of concrete by new protective coating. Construction and Building Materials, 220, 245–252.

Escadeillas, G., Hornain, H. (2008). “La durabilite´ des be´tons vis-a`-vis des environnements chimiquement agressifs.” In: Presses de l’ENPC (Ed.) La Durabilite´ Des Be´tons, Chap. 12, 613–705.

Esfandi, E. J., Sydney, R., & Jones, R. M. (2004). Evaluation of Protective Coatings for Concrete.

Fan, Y. F., and Luan, H. Y. (2013). “Pore structure in concrete exposed to acid deposit.” Construction and Building Materials, 49, 407–416.

Fattuni, N. I., and Hughes, B. P. (1983). Effect of acid attack on concrete with different admixtures or protective coatings. Cement and Concrete Research, 13(5), 655–665.

Fattuhi, Nijad I, and Hughes, B. P. (1988-a). Ordinary Portland cement mixes with selected admixtures subjected to sulfuric acid attack. Materials Journal, 85(6), 512–518.

Fattuhi, N I, and Hughes, B. P. (1988-b). The performance of cement paste and concrete subjected to sulphuric acid attack. Cement and Concrete Research, 18(4), 545–553.

Gaze, M. E., and Crammond, N. J. (2000). “Formation of thaumasite in a cement:lime:sand mortar exposed to cold magnesium and potassium sulfate solutions.” Cement and Concrete Composites, 22(3), 209–222.

Garvin, S., Hartless, R., Smith, M., Manchester, S., and Tedd, P. (2000). “Risks of contaminated land to buildings, building materials and services: A literature review.” Building Research Establishment (BRE) and M A Smith Environmental Consultancy, Watford, UK.

Ghrici, M., Kenai, S., and Said-Mansour, M. (2007). “Mechanical properties and durability of mortar and concrete containing natural pozzolana and limestone blended cements.” Cement and Concrete Composites, 29(7), 542–549.

Girardi, F., and Maggio, R. D. (2011). “Resistance of concrete mixtures to cyclic sulfuric acid exposure and mixed sulfates: Effect of the type of aggregate.” Cement and Concrete Composites, 33, 276–285.

Glasser, F. P., Marchand, J., and Samson, E. (2008). “Durability of concrete — Degradation phenomena involving detrimental chemical reactions.” Cement and Concrete Research, 38(2), 226–246.

Gu, L., Visintin, P., and Bennett, T. (2018). Evaluation of accelerated degradation test methods for cementitious composites subject to sulfuric acid attack; application to conventional and alkali-activated concretes. Cement and Concrete Composites, 87, 187–204.

Gutberlet, T., Hilbig, H., and Beddoe, R. E. (2015). “Acid attack on hydrated cement — Effect of mineral acids on the degradation process.” Cement and Concrete Research, 74, 35–43.

Gutierrez-Padilla, M. G. D. (2007). “Activity of sulfur oxidizing microorganisms and impacts on concrete pipe corrosion.” 224 pages.

Hewayde, E., Nehdi, M., Allouche, E., and Nakhla, G. (2007). “Neural network prediction of concrete degradation by sulphuric acid attack.” Structure and Infrastructure Engineering: Maintenance, Management, Life-Cycle Design and Performance, 3:1, 17-27.

Hobbs, D. W., and Taylor, M. G. (2000). “Nature of the thaumasite sulfate attack mechanism in field concrete.” Cement and Concrete Research, 30(4), 529–533.

House, M. W., and Weiss, W. J. (2014). “Review of microbially induced corrosion and comments on needs related to testing procedures.” In 4th International Conference on the Durability of Concrete Structures, Purdue University, West Lafayette, IN, USA.

Hou, D., Wu, C., Yin, B., Hua, X., Xu, H., Wang, X., Li, S., Zhou, Y., Jin, Z., Xu, W., and Lu, H. (2021). Investigation of composite silane emulsion modified by in-situ functionalized graphene oxide for cement-based materials. Construction and Building Materials, 304(August).

Huang, H., Fang, S., Luo, S., Hu, J., Yin, S., Wei, J., & Yu, Q. (2021). Multiscale modification on acrylic resin coating for concrete with silicon/fluorine and graphene oxide (GO) nanosheets. Construction and Building Materials, 305, 124297.

Islander, R. L., Devinny, J. S., Mansfeld, F., Postyn, A., and Shih, H. (1991). "Microbial ecology of crown corrosion in sewers." Journal of Environmental Engineering, 117(6), 751–770.

ISO 7150-1. "Water quality — Determination of ammonium — Part 1: Manual spectrometric method".

ISO 7150-2. "Water quality — Determination of ammonium — Part 2: Automated spectrometric method".

Ibrahim, M., Al-Gahtani, A. S., Maslehuddin, M., & Dakhil, F. H. (1999). Use of surface treatment materials to improve concrete durability. Journal of Materials in Civil Engineering, 11(1), 36–40.

Ibrahim, M., Salami, B. A., Amer Algaifi, H., Kalimur Rahman, M., Nasir, M., & Ewebajo, A. O. (2021). Assessment of acid resistance of natural pozzolan-based alkali-activated concrete: Experimental and optimization modelling. Construction and Building Materials, 304(September), 124657.

Israel, D., Macphee, D., and Lachowski, E. (1997). "Acid attack on pore-reduced cements." Journal of Materials Science, 2, 1–8.

Irico, S., De Meyst, L., Qvaeschning, D., Alonso, M. C., Villar, K., and De Belie, N. (2020). Severe sulfuric acid attack on self-compacting concrete with granulometrically optimized blast-furnace slag-comparison of different test methods. Materials, 13(6), 1431.

Jahani, F., Devinny, J., Mansfeld, F., Rosen, I., Sun, Z., and Wang, C. (2001). “Investigations of sulfuric acidcorrosion of concrete. I: Modeling and chemical observations.” Journal of Environmental Engineering, 127(7), 572-579.

Jauberthie, R., and Rendell, F. (2003). “Physicochemical study of the alteration surface of concrete exposed to ammonium salts.” Cement and Concrete Research, 33, 85–91.

Jiang, G., Liu, Y., Li, X., & Sun, X. (2023). Mathematical Modelling for the Concrete Corrosion of Sewer Systems. In Microbiologically Influenced Corrosion of Concrete Sewers: Mechanisms, Measurements, Modelling and Control Strategies (pp. 159–181). Springer.

Jia, L., Shi, C., Pan, X., Zhang, J., and Wu, L. (2016). Effects of inorganic surface treatment on water permeability of cement-based materials. Cement and Concrete Composites, 67, 85–92.

Jirasit, F., Jaturapitakkul, C., Siripanichgorn, A., and Kiattikomol, K. (1999). Effects of Cement and Fly Ash Contents in Concreteagainst Sulfuric Acid Attack. KMUTT Research and Development Journal, 22(2), 27–46.

Khan, H. A., Castel, A., Khan, M. S. H., and Mahmood, A. H. (2019). Durability of calcium aluminate and sulphate resistant Portland cement based mortars in aggressive sewer environment and sulphuric acid. Cement and Concrete Research, 124(August), 105852.

Law, K.-Y., and Zhao, H. (2016). Surface wetting: characterization, contact angle, and fundamentals. Springer International Publishing Basel, Switzerland.

Leemann, A., Lothenbach, B., and Hoffmann, C. (2010 “a”). “Biologically induced concrete deterioration in a wastewater treatment plant assessed by combining microstructural analysis with thermodynamic modeling.” Cement and Concrete Research, 40, 1157–1164.

Leemann, A., Lothenbach, B., Siegrist, H., and Hoffmann, C. (2010 “b”). “Influence of water hardness on concrete surface deterioration caused by nitrifying biofilms in wastewater treatment plants.” International Biodeterioration and Biodegradation, 64(6), 489–498.

Leung, C. K. Y., Zhu, H.-G., Kim, J.-K., & Woo, R. S. C. (2008). Use of polymer/organoclay nanocomposite surface treatment as water/ion barrier for concrete. Journal of Materials in

Civil Engineering, 20(7), 484–492.

Li, G., Yue, J., Guo, C., & Ji, Y. (2018). Influences of modified nanoparticles on hydrophobicity of concrete with organic film coating. Construction and Building Materials, 169, 1–7.

Liu, Z., and Hansen, W. (2016). Effect of hydrophobic surface treatment on freeze-thaw durability of concrete. Cement and Concrete Composites, 69, 49–60.

Makhloufi, Z., Kadri, E. H., Bouhicha, M., and Benaissa, a. (2012). "Resistance of limestone mortars with quaternary binders to sulfuric acid solution." Construction and Building Materials, 26(1), 497–504.

Martins, M. C., Langaro, E. A., Macioski, G., & Medeiros, M. H. F. (2021). External ammonium sulfate attack in concrete: Analysis of the current methodology. Construction and Building Materials, 277, 122252.

Marchand, J., Odler, I., & Skalny, J. P. (2001). Sulfate attack on concrete. CRC Press.

Macías, A., Goñi, S., and Madrid, J. (1999). "Limitations of Köch-Steinegger test to evaluate the durability of cement pastes in acid medium." Cement and Concrete Research, 29(12), 2005–2009.

Mahmoud, M. H., and Bassuoni, M. T. (2019). Performance of concrete with alkali-activated materials and nanosilica in acidic environments. Journal of Materials in Civil Engineering, 31(3), 4019009.

Mbessa, M., and Pe´ra, J. (2001). "Durability of high-strength concrete in ammonium sulfate solution" Cement and Concrete Research, 31, 1227–1231.

Mehta, P Kumar, and Monteiro, P. J. M. (2014). Concrete: microstructure, properties, and materials. McGraw-Hill Education.

Mehta, P K. (1985). Studies on chemical resistance of low water/cement ratio concretes. Cement and Concrete Research, 15(6), 969–978.

Merachtsaki, D., Tsardaka, E. C., Anastasiou, E., & Zouboulis, A. (2021). Anti-corrosion properties of magnesium oxide/magnesium hydroxide coatings for application on concrete

surfaces (sewerage network pipes). Construction and Building Materials, 312(November), 125441.

Merachtsaki, D., Tsardaka, E.-C., Tsampali, E., Simeonidis, K., Anastasiou, E., Yiannoulakis, H., & Zouboulis, A. (2020). Study of corrosion protection of concrete in sewage systems with magnesium hydroxide coatings. Environmental Sciences Proceedings, 2(1), 27.

Miletić, S., Ilić, M., Ranogajec, J., Marinovič-Neducin, R., and Djurić, M. (1998). "Portland ash cement degradation in ammonium-sulfate solution." Cement and Concrete Research, 28(5), 713–725.

Monteny, J., De Belie, N., Vincke, E., Verstraete, W., and Taerwe, L. (2001). "Chemical and microbiological tests to simulate sulfuric acid corrosion of polymer-modified concrete." Cement and Concrete Research, 31, 1359–1365.

Monteny, J., Vincke, E., Beeldens, A., De Belie, N., Taerwe, L., Van Gemert, D., and Verstraete, W. (2000). "Chemical, microbiological, and in situ test methods for biogenic sulfuric acid corrosion of concrete." Cement and Concrete Research, 30, 623–634.

Mori, T., Nonaka, T., Tazaki, K., Koga, M., Hikosaka, Y., and Noda, S. (1992). "Interactions of nutrients, moisture and pH on microbial corrosion of concrete sewer pipes." Water Research, 26(1), 29–37.

Moon, S., and Lee, K. J. (2017). Simultaneous control of size and surface functionality of silica particle via growing method. Advanced Powder Technology, 28(11), 2914–2920.

Muthu, M., Yang, E. H., and Unluer, C. (2021). Effect of graphene oxide on the deterioration of cement pastes exposed to citric and sulfuric acids. Cement and Concrete Composites, 124(February), 104252.

Nagele, E., Hillemeier, B., and Hilsdorf, H. (1984). "Attack of ammonium salt solutions of concrete." Betonwerk Fertigteil Technik, 50(11), 742–751.

O'Connell, M., McNally, C., and Richardson, M. G. (2010). "Biochemical attack on concrete in wastewater applications: A state of the art review." Cement and Concrete Composites, 32(7), 479–485.

Olmstead, W.M., and Hamlin, H. (1900). “Converting portions of the Los Angles outfall sewer into a septic tank.” Engineering News, 44, 317- 318.

Özalp, F., Yilmaz, H. D., Zeytun, S., & Akcay, B. (2023). Effects of EAF Slag, Steel Fiber, and Polyurea Coating on Mechanical Properties and Sulfuric Acid Resistance of Concrete Pipes. Journal of Pipeline Systems Engineering and Practice, 14(2), 1–12.

Pan, X., Shi, Z., Shi, C., Ling, T.-C., and Li, N. (2017). A review on concrete surface treatment Part I: Types and mechanisms. Construction and Building Materials, 132, 578–590.

Pan, X., Shi, Z., Shi, C., Ling, T.-C., and Li, N. (2017). A review on surface treatment for concrete--Part 2: Performance. Construction and Building Materials, 133, 81–90.

Parker, C. D. (1951). “Mechanics of corrosion of concrete sewers by hydrogen sulfide.” Sewage and Industrial Wastes, 23(12), 1477–1485.

Pavlík, V. (1994a). “Corrosion of hardened cement paste by acetic and nitric acids part I: Calculation of corrosion depth.” Cement and Concrete Research, 24(3a), 551–562.

Pavlík, V. (1994b). “Corrosion of hardened cement paste by acetic and nitric acids part II: Formation and chemical composition of the corrosion products layer.” Cement and Concrete Research, 24(8b), 1495–1508.

Pavlík, V., and Unčík, S. (1997). “The rate of corrosion of hardened cement pastes and mortars with additive of silica fume in acids.” Cement and Concrete Research, 27(11), 1731–1745.

Pavlík, V. (2000). “Effect of carbonates on the corrosion rate of cement mortars in nitric acid.” Cement and Concrete Research, 30, 481–489.

Pepenar, I. (2009). “Degradation of reinforced concrete structures in ammonium nitrate environments.” In Proceedings International RILEM TC 211-PAE Final Conference on Concrete in Aggressive Aqueous Environments: Performance, Testing and Modelling, Toulouse, France, 442–448.

PCA IS001 (2007). “Effects of substances on concrete and guide to protective treatments.” Portland Cement Association.

Pigino, B., Leemann, A., Franzoni, E., and Lura, P. (2012). Ethyl silicate for surface treatment of concrete - Part II: Characteristics and performance. Cement and Concrete Composites, 34(3), 313–321.

Rahman, M. M., & Bassuoni, M. T. (2014). Thaumasite sulfate attack on concrete: Mechanisms, influential factors and mitigation. Construction and Building Materials, 73, 652–662.

Roghanian, N., and Banthia, N. (2019). Development of a sustainable coating and repair material to prevent bio-corrosion in concrete sewer and waste-water pipes. Cement and Concrete Composites, 100, 99–107.

Rodrigues, A., Duchesne, J., Fournier, B., Durand, B., Rivard, P., and Shehata, M. (2012). "Mineralogical and chemical assessment of concrete damaged by the oxidation of sulfide-bearing aggregates: Importance of thaumasite formation on reaction mechanisms." Cement and Concrete Research, 42(10), 1336–1347.

Sakr, M. R., and Bassuoni, M. T. (2021). Silane and methyl-methacrylate based nanocomposites as coatings for concrete exposed to salt solutions and cyclic environments. Cement and Concrete Composites, 115(May 2020), 103841.

Sakr, M. R., Bassuoni, M. T., and Taha, M. R. (2019). Effect of coatings on concrete resistance to physical salt attack. ACI Materials Journal, 116(6), 255–267.

South African National Standard (SANS) 6242. (2002). "Acid insolubility of aggregates." SABS Standards Division, Pretoria.

Scarfato, P., Di Maio, L., Fariello, M. L., Russo, P., & Incarnato, L. (2012). Preparation and evaluation of polymer/clay nanocomposite surface treatments for concrete durability enhancement. Cement and Concrete Composites, 34(3), 297–305.

Schneider, U., and Chen, S.W. (1998). "The chemomechanical effect and the mechanochemical effect oon high-performance concrete subjected to stress corrosion." Cement and Concrete Research, 28(4), 509–522.

Sersale, R., Frigione, G., and Bonavita, L. (1998). "Acid depositions and concrete attack: Main influences." Cement and Concrete Research, 28(1), 19–24.

Siad, H., Lachemi, M., Sahmaran, M., and Hossain, K. M. A. (2015). Effect of glass powder on sulfuric acid resistance of cementitious materials. Construction and Building Materials, 113, 163–173.

Skalny, J., Marchand, J., and Odler, I. (2002). “Sulfate Attack on Concrete.” Spon Press, London and New York.

Soleimani, S., Isgor, O. B., and Ormeci, B. (2013). “Resistance of biofilm-covered mortars to microbiologically influenced deterioration simulated by sulfuric acid exposure.” Cement and Concrete Research, 53, 229–238.

Soroushian, P., Chowdhury, H., and Ghebrab, T. (2009). Evaluation of water-repelling additives for use in concrete-based sanitary sewer infrastructure. Journal of Infrastructure Systems, 15(2), 106–110.

Stephen Garvin, Richard Hartless, Mike Smith, S. M. and P. T. (2000). “Risks of contaminated land to buildings, building materials and services: A literature review.” BRE (and M A Smith Environmental Consultancy) R&D Technical Report P331.

Stark, J., & Bollmann, K. (1999). Laboratory and field examinations of ettringite formation in pavement concrete. Special Publication, 177, 183–198.

Tagnit-hamou, A., Saric-coric, M., and Rivard, P. (2005). “Internal deterioration of concrete by the oxidation of pyrrhotitic aggregates.” Cement and Concrete Research, 35, 99–107.

Tian, B., and Cohen, M. D. (2000). “Does gypsum formation during sulfate attack on concrete lead to expansion?” Cement and Concrete Research, 30, 117–123.

Torii, K., and Kawamura, M. (1994). “Effects of fly ash and silica fume on the resistance of mortar to sulfuric acid and sulfate attack.” Cement and Concrete Research, 24, 361-370.

Torrenti, J. M., Nguyen, V. H., Colina, H., Le Maou, F., Benboudjema, F., and Deleruyelle, F. (2008). “Coupling between leaching and creep of concrete.” Cement and Concrete Research, 38, 816–821.

U.S. EPA. (1991). “Hydrogen sulfide corrosion in wastewater collection and treatment systems: Report to congress.” Technical Report.

Vipulanandan, C., & Liu, J. (2002). Glass-fiber mat-reinforced epoxy coating for concrete in sulfuric acid environment. Cement and Concrete Research, 32(2), 205–210.

Vincke, E., Wanseele, E. V., Monteny, J., Beeldens, A., and Belie, N. D. (2002). “Influence of polymer addition on biogenic sulfuric acid attack of concrete.” International Biodeterioration and Biodegradation, 49, 283–292.

Vishwakarma, V., Uthaman, S., Dasnamoorthy, R., & Kanagasabai, V. (2020). Investigation on surface sulfate attack of nanoparticle-modified fly ash concrete. Environmental Science and Pollution Research, 27(33), 41372–41380.

Wang, Y., Su, F., Guo, Y., Yang, H., Ye, Z., & Wang, L. (2022). Predicting the microbiologically induced concrete corrosion in sewer based on XGBoost algorithm. Case Studies in Construction Materials, 17(September), e01649.

Wang, X., and Pan, Z. (2017). Chemical changes and reaction mechanism of hardened cement paste–(NH4)2SO4–H2O system. Construction and Building Materials, 152, 434–443.

Woo, R. S. C., Zhu, H., Chow, M. M. K., Leung, C. K. Y., & Kim, J.-K. (2008). Barrier performance of silane--clay nanocomposite coatings on concrete structure. Composites Science and Technology, 68(14), 2828–2836.

Wong, L. L., Asrah, H., Rahman, M. E., and Mannan, M. A. (2015). “Effects of aggressive ammonium nitrate on durability properties of concrete using sandstone and granite aggregates.” World Academy of Science, Engineering and Technology, 73.

Wu, M., Wang, T., Wu, K., & Kan, L. (2020). Microbiologically induced corrosion of concrete in sewer structures: A review of the mechanisms and phenomena. Construction and Building Materials, 239, 117813.

Xu, S., Ma, Q., & Wang, J. (2018). Combined effect of isobutyltriethoxysilane and silica fume on the performance of natural hydraulic lime-based mortars. Construction and Building Materials, 162, 181–191.

Xu, B., and Zhang, Q. (2021). Preparation and properties of hydrophobically modified nano-SiO2 with hexadecyltrimethoxysilane. ACS Omega, 6(14), 9764–9770.

Yuan, H., Dangla, P., Chatellier, P., & Chaussadent, T. (2015). Degradation modeling of concrete submitted to biogenic acid attack. Cement and Concrete Research, 70, 29–38.